Spinal cord regeneration progresses via developmental and non-developmental mechanisms in *X. tropicalis*

Avery Angell Swearer

A dissertation

submitted in partial fulfillment of the

requirements for the degree of

Doctor of Philosophy

University of Washington

2025

Reading Committee:

Andrea Wills, Chair

Celeste Berg

Lisa Maves

Program Authorized to Offer Degree:

Molecular and Cellular Biology

University of Washington

Abstract

Spinal cord regeneration progresses via developmental and non-developmental mechanisms in *X. tropicalis*

Avery Angell Swearer

Chair of the Supervisory Committee:
Andrea Wills
Biochemistry

Human spinal cord regeneration is hampered by the inability of resident neural stem cells to regenerate developmentally derived neuron diversity and organization after injury. Unlike humans, the *Xenopus tropicalis* spinal cord is capable of functional regeneration after amputation, although the regenerative extent and mechanisms driving neural diversity and patterning remain unknown. During my dissertation work, I investigated if the *X. tropicalis* spinal cord regenerates cell diversity and patterning via the same developmental mechanisms with which it was originally made. First, I showed that the spinal cord dorsal/ventral axis is re-established by Shh signaling after injury in a similar manner to embryogenesis (Angell Swearer, Perkowski, et al. 2025). Next, I found that spinal cord regeneration deploys cell-type-specific developmental and non-developmental strategies to restore neuron diversity, in a divergence from the traditional regenerative paradigm (Angell Swearer et al. 2025, preprint). Overall, these results indicate that successful regeneration recruits a dynamic combination of developmental and non-developmental signals to complete functional healing.

TABLE OF CONTENTS

LIST OF FIGURES

ACKNOWLEDGEMENTS

I would like to acknowledge the Coast Salish Peoples of this land which touches the shared waters of all tribes and bands within the Suquamish, Tulalip, and Muckleshoot nations, upon whose land this work has been undertaken.

First I would like to thank my committee members—Andrea Wills, Olivia Bermingham-McDonogh, Celeste Berg, Jeff Rasmussen, and Lisa Maves—for their time, guidance, and constructive feedback. You successfully guided me through several changes in project aims, including the switch from studying Pbx3 and Meis1 transcription factors to the completely separate goal of creating a neuron atlas. I also want to thank the MCB program, especially Maia Low and Denise Barnes, for providing me with endless guidance. I want to thank my MCB cohort, especially LuLu Callies, for being my go-to for single cell RNA-sequencing questions. I want to thank my mentors, Stephan Zweifel, Jennifer Wolff, Yasuhiko Kawakami, Aniket Gore, and Brant Weinstein for inspiring my love of science and helping me get to where I am today.

I want to thank my mentor, Andrea Wills, for being the best mentor a PhD student could hope for. Thank you for encouraging me to be the best scientist I could be while providing the support I needed to make that happen. Your enthusiastic and conscientious mentorship will forever serve as a model to me and others of how to be a positive and effective mentor.

I want to thank my current lab mates and alumni: Anneke, Claire, Jeet, Gavin, Morgan, Beatrice, Yelena, Kalle, Hannah, Thiago, and Sam. Your support and companionship have made the last 5 years the best in my life (no small feat given grad school's reputation). Anneke, Claire, and Jeet: I deeply appreciate the time and effort you spent walking me through experiments and guiding me through the beginning of my project. Gavin: thank you for being half of mid-bay, I will forever appreciate your patience as I learned to code and asked dumb questions about

statistics. To Beatrice, Yelena, Kalle, Hannah, and Thiago- thank you for being my primary support team, hype squad, trivia group, and geoguessr crew. I will always appreciate not only your scientific feedback, but also your friendship, camaraderie, and never-ending support. I will miss you more than I can say. Thank you to my undergraduate students, Sam, Iba, and Ashi, for taking on the fun but challenging experiments I couldn't- thank you for giving me the opportunity to teach you. Thank you especially to Sam, whose clever experiments and exploratory coding propelled many of our research findings and publications.

To my family, thank you for being my first team. Especially to my mom, for inspiring my love of science, and to my sister, for actually remembering what I work on (and for other things like her unrelenting support and consistent phone calls, I suppose).

To my Seattle family: Ashe, Nicel, Camila, Shanon, Lauren, Kazia, Liv, Emily, Jasper, Maya, Erin, and so many others. Your continued friendship has kept me sane all these years- thank you for being such a source of joy and love. I feel so lucky to share my life with such amazing people. I'm so thankful that while things in life change these friendships will remain. To my cat, Juniper, and my dog, Haven, your enthusiastic companionship during the long days of coding and writing made it all worthwhile.

Lastly, I want to thank my partner Audrey, without whose support I would not be here today. I could write pages about you, so I'll stick to just the simple facts. Thank you for coming to Seattle with me. Thank you for making the best friends that I can steal. Thank you for giving me a house to distract myself with. Thank you for feeding me. Thank you for talking me through tears and crash outs and for being patient through grant deadlines and paper writing. Thank you for being my biggest supporter and the reason I want to succeed. I'm so proud of how far we've come and I'm so excited to see where we go.

DEDICATION

For my found family: Audrey, Juniper, and Haven.

Chapter 1. INTRODUCTION

Full or partial paralysis due to traumatic spinal cord injury (SCI) remains one of the most debilitating afflictions in human medicine. With an average injury age of 43, SCI requires lifelong management and places a severe physical, psychological, and economic burden on patients and their families (SCIMS 2024). Despite the advent of modern medicine, established treatment for SCI only minimizes additional damage without treating the underlying injury (Ralph et al. 2024).

In mammals, paralysis stems from the inability of the spinal cord to repopulate lost cells and repair axon connectivity. Primary traumatic injury shears axons and damages local neuron populations, which leads to axon dieback and neuron apoptosis (Katoh et al. 2019). In response, cystic cavities form alongside a glial scar, generated by fibrosis and abnormal numbers of hypertrophic astrocytes, or reactive astrogliosis. This scar protects the tissue from infection but inhibits axon reinnervation (Katoh et al. 2019; Wang et al. 2019). Recent clinical research has started to tackle this problem by combatting different aspects of this injury response in humans (reviewed in Ralph et al. 2024). The most prevalent approach is stem cell therapy, utilizing transplantation of autologous mesenchymal stem cells within a synthetic matrix into the injury site to try and reestablish cell populations and prevent a fibrotic scar (Dasari 2014). However, the risk of cancer or other complications during the process remains high (Lee et al. 2013). In contrast, inducing endogenous glial cells to replenish lost neurons, or *in vivo* neuronal reprogramming, is less invasive and avoids these risks (Chen and Li 2022). This process promotes the expression of neurogenic transcription factors in resident glial cells to reprogram cells into multipotent neuroblasts. For example, Sox2 or NeuroD1 can reprogram astrocytes into neuroblasts (Wang et al. 2016; Su et al. 2014), which in combination with growth factors and

expression of Ngn2 can stimulate neurogenesis in mice (Puls et al. 2020). This process not only aids in neuron repopulation but also may reroute astrocytes from contributing to inhibitory scar formation.

The goal of inducing endogenous regeneration of neuronal populations is complicated by the complex neuron diversity and organization found within the uninjured spinal cord (Rodemer et al. 2020). This spinal cord consists of incoming sensory nerves, numerous types of interconnected dorsal interneurons, and ventral motor neurons with axons leaving the spinal cord to innervate specific muscles (Figure 1.1A) (Watson and Kayalioglu 2009). This complexity and organization must be regenerated in order to recover balanced neural connectivity and functional recovery. Several studies have found that expression of different transcription factors during neuronal reprogramming can effectively produce different neuron types, but it is unclear how this process is finetuned in order to produce the correct proportion of different neurons necessary for recovery (reviewed in Chen and Li 2022).

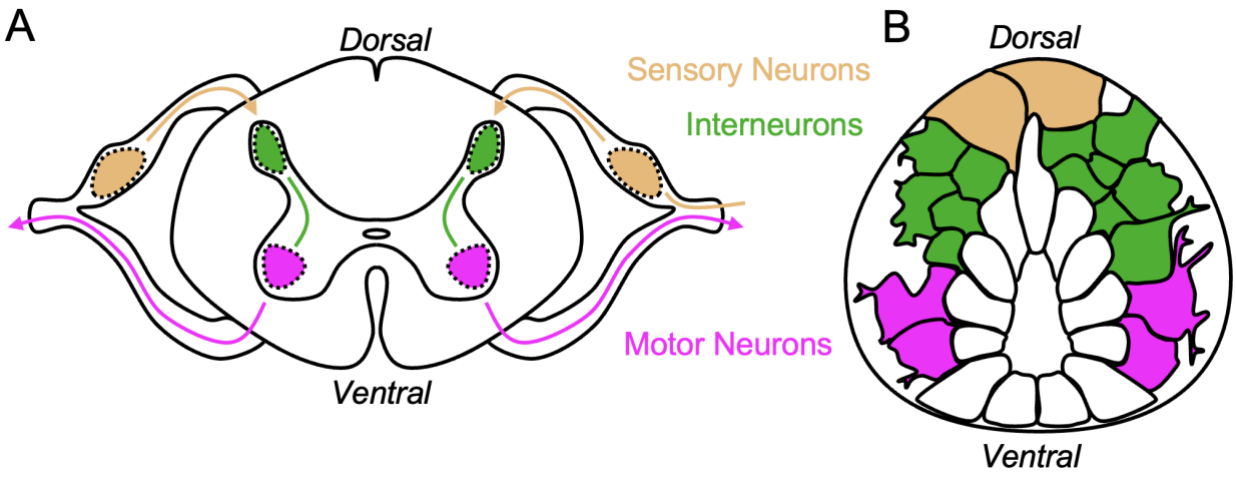

Figure 1.1. Diagram of the human and *Xenopus tropicalis* spinal cords with sensory neurons, interneurons, and motor neurons labelled. A) Human spinal cord with neuron cell body domains labelled with colored dotted regions. Major axon pathways indicated by colored lines. B) *X. tropicalis* spinal cord with cells labeled by color (adapted from Roberts et al. 2012). Diagrams not to scale: human adult spinal cord width ~ 14,000 µm, average stage 41 *X. tropicalis* spinal cord width ~20 µm.

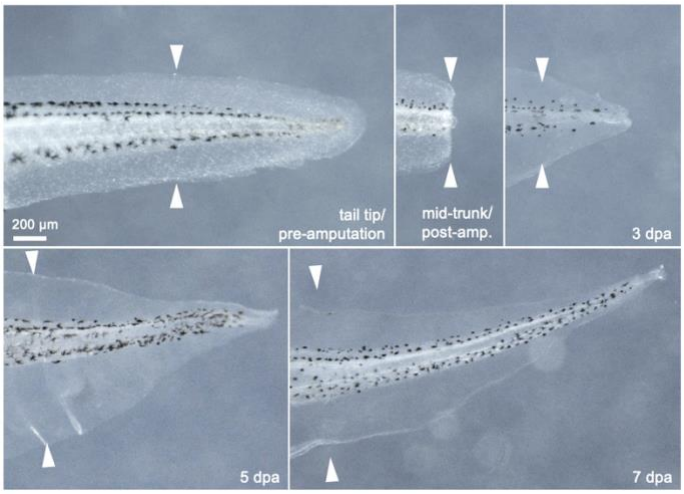

Figure 1.2. *X. tropicalis* spinal cord regeneration over 7 days post amputation (dpa). Samples were collected before or after amputation at stage 41 for the tail tip and mid-trunk images. The rest were collected at 3dpa, 5dpa, and 7 dpa (days post amputation). All samples were imaged brightfield. Animals were fed starting at 3dpa. Scale bar is 200 µm. Adapted from Angell Swearer et al. 2025.

In contrast to mammalian regeneration, western clawed frog (*Xenopus tropicalis*) tadpoles are able to completely regenerate spinal cord function within a week of tail amputation (Figure 1.2) (Edwards-Faret et al. 2017). Remarkedly, *X. tropicalis* tadpoles also have the same diverse set of precisely organized neuron types as humans, including centralized sensory, inter-, and motor neurons that allow tail function (Figure 1.1B). Researching how recovery after SCI in regenerative-competent animals such as *X. tropicalis* may provide the missing context needed to guide neuronal reprogramming for SCI therapy in humans.

In regeneration-competent animals, multipotent neural stem/progenitor cells (broadly called NS/PCs) retain the ability to activate and proliferate after injury to restore lost neurons instead of triggering reactive astrogliosis and generating an inhibitory scar (Lee-Liu et al. 2013). Neurons repopulate the new tissue to support functional recovery. While intuitively one might expect that the spinal cord is thus completely restored to pre-injury complexity, to what extent neural diversity and organization is recovered remains unclear. Only recently has research begun to tackle this question. Axolotls restore dorsal/ventral NS/PC patterning post injury in a process mirroring developmental specification of neuronal domains, though it is unclear if neurons are then formed from these specific domains via neurogenesis (Schnapp et al. 2005; Mchedlishvili et

al. 2007). In zebrafish, motor neurons have been found in the regenerating tissue, indicating that regenerated neurons have distinct identities (Reimer et al. 2009). In addition, these neurons were BrdU+, indicating that they were derived from proliferative neurogenesis (aka the generation of neurons from mitotically active progenitors), like they are during development (Figure 1.3). However non-developmental mechanisms such as transdifferentiation of radial glia to NS/PCs are a critical contributor to spinal cord neurogenesis after injury in axolotls and zebrafish (Zhou et al. 2023; Reimer et al. 2009; reviewed in Cigliola et al. 2020), and in axolotls neuron displacement from the uninjured anterior tissue into posterior regenerating tissue also contributes to neuron repopulation (Zhang et al. 2003) (Figure 1.3). Overall, the characterization of progenitor and neuron diversity post injury is surprisingly unexplored, and the identification of which mechanisms underlie neuron repopulation and if those mechanisms are cell-type specific is lacking.

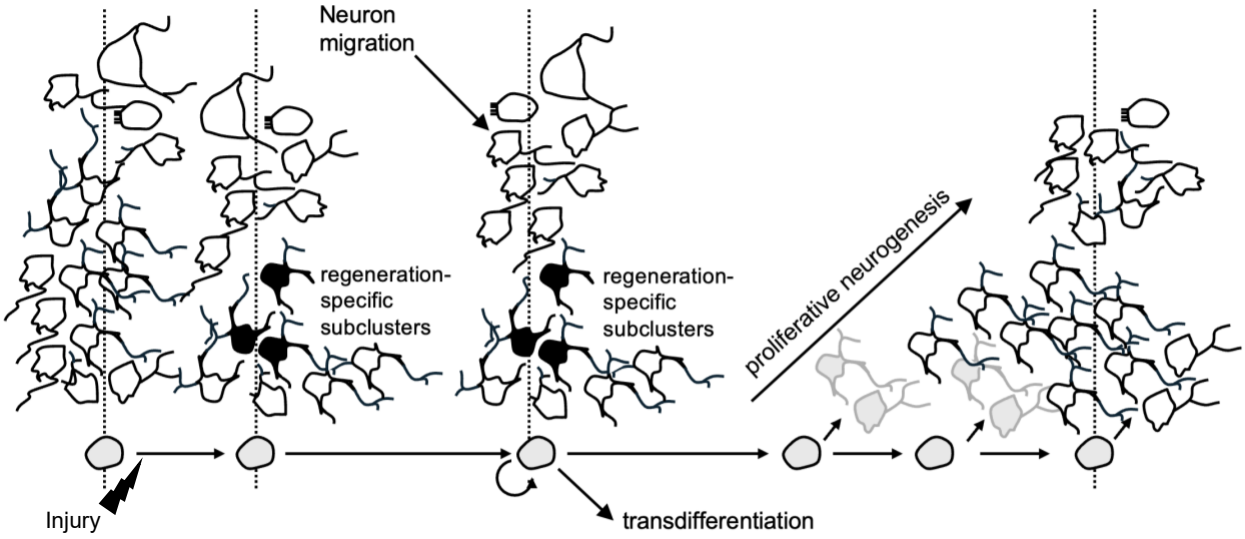

Figure 1.3. Mechanisms of neural regeneration. In other animals, spinal cord regeneration proceeds via developmental mechanisms such as proliferative neurogenesis as well as via unique mechanisms such as regeneration-specific subclusters, transdifferentiation, or neuron migration (Saraswathy et al. 2024; Zhang et al. 2003; Echeverri and Tanaka 2002).

Recent studies indicate that neuron identity plays an important role in regeneration. In mammals, Shox2-expressing V2a and spinocerebellar neurons express a cohort of regeneration associated genes, which seem to promote structural remodeling post injury (Matson et al. 2022). In zebrafish, a similar population of transient, regeneration-specific induced-Neurons (iNeurons) similarly express regeneration associated genes, specifically *atf3* and *vamp4*, which are necessary for complete regeneration post-transection likely due to their role in neural plasticity (Saraswathy et al. 2024). Lineage tracing indicates that the iNeuron population is primarily composed of surviving neurons from pre-injury tissue. iNeurons express markers of various neuron types, indicating that many neurons give rise to this transient cell population, although it's unclear which types do and do not specifically contribute (Saraswathy et al. 2024). iNeurons have not yet been established in other species, although studies in mice did identify a rare population of spinocerebellar neurons that express regeneration-associated genes such as *atf3* after injury. In *Xenopus*, a universal regeneration-specific neuron subtype has not yet been identified, although a subset of motor neurons express Leptin and Leptin Receptor post injury (Aztekin et al. 2019; Kakebeen et al. 2020), indicating that there may be cell-type specific changes in neuron identity after injury in these animals as well. Leptin signaling often plays a neuroprotective role during homeostasis and disease, although its exact role during spinal cord regeneration is unclear (Tan et al. 2023).

Amongst these animals capable of strong spinal cord regeneration, *Xenopus tropicalis* is uniquely a larval-only model of regeneration. In comparison to the study of adult mouse and zebrafish spinal cord transection, *Xenopus* spinal cord regeneration occurs during their larval tadpole stages, as they lose the ability to regenerate post-metamorphosis. *X. tropicalis* is thus an ideal model in which to study the interplay between developmental (i.e. proliferative

neurogenesis) and regenerative-specific (i.e. transient neuron populations, neuron displacement) models of neural recovery (Figure 1.3).

During my PhD, I used immunohistochemistry, HCR, and single-cell RNA-sequencing to establish an atlas of progenitor and neuron diversity and organization in the regenerating *X. tropicalis* spinal cord. I then tested what developmental and regenerative specific mechanisms underlie the regeneration of this diversity using small molecule inhibitors and lineage tracing. I found that spinal cord regeneration uses developmental and non-developmental mechanisms of recovery.

Chapter 2. SHH SIGNALING DIRECTS DORSAL VENTRAL PATTERNING IN THE REGENERATING *X. TROPICALIS* SPINAL CORD

Chapter 2 is adapted with minimal modification from:

Angell Swearer, A.,* Perkowski, S,* and Wills, A. 2025. Shh signaling directs dorsal ventral patterning in the regenerating *X. tropicalis* spinal cord. Developmental Biology, 520, pp.191-199. DOI: 10.1016/j.ydbio.2025.01.015.

**These authors contributed equally to this work. SP and I contributed to the project design, experimental methods, and writing. AW lead the conceptual design and writing of this work.*

2.1. Abstract

Tissue development and regeneration rely on the deployment of embryonic signals to drive progenitor activity and thus generate complex cell diversity and organization. One such signal is Sonic Hedgehog (Shh), which establishes the dorsal-ventral (D/V) axis of the spinal cord during embryogenesis. However, the existence of this D/V axis and its dependence on Shh signaling during regeneration varies by species (Schnapp et al. 2005; Sun et al. 2018). Here we investigate the function of Shh signaling in patterning the D/V axis during spinal cord regeneration in *Xenopus tropicalis* tadpoles. We find that neural progenitor markers Msx1/2, Nkx6.1, and Nkx2.2 are confined to dorsal, intermediate and ventral spatial domains, respectively, in both the uninjured and regenerating spinal cord. These domains are altered by perturbation of Shh signaling. Additionally, we find that these D/V domains are more sensitive to Shh perturbation during regeneration than uninjured tissue. The renewed sensitivity of these neural progenitor cells to Shh signals represents a regeneration specific response and raises questions about how responsiveness to developmental patterning cues is regulated in mature and regenerating tissues.

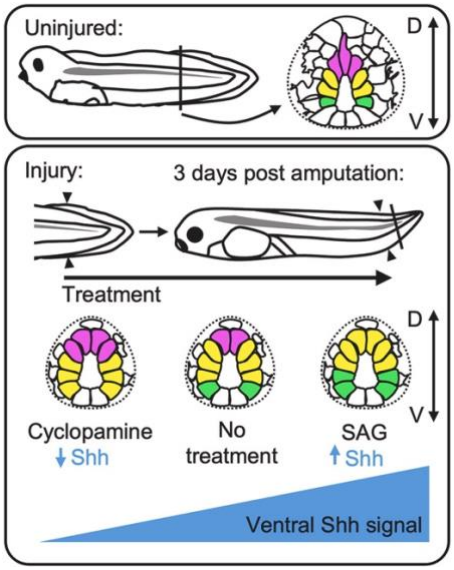

Figure 2.1. Graphical Abstract. Shh drives NPC patterning after spinal cord amputation. In uninjured tadpoles, neural progenitor cells (NPCs) are dorsal/ventrally (D/V) patterned. By 3 days post amputation, this patterning regenerates, driven by ventral Shh signaling in a recapitulation of development. Inhibition of Shh using cyclopamine dorsalizes the regenerating spinal cord, whereas increasing Shh signaling with SAG ventralizes the spinal cord.

2.2. Introduction

Regeneration is often understood through the lens of development, as both processes must generate and pattern complex tissue. During embryogenesis, positional identity in the vertebrate spinal cord is established through opposing gradients of secreted dorsal bone morphogenetic protein (BMP) and ventral Sonic hedgehog (Shh) signals, which are interpreted through a transcription factor code to yield distinct dorsal, intermediate, and ventral neural progenitor cell (NPC) domains (Lee and Pfaff 2001; Briscoe et al. 2000). More specifically, this gradient of Shh originates from the ventrally-located notochord and floor plate and is canonically interpreted through Gli transcription factors. In the presence of the Shh ligand, these factors are converted from transcriptional repressors to activators, and they then drive expression of ventral NPC identities and repression of dorsal identities (Briscoe and Thérond 2013). Each unique NPC domain along the Dorsal/Ventral (D/V) axis later gives rise to a similarly spatially restricted

domain of post-mitotic neurons, which work together to mediate the many types of afferent and efferent neural impulses of the spinal cord (Briscoe and Ericson 1999; Alaynick et al. 2011). The basic features of this developmental patterning mechanism are fundamentally conserved in vertebrates, with fish, frogs, chicks, mice, and others all showing disruptions of spinal cord patterning when BMP or Shh are perturbed (Chen et al. 2001; Barth et al. 1999; Marti et al. 1995; Zechner et al. 2007; Lee et al. 2000; Chiang et al. 1996; Ramsbottom et al. 2014; Miller et al. 2004). Shh also acts in a mitogenic role to support NPC proliferation in both the embryonic and mature CNS in the chick, mouse, and zebrafish, and in the regenerating CNS of zebrafish and axolotls (Yang et al. 2019; Rowitch et al. 1999; Lai et al. 2003; Schnapp et al. 2005; Reimer et al. 2009; Feijóo et al. 2011).

In animals that can regenerate, one might intuitively expect that regeneration of spinal cord cell types would re-use the same developmental mechanisms to pattern lost tissue. However, there are examples that both support and oppose this paradigm. Across the vertebrate phylum, BMP and Shh are understood to be required for regeneration, as the absence of these signals leads to incomplete regeneration in zebrafish, *Xenopus*, axolotls, newts and lizards (Romero et al. 2018; Smith et al. 2006; Makanae et al. 2016; Taniguchi et al. 2014; Schnapp et al. 2005; Singh et al. 2018; Slack et al. 2004; Sun et al. 2018). The role of these signals, specifically Shh, in conferring positional identity to the regenerated neural progenitors varies among these species. In axolotls (*Ambystoma mexicanum*), Shh specifies ventral neural stem/progenitor cell domains during regeneration, a process that can be disrupted by inhibition of Shh signaling (Schnapp et al. 2005). However, axolotls also appear to take advantage of the existing pattern in the mature spinal cord, as most regenerated daughter cells occupy the dorsoventral position of their parent (Mchedlishvili et al. 2007). Thus, both the *de novo*

establishment of positional identity by Shh and the positional identity of pre-existing progenitors may contribute to D/V patterning in the regenerated spinal cord. By contrast, in green anole lizards (*Anolis carolinensis*), the spinal cord regenerates as a ubiquitously Shh+ ependymal tube, in which Shh serves to specify surrounding mesoderm but has no proven influence in generating a D/V axis (Sun et al. 2018). Thus the role of Shh in directing D/V patterning in the regenerated spinal cord is less universal than its role in the developing spinal cord.

Xenopus tadpoles occupy a unique niche among regeneration-competent animals because they are capable of functional spinal cord regeneration prior to metamorphosis, but they lose that ability as adults (Muñoz et al. 2015). In *X. laevis*, Shh is expressed in the regenerating notochord following injury, and this signal is necessary for the full regeneration of not only the spinal cord, but also the muscle and notochord (Taniguchi et al. 2014). However, it is not clear that the requirement for Shh in regeneration derives from its canonical functions through Gli transcription factors. Most notably, knockdown of Gli2 and treatment with the Gli1/2 inhibitor GANT61 does not impair global regeneration in *X. laevis*. Rather, a non-canonical Shh pathway of Ca2+-dependent activation and coordination of proliferation in neural and muscle progenitor cells is thought to direct the Shh-dependent aspects of regenerative growth in the tail (Hamilton et al. 2021). This reported lack of function for Gli1/2 during regeneration could be due to the absence of D/V patterning during regeneration, leading us to question whether these D/V domains are regenerated and if Shh retains any developmental patterning function during regeneration in *Xenopus*.

Here we interrogated the basis for D/V patterning during regeneration of the spinal cord in *Xenopus tropicalis*, a diploid relative of *X. laevis* that shares many of the latter's regenerative features and mechanisms (Kakebeen and Wills 2019). We specifically sought to determine

whether the regenerating spinal cord recapitulates the D/V organization of the embryonic spinal cord by examining expression of dorsal, intermediate, and ventral NPC markers. Next, we asked whether this organization is dependent on Shh through gain- and loss-of-function perturbations. Finally, we sought to identify whether positional identity in the uninjured spinal cord is plastic or fixed by asking whether perturbations of Shh change the balance of positional identity in uninjured tadpoles as compared to regenerating tadpoles.

2.3. Results

2.3.1. Dorsal, intermediate, and ventral NPC domains exist in the uninjured, regenerative-stage spinal cord

Our first goal was to confirm that NPCs were organized into spatially restricted dorsal, intermediate, and ventral domains in uninjured, regenerative-stage *X. tropicalis* tadpoles. To this end, we identified an antibody against two transcription factor paralogs, Msx1 and Msx2, which have conserved expression in dorsal NPCs of the developing spinal cord downstream of BMP signaling (Liem et al. 1995; Timmer et al. 2002; Schlosser and Ahrens 2004). We then selected two transcription factors downstream of Shh signaling, Nkx6.1 and Nkx2.2, as intermediate and ventral markers, respectively. These genes are known to be expressed in intermediate and ventral domains of the developing spinal cord in *Xenopus* (Ramsbottom et al. 2014; Koide et al. 2006; Peyrot et al. 2011). We performed immunofluorescence for Msx1/2, Nkx2.2, and Nkx6.1 to assess expression of these markers in the uninjured spinal cord of regenerative stage 46 uninjured tadpoles (Figure 2.2). In lateral views and transverse sections, each marker was expressed in their expected D/V domains.

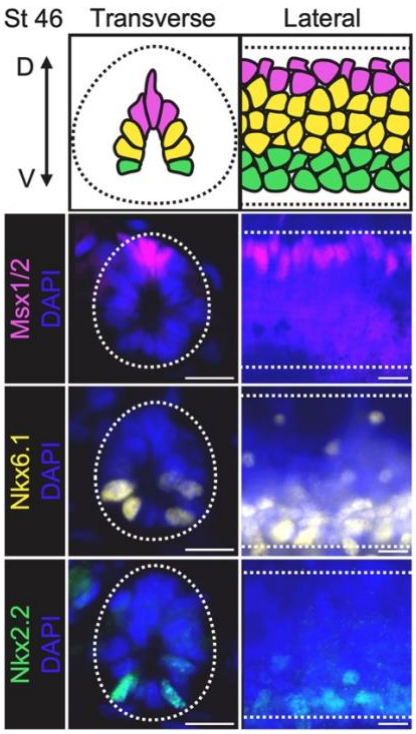

Figure 2.2. Dorsal, intermediate, and ventral NPC domains are visible in the uninjured, regenerative-stage spinal cord. Top, diagram of stage 46 uninjured regenerative-stage spinal cord. Bottom, transverse and lateral images visualizing dorsal markers Msx1 and Msx2 (Msx1/2: 4G1), intermediate marker Nkx6.1 (F44A10), and ventral marker Nkx2.2 (74-5A5). D = Dorsal, V = Ventral, dotted line indicates spinal cord boundary. Scale bars = 10 μm.

2.3.2. Dorsal, intermediate, and ventral NPC domains are present within the regenerating X. tropicalis spinal cord

Having confirmed D/V NPC domains in uninjured tissue, we next asked if this organization is recapitulated in the regenerating spinal cord. It was previously reported that some regenerative animals such as the axolotl do regenerate regionalized D/V domains, but others, like the green anole lizard, only regenerate a ventralized ependymal tube. To determine if these D/V NPC domains are present during *Xenopus* regeneration, we amputated the posterior third of the tail of stage 41 tadpoles, as we have previously (Kakebeen et al. 2020). Tadpoles were allowed to regenerate for 2, 3, or 4 days post amputation (dpa), before they were collected and stained for Msx1/2, Nkx6.1, or Nkx2.2 in transverse section and whole mount preparations (Figure 2.3A).

We found that throughout the surveyed time period, Msx1/2, Nkx6.1, and Nkx2.2 are regionally localized into dorsal, intermediate and ventral domains in the regenerating spinal cord (Figure 2.3B–D). In order to quantify this NPC localization pattern, we measured the position of cells expressing each marker in whole mount images and normalized this position to spinal cord width or length (Figure 2.3E). Localization of Msx1/2+ cells are clearly biased to the dorsal spinal cord, with Nkx6.1+ cells positioned intermediately and Nkx2.2+ cells ventrally. Interestingly, we identified not only a D/V NPC axis, but also A/P regionalization of these markers during regeneration. Specifically, Msx1/2+ cells were more strongly regionalized posteriorly, while Nkx2.2+ cells were more strongly regionalized anteriorly (Figure 2.3E). From these data, our principal conclusion was that the regenerated spinal cord is indeed patterned along the D/V axis, eventually recovering a similar organization to its pre-injury condition. In this regard, the *X. tropicalis* spinal cord more closely resembles that of the axolotl, in which NPCs are also organized dorsal-ventrally, rather than the anole, which is radially ventralized (Sun et al. 2018).

2.3.3. Shh signaling is necessary and sufficient for D/V NPC patterning during regeneration

We next asked what mechanisms help specify NPC positional identity along the D/V axis during the rapid progenitor proliferation and cell movements that accompany regeneration. Here we hoped to discriminate between two possible mechanisms for D/V patterning during regeneration. By one mechanism, D/V domains could be maintained via the simple mechanism of clonal restriction to parental domains. In this model, each newly born NPC would retain the positional identity of its parent, and morphogens such as BMP or Shh would be dispensable for positional identity in the regenerate. Alternatively, regenerating neural progenitors could be multipotent with respect to positional identity, and extrinsic signals such as Shh would be

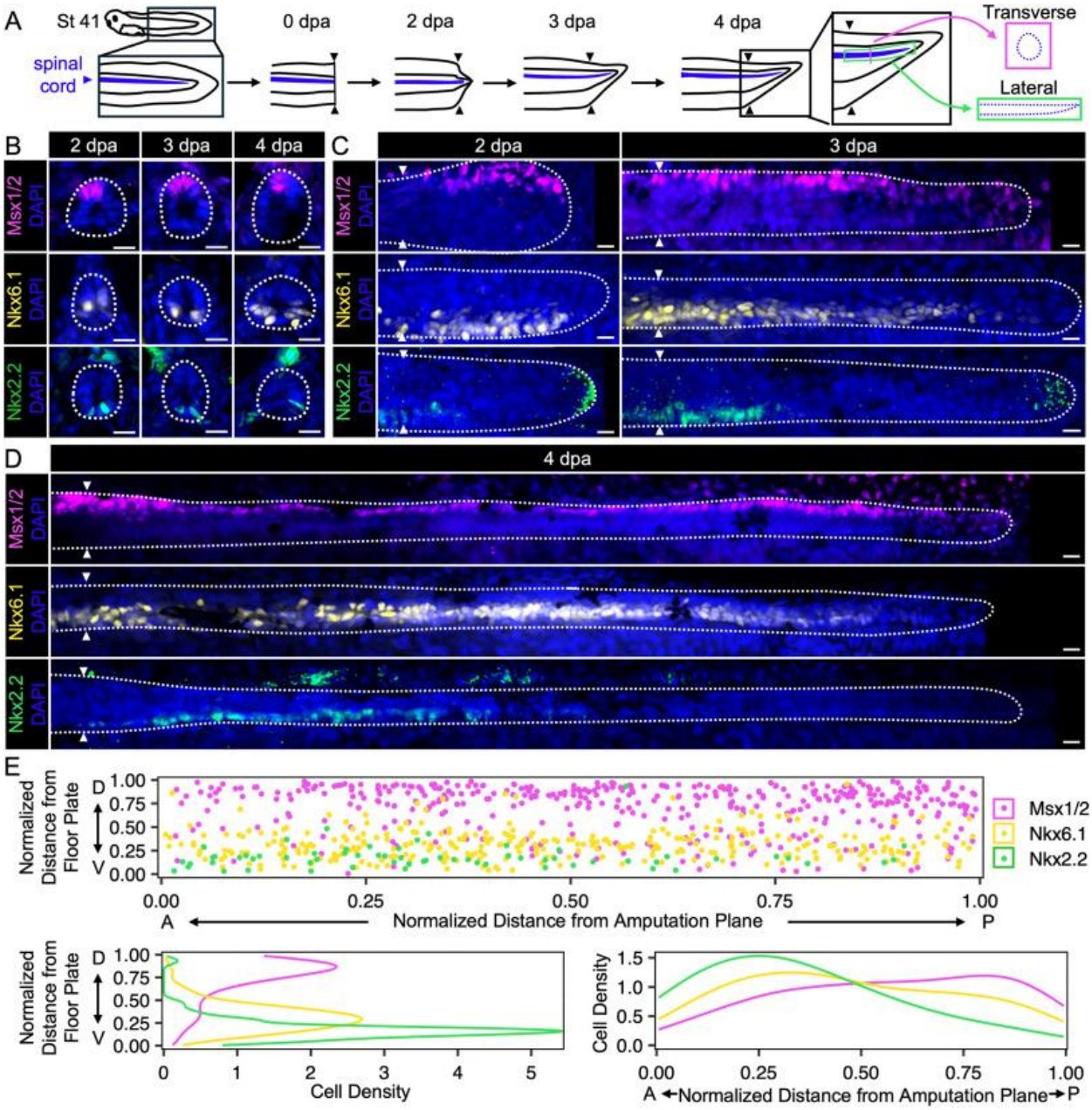

Figure 2.3. Dorsal, intermediate, and ventral NPC domains are present within the regenerating *X. tropicalis* spinal cord. A. Experimental design for sample collection post amputation. B**.** Images of transverse sections visualizing dorsal marker Msx1/2, intermediate marker Nkx6.1 and ventral marker Nkx2.2 at 2, 3, or 4 dpa. C-D. Images of whole mount tadpoles visualizing Msx1/2, Nkx6.1 and Nkx2.2 at 2, 3, or 4 dpa. E**.** Top, scatter plot showing cumulative cells based on their distance from floor plate or amputation planes, normalized to spinal cord width or length. Bottom, smoothed cell density plots illustrating regionalized distribution of D/V markers over the D/V axis and A/P axis, respectively. For all images in this figure, paired triangles represent amputation plane and dotted lines represent spinal cord boundary. n = 17–20 animals per marker. D = Dorsal, V = Ventral. Scale bar = 10 μm.

required to reestablish D/V progenitor domains. Research in axolotls has shown that both mechanisms can be active during regeneration (Schnapp et al. 2005; Mchedlishvili et al. 2007). In *Xenopus*, both Shh and BMP are required for regeneration (Taniguchi et al. 2014; Slack et al. 2004). However, that does not necessarily imply that their D/V patterning functions are specifically required, since both these signals have pleiotropic effects that also include regulation of cell proliferation. In light of the non-canonical functions for Shh during regeneration, the role for Shh in D/V patterning was particularly called into question (Hamilton et al. 2021). Therefore, we set out to directly ask whether perturbation of Shh disrupted D/V patterning in the regenerate.

Before testing whether Shh is essential for the patterning of NPCs during regeneration in *X. tropicalis*, we first asked where and when *shh* is expressed during regeneration. Visualization of *shh* transcripts via in situ hybridization showed continued low expression of *shh* in the stage 41 uninjured tadpole tail. Expression of *shh* is found within the regenerating notochord starting as early as 8 hpa, and expression increases in intensity in the regenerating notochord and spinal cord floor plate starting at 2 dpa (Figure 2.4A). This early expression of *shh* within the regenerating notochord matches with previously reported results in *Xenopus laevis* and zebrafish (Romero et al. 2018; Taniguchi et al. 2014). The expression of *shh* along with floor plate marker *foxa2* (Figure S1) in the spinal cord is notable because previous studies done in *Xenopus laevis* only observed *shh* expression in the notochord, and not the floor plate, during regeneration (Taniguchi et al. 2014). This floor plate expression suggests a possible divergence between the two species. Overall, these results place *shh* expression at the right time and place to have an early effect on the D/V axis, as expected from previous studies in *Xenopus laevis* and other vertebrates.

To test Shh's functional role in shaping the D/V axis during regeneration, we used the

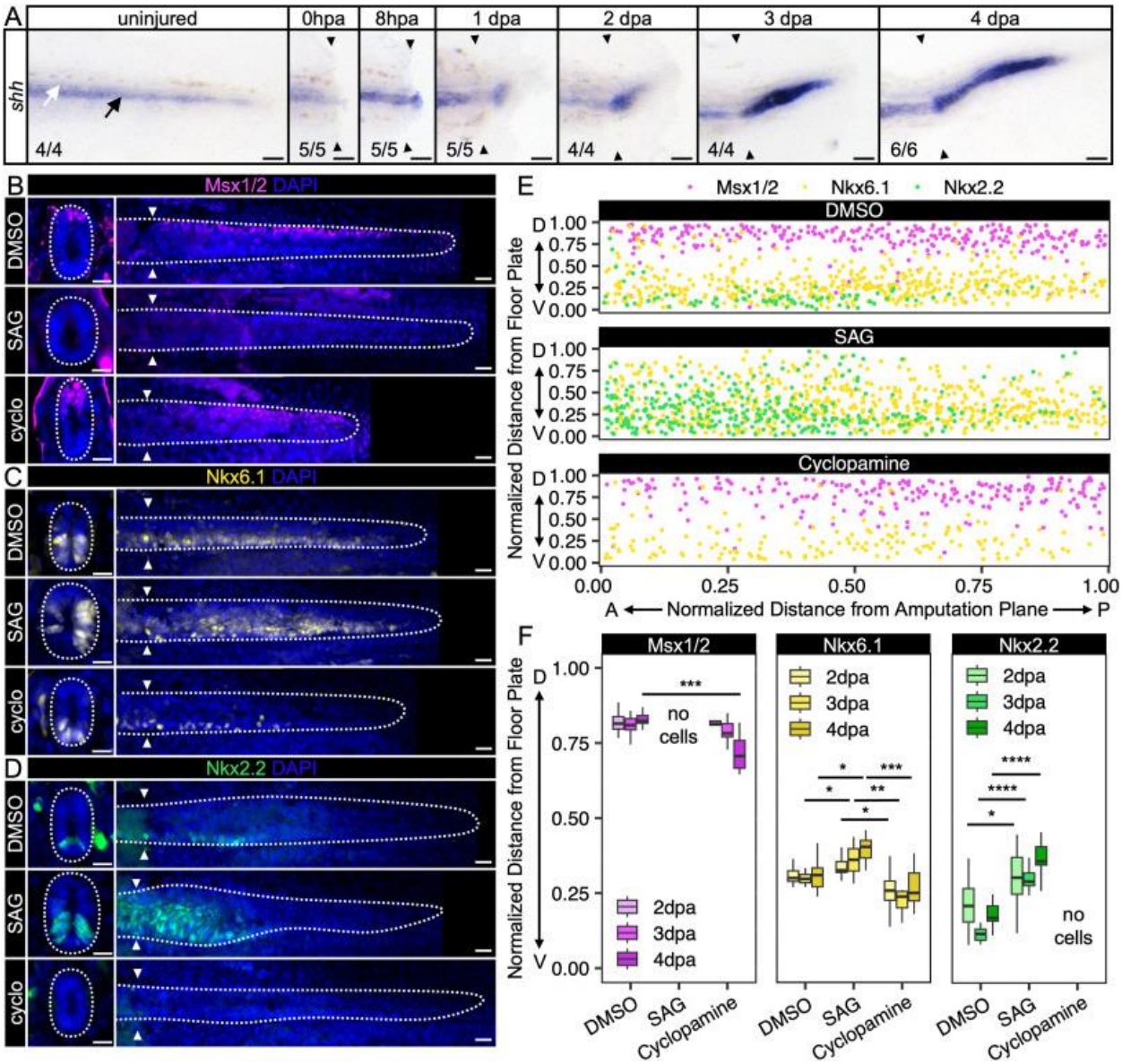

Figure 2.4. Shh signaling is necessary and sufficient for D/V NPC patterning during regeneration. A. Images of in situ hybridization visualizing *shh* expression at 0 h post amputation (hpa), 8 hpa, 1 dpa, 2 dpa, 3 dpa, and 4 dpa. n/n is noted. Scale bar = 100 µm. White arrow indicates spinal cord, black arrow indicates notochord B-D. Images of transverse sections (left) or lateral views (right) of tadpoles treated with DMSO, Shh agonist SAG or Shh inhibitor cyclopamine ("cyclo") for full 3 dpa and stained for Msx1/2 (B), Nkx6.1 (C), Nkx2.2 (D). Scale bar = 10 µm. n = 10–17 animals per condition. E. Scatter plot showing cumulative cells based on their distance from floor plate or amputation planes, normalized to spinal cord width or length after DMSO, SAG, or cyclopamine treatment for 3 dpa. D = Dorsal, V = Ventral. n = 10–17 animals per condition F. Quantification of average normalized distance from floor plate after treatment with DMSO, SAG, or cyclopamine treatment over 2, 3, and 4 dpa. n = 6–17 tadpoles per condition. Significance was determined by one-way ANOVA followed by Tukey's multiple comparisons test or by pairwise two-sample Wilcoxon tests ($*p < 0.05$, $**p < 0.01$, $***p < 0.001$,

∗∗∗∗p < 0.0001). For all images in this figure, dotted white lines represent spinal cord boundary and paired triangles represent amputation plane.

hedgehog pathway inhibitor cyclopamine and agonist SAG to modulate Shh activity. Cyclopamine and SAG have both been used to inhibit Shh signal transduction in *Xenopus* and other vertebrates (Hamilton et al. 2021; Peyrot et al. 2011; Martin et al. 2007; Satoh et al. 2006; Lewis and Krieg 2014). Because high doses of cyclopamine completely prevent spinal cord and tail regeneration, we performed a dose-response curve to identify doses that did not globally impair regeneration of the spinal cord. This assay allowed us to isolate the effect of Shh modulation on spinal cord patterning (Figure S2A–E).

Following treatment with SAG, the dorsal Msx1/2+ domain was lost but the intermediate Nkx6.1+ and ventral Nkx2.2+ domains expanded significantly (Figure 2.4B–F). The opposite result was seen following treatment with cyclopamine: the spinal cord exhibited an expansion of the Msx1/2+ domain, reduction of the Nkx6.1+ domain, and complete absence of the Nkx2.2+ domain. These two complementary results demonstrate that Shh is required for normal repatterning of NPCs after injury, outside of its reported non-canonical mitogenic function in supporting stem cell proliferation. Finally, we visualized *shh* expression after DMSO, cyclopamine, or SAG treatment until 3 dpa. We saw no change in *shh* expression after cyclopamine treatment, but a reduction in expression after SAG compared to DMSO (Figure S2F–H). Our result suggests that activating Shh signaling serves to repress expression of *shh* itself in the tadpole spinal cord, adding nuance to our understanding of hedgehog signaling as a feedback-regulated pathway (Cohen et al. 2015).

2.3.4. Restricted window for sensitivity to shh perturbation post amputation

To determine how the Shh signal response may change over the course of regeneration,

we performed 1 day-restricted treatments of cyclopamine and SAG from 1 to 4 days post amputation and stained for the intermediate marker Nkx6.1 at 4 dpa. We chose Nkx6.1 because of its broad range of expression in lateral views (Figure 2.5A). We observed that treatment with SAG during the initial 1 day period after injury resulted in a significant expansion of the Nkx6.1+ domain. SAG treatment after 1 dpa resulted in expansion of the Nkx6.1 domain, but no significant change in average dorsal-ventral position of cells. Treatment with cyclopamine only resulted in a significant change in the Nkx6.1+ domain when tadpoles were treated during the whole course, 1–2, and 2–3 dpa. Previously, treatment with cyclopamine during regeneration did not significantly affect the average position of the Nkx6.1+ domain, a difference that we ascribe to refreshing the media every 24 h for this experiment but not previously. We attribute the observed lack of sensitivity to cyclopamine treatment within the first day after injury to the return of normal Shh signal transduction levels after removal of cyclopamine from the media. Treatment with either drug had no effect on the position of the Nkx6.1+ domain after 3 days post amputation (Figure 2.5B–S3). From these results we find that the Nkx6.1 expression domain is sensitive to Shh perturbation immediately after injury but loses sensitivity after three days of regeneration.

2.3.5. Regenerating cells have stronger response to shh perturbation compared to uninjured cells

In the absence of injury, *shh* is still weakly expressed in the notochord and floor plate. This observation made us question how much Shh signaling might be contributing to the ongoing maintenance of NPC identity in the uninjured tadpole. To address this question, we asked whether regionalized NPCs changed their domain boundaries when Shh was perturbed in uninjured tadpoles, and we compared this effect with Shh perturbation in anterior spinal cord tissue of injured tadpoles (tissue anterior to the amputation plane) and with Shh perturbation in

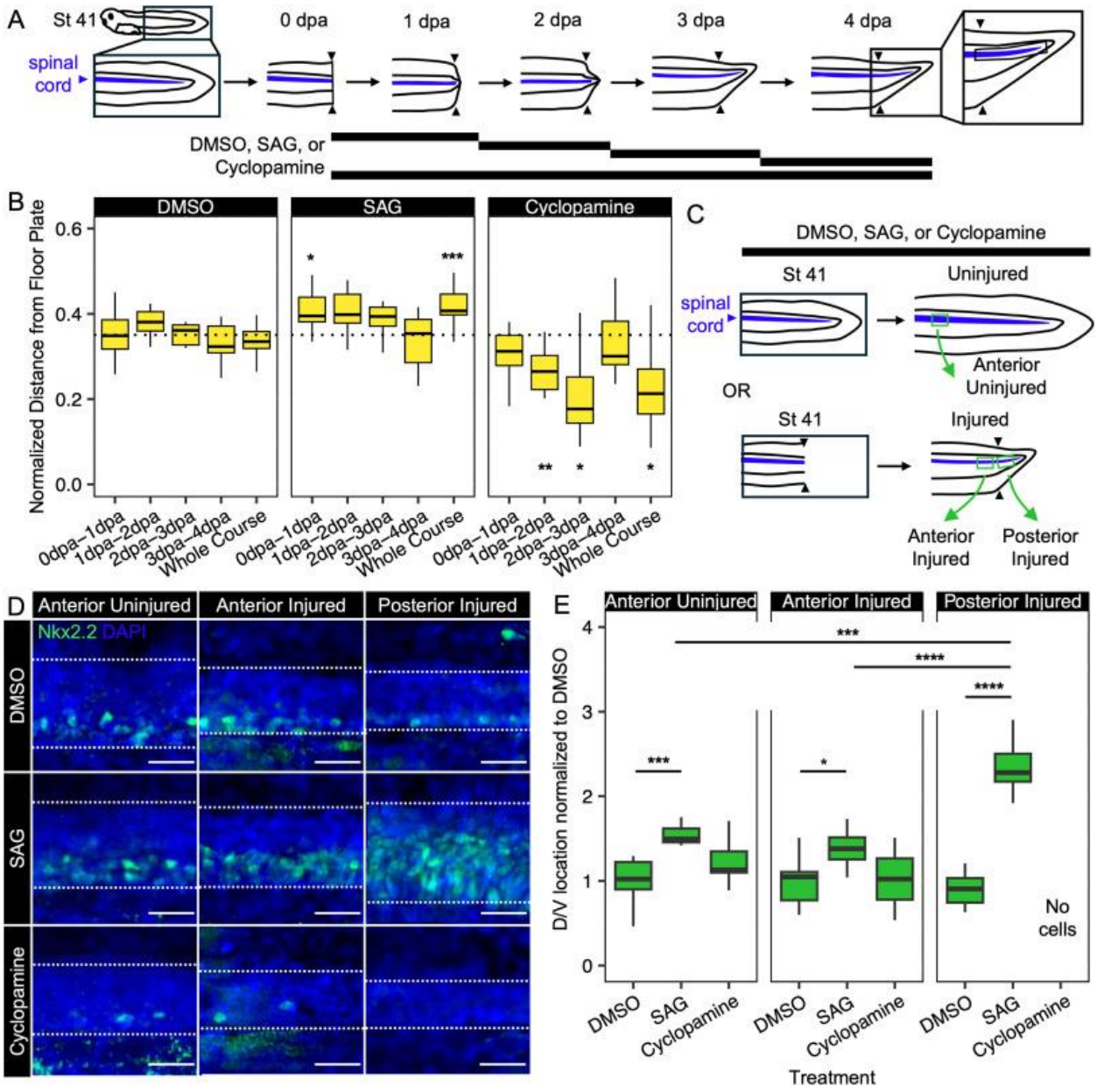

Figure 2.5. Regenerating NPCs are more sensitive to Shh modulation before 3 dpa and compared to uninjured cells. A. Experimental design for DMSO, SAG, or cyclopamine treatment during regenerative timepoints. B. Quantification of average normalized distance of Nkx6.1+ cells from the floor plate after treatment with DMSO, SAG, or cyclopamine during specific regenerative timepoints, where the dotted black line represents average DMSO normalized D/V location across all timepoints. n = 9–15 tadpoles. Significance was determined by one-way ANOVA followed by Tukey's multiple-comparisons test or by pairwise two-sample Wilcoxon tests ($*p < 0.05$, $**p < 0.01$, $***p < 0.001$, $****p < 0.0001$), against comparative DMSO timepoint. C. Experimental design for collection of Anterior Uninjured, Anterior Injured, and Posterior Injured tissue after DMSO, SAG, or Cyclopamine treatment for 3 dpa. D. Images showing lateral views visualizing ventral marker Nkx2.2 within the Anterior Uninjured, Anterior Injured, or Posterior Injured spinal cord after treatment with DMSO, SAG, or cyclopamine.

Dashed white lines represent spinal cord boundary. Scale bar = 10 μm. E. Quantification of (D), with D/V location normalized to DMSO. n = 8–11 tadpoles per condition. Significance was determined by pairwise two-sample Wilcoxon tests (∗p < 0.05, ∗∗p < 0.01, ∗∗∗p < 0.001, ∗∗∗∗p < 0.0001).

regenerating spinal cord tissue (tissue posterior to the amputation plane). Using the same protocol used for the injured tadpoles, we treated uninjured stage 41 tadpoles with SAG or cyclopamine for three days. We then stained for ventral marker Nkx2.2, chosen because of its high sensitivity to Shh perturbation (Figure 2.5C). We found that the Nkx2.2+ domain remains sensitive to Shh perturbation in the anterior tail of uninjured and injured tadpoles during the stages we were investigating. However, when compared with what we see in the regenerating spinal cord, the domain expansion following treatment with SAG was less extensive, and cyclopamine did not completely ablate expression of Nkx2.2 (Figure 2.5D). This result suggests that while NPC identity remains plastic in the spinal cord of uninjured stage 41 tadpoles and can be modulated by perturbation of Shh, regenerating tissue is the most sensitive to Shh perturbation.

2.4. Discussion

Our principal motivation in undertaking this study was to determine whether the D/V axis of the spinal cord is re-established after injury in *X. tropicalis*, and whether perturbation of Shh signaling influenced that axial patterning. Our study confirms that uninjured, regenerative stage *Xenopus tropicalis* tadpoles maintain expression of developmental markers of D/V NPC domains, and it demonstrates that these domains are re-established during regeneration. We also show that D/V patterning is dependent on Shh signaling in a similar manner to embryogenesis, with Shh activating expression of the intermediate and ventral domain transcription factors and inhibiting expression of dorsal markers. In this regard, our results in *X. tropicalis* align with

previous studies done in axolotls (Schnapp et al. 2005). We also demonstrate that regenerating cells show greater sensitivity to Shh perturbations than uninjured cells.

2.4.1. D/V patterning is dependent on Shh signaling during regeneration

There are at least two mechanisms by which dorsal-ventral patterning information could be propagated from preexisting cells to new cells in the regenerating spinal cord. One is that NPCs near the amputation site could acquire a dorsal or ventral identity during development, retain this identity after injury, and undergo mitosis to create progeny with that same positional identity. Alternatively, secreted signals like Shh might be continually required for positional identity in NPCs, and during regeneration these signals would dictate the positional identity of new NPCs, which otherwise would be multipotent. Both mechanisms contribute to axolotl regeneration (Schnapp et al. 2005; Mchedlishvili et al. 2007).

Our data support the second model, as we have shown that Shh patterns regenerating NPCs following tail amputation in *Xenopus tropicalis*. Treatment with the Shh inhibitor cyclopamine leads to a significant reduction in Nkx6.1+ cells and the complete absence of Nkx2.2+ cells, results that match with previous studies showing that high and sustained levels of Shh are necessary for the activation of Nkx2.2 expression (Dessaud et al. 2007). Treatment with SAG conversely leads to an increase in Shh activity, causing expansion of Nkx6.1 and Nkx2.2 into more dorsal positions, and the consequent repression of Msx1/2. Unexpectedly, our data showed not only a D/V axis within the regenerating spinal cord, but also an A/P axis of NPC domains. There are a number of signals that may regulate NPC domains orthogonally to the Shh signal. These possibilities include posteriorizing signals that are well known to act in spinal cord regeneration, such as FGF and Wnt (Lin and Slack 2008). Overall, our study demonstrates that, as in the axolotl and in contrast to the anole, *Xenopus* depends upon extrinsic signals to

reestablish D/V patterning in the spinal cord after injury. Whether the clonal restriction mechanism utilized in the first model is at all utilized in *Xenopus* remains an intriguing question and open in the comparative study of regeneration across vertebrate species.

2.4.2. Species differences in Shh signaling during spinal cord regeneration

The most parsimonious mechanism for the patterning activity we observe would be for Shh to act through Gli-dependent activation of ventral transcription factors and cross-repression of dorsal transcription factors, as thoroughly described in mouse and chick embryogenesis (Lee and Pfaff 2001; Briscoe and Ericson 1999). However, recent work in *Xenopus laevis* suggests that Gli1 and Gli2 are dispensable for regenerative growth of the spinal cord (Sun et al. 2018). There are several lenses through which we believe our results can be resolved with that study, though these require further testing to fully address. The first possibility, which we consider the most likely, is that the signal transduction mechanism of Shh as a mitogen in spinal cord regeneration may be distinct from its transduction as a morphogen. It may therefore be that Shh acts through Gli-independent non-canonical Ca2+ dependent mechanisms to direct growth, while it acts through canonical signaling to establish patterning. We note that the doses of cyclopamine we report here are much lower than those used to repress proliferative growth during regeneration (Sun et al. 2018), and so the sensitivity of each of these pathways to ligand binding may differ. Assessment of spinal cord patterning under Gli-inhibited conditions in *X. laevis* would clarify whether this explanation is most likely. Alternatively, it is plausible that there are species-specific mechanisms in *X. tropicalis* and *X. laevis*, with the latter relying less on canonical Shh signaling than the former. We note that the localization of *shh* transcripts does seem to vary between these species, as discussed below. Another question for further study is how the perturbation of NPC positional identity by Shh is propagated to post-mitotic neurons and

ultimately impacts spinal cord function. Future work will interrogate the composition and organization of post-mitotic neurons in the regenerating spinal cord, as well as the effects of Shh perturbation on motor function.

The source of Shh signal has intriguing differences among regenerative amphibians. During development, both the notochord and the floor plate express *shh* and participate in patterning. However, the axolotl does not regenerate its notochord, leaving the floor plate as the sole source of Shh during regeneration (Schnapp et al. 2005). In contrast, *Xenopus laevis* regenerates the notochord, but it is unclear whether it regenerates the floor plate, as *in situ* hybridization shows no expression of *shh* in the regenerating spinal cord (Taniguchi et al. 2014; Sugiura et al. 2004), but scRNAseq data show a *shh*+/*foxa2*+ neural cluster in the regenerate (Aztekin et al. 2019). Here we show that in *Xenopus tropicalis*, a morphologically distinct *shh*-expressing floor plate and notochord are each regenerated, with expression of *shh* detected in each by *in situ* hybridization. As both structures express *shh*, both may contribute as sources of secreted Shh that influence positional identity in the neighboring NPCs of the spinal cord.

2.4.3. The NPC response to Shh shifts following injury

During development of the non-regenerative mouse and chick, spinal cord maturation is accompanied by a rapid decrease in the number of NPCs lining the central canal. During this time, the Shh signal that was integral to the initial patterning of the neural tube also diminishes, until it finally appears to vanish in the postnatal spinal cord (Cañizares et al. 2020; Fu et al. 2003). Expression of dorsal-ventral patterning genes is also significantly altered in the mature spinal cord, as expression of Nkx2.2 as well as dorsal markers diminish, and the entire ependyma becomes Nkx6.1+ (Fu et al. 2003; Rodrigo Albors et al. 2023). In contrast to these observations in non-regenerative amniotes, adult axolotls retain expression of Shh in the floor plate (Schnapp

et al. 2005; Sun et al. 2018). We find that *Xenopus tropicalis* tadpoles, like axolotls, maintain embryonic patterning factors in the spinal cord in regenerative-stage tadpoles. The maintenance of progenitor domains may be related to the fact that anamniotes like *Xenopus*, axolotls, and zebrafish must undergo a second round of neurogenesis during their larval stages to generate adult neuronal types (Wullimann et al. 2005).

We demonstrate that Shh continues to be expressed in the notochord and floor plate up until tadpole stages, and that Nkx2.2+, Nkx6.1+, and Msx1/2+ domains retain their embryonic positions through these stages as well. We also present evidence that the anterior tissue in both uninjured and injured tadpoles remains sensitive to Shh activation or inhibition, with greater sensitivity in regenerating NPCs. Sensitivity to Shh perturbation subsequently declines until 3 dpa, after which there is no change to the positioning of the Nkx6.1 domain in response to cyclopamine or SAG treatment. This decline could represent the progenitors reaching a more mature state and corresponds roughly with the onset of neurogenesis in the anterior regenerate. Both the ongoing sensitivity of NPC domains to Shh perturbation and the continued expression of Shh past its initial role in dorsal-ventral patterning have interesting implications for the role in cell fate plasticity of the *X. tropicalis* spinal cord. *Xenopus* are notable in that regenerative competence declines with age, and so one aspect of regenerative competence may be tied to the ability of regenerative NPCs to respond to Shh. Future work will interrogate the plasticity of NPC fate in non-regenerative stages.

2.5. Methods

2.5.1. Xenopus tropicalis amputation assay

NF stage 41 tadpoles were anesthetized with 0.05% MS-222 in 1/9x MR and tested for response

to touch prior to amputation surgery. Once fully anesthetized, a sterilized scalpel was used to amputate the posterior third of the tail. Amputated tadpoles were removed from anesthetic media within 10 min of amputation into new 1/9x MR. Tadpoles were kept at a density of no more than 2.5 tadpoles per mL. Tadpoles were fixed for 1 h in 1x MEM with 3.7% formaldehyde at room temperature at 2 dpa (days post amputation), 3 dpa, or 4 dpa.

2.5.2. Immunohistochemistry

For whole mount immunohistochemistry, fixed tadpoles were permeabilized by washing 3 × 15 min in PBS +0.01% Triton X-100 (PBT) with the exception of tadpoles stained for Nkx2.2, which were washed with 0.05% Triton X-100 for the entire protocol. Tadpoles were blocked for 1 h at room temperature in 10% CAS-block (Invitrogen #00–8120) in PBT, with the exception of tadpoles stained for Msx1/2, which were incubated at 4 °C overnight in 10% CAS-block. Then, tadpoles were incubated in primary antibody [1:10 mouse Msx1/2 (4G1, DSHB); 1:10 mouse Nkx2.2 (74.5A5, DSHB); 1:50 mouse Nkx6.1 (F55A10, DSHB)] diluted in 100% CAS-block overnight at 4 °C. Tadpoles were then washed 3 × 10 min at room temperature in PBT and blocked for 30 min in 10% CAS-block in PBT. Secondary antibody (goat anti-mouse 594, ThermoFisher A11032) was diluted 1:500 in 100% CAS-block and incubated for 2 h at room temperature. Tadpoles were then washed 3 × 10 min in PBT followed by a 10-min incubation in 1:2000 DAPI (Sigma D9542) before being washed with 1xPBS for 10 more minutes. Isolated tails were mounted on slides in ProLong Diamond (ThermoFisher P36961). For cryosectioned immunohistochemistry, fixed tadpoles were washed with 3 × 15 min with 1X PBS, 1 × 15 min 15% sucrose with 1X PBS, then overnight at 4 °C. Tadpoles were then transferred into OCT (Thermofisher 23-750-571) and kept at −80 °C until sectioning with a Leica CM3050 S Cryostat. Immunohistochemistry proceeded as described above. Images were acquired using a Leica DM

5500 B microscope using a 20X or 40X objective and processed using FIJI image analysis software. 3–8 transverse sections were imaged per marker from a single animal, with 4–10 animals processed per condition.

2.5.3. Whole mount in situ *hybridization*

Embryos and tadpoles were fixed overnight in 1x MEM with 3.7% formaldehyde at 4 °C. *Xenopus tropicalis* multibasket in situ hybridization protocols were followed as described (Khokha et al. 2002), with the notable change that pre-hybridization was always performed overnight. Isolated tails were mounted on slides in ProLong Diamond (ThermoFisher P36961) and imaged on a Leica M205 FA with a color camera. For cross-sections, tadpoles were stained and then cryosectioned as described above. Probes were synthesized using the following primer pairs designed against a single exon of each mRNA: *shh* (forward – gctttctacacctgccttgc, reverse – taatacgactcactatagggtgagtcatgagtcggtctgc), *foxa2* (forward – aactgcagcagctttggaa, reverse – taatacgactcactatagggcccgtttaagagtaagaactgagg. RefSeq annotation derived from Xenbase (http://www.xenbase.org/, RRID:SCR_003280) (Fisher et al. 2023) genome v10.0.

2.5.4. Pharmacological inhibition

Cyclopamine (Cayman Chemical, 11321) was resuspended to a 10 mM stock in DMSO, and SAG (GLPBio, GC50135) to a 5 mM stock in DMSO. Uninjured and injured tadpoles were reared with 0.01% DMSO, 500 nM SAG or 1 μM cyclopamine diluted in 1/9x MR until collection at 2 dpa, 3 dpa, or 4 dpa following treatment. Other concentrations were used in establishing doses and are reported in Figure 2.S2.

2.5.5. Quantification and statistical analysis

Whole mount immunostained tail images were processed in Fiji (Schindelin et al. 2012) and the regenerate spinal cord was isolated using the Straighten tool. Segmentation, counting and measurements of Nkx6.1+/Nkx2.2+/Msx + cells were done using the Fiji Analyze Particles tool. Dorsal/Ventral position after DMSO, cyclopamine, or SAG treatment were compared using one-way ANOVA followed by Tukey's multiple-comparisons test or pairwise Wilcoxon two-sample tests depending on normality of data. The Shapiro-Wilk test was used to assess normality. N (number of animals) is reported for regeneration experiments on graphs. The data for each marker consists of at least two independent experiments. Information regarding statistics can be found in the figure legend or on the figure panel with the data. Boxplots and stacked bar plots were generated using the R package ggplot2 (Wickham 2016).

2.6. Acknowledgements

We thank members of the Wills lab for critical comments during the preparation of this manuscript and support in frog husbandry. We thank Laura Borodinsky and Andrew Hamilton for feedback on a preliminary paper draft. We thank the Tom Reh and Jennifer Kong labs at UW for access and training on their cryostats. We thank Jennifer Kong for consultation about the use of SAG. We thank Xenbase (http://www.xenbase.org/, RRID:SCR_003280) for curation of genomic and literature information, and the National *Xenopus* Resource for frogs. AAS was supported by the Cellular and Molecular Biology Training Grant NRSA 5T32GM136534-02 from NIGMS. SBP was supported by a Mary Gates Research Scholarship. This work was supported by NINDS R01NS099124 to AEW.

2.7. Supplemental Figures

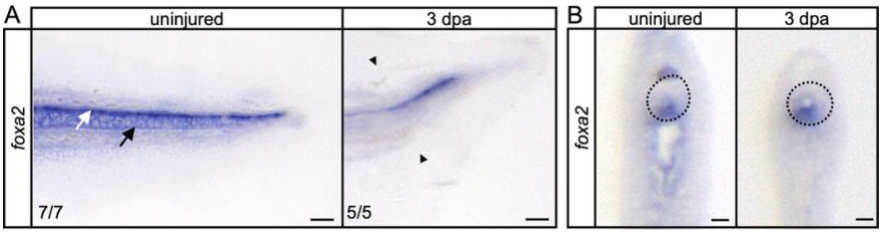

Figure 2.S1. *foxa2* is present within the regenerating spinal cord floor plate. Images of *in situ* hybridization visualizing *foxa2* expression at uninjured and 3 dpa in lateral view (A) and transverse (B). A. White arrow indicates spinal cord floor plate, black arrow indicates notochord. Scale bar = 100 μm. Paired triangles represent amputation plane. n/n is noted. B. Dotted line represents spinal cord border. Scale bar = 10 μm.

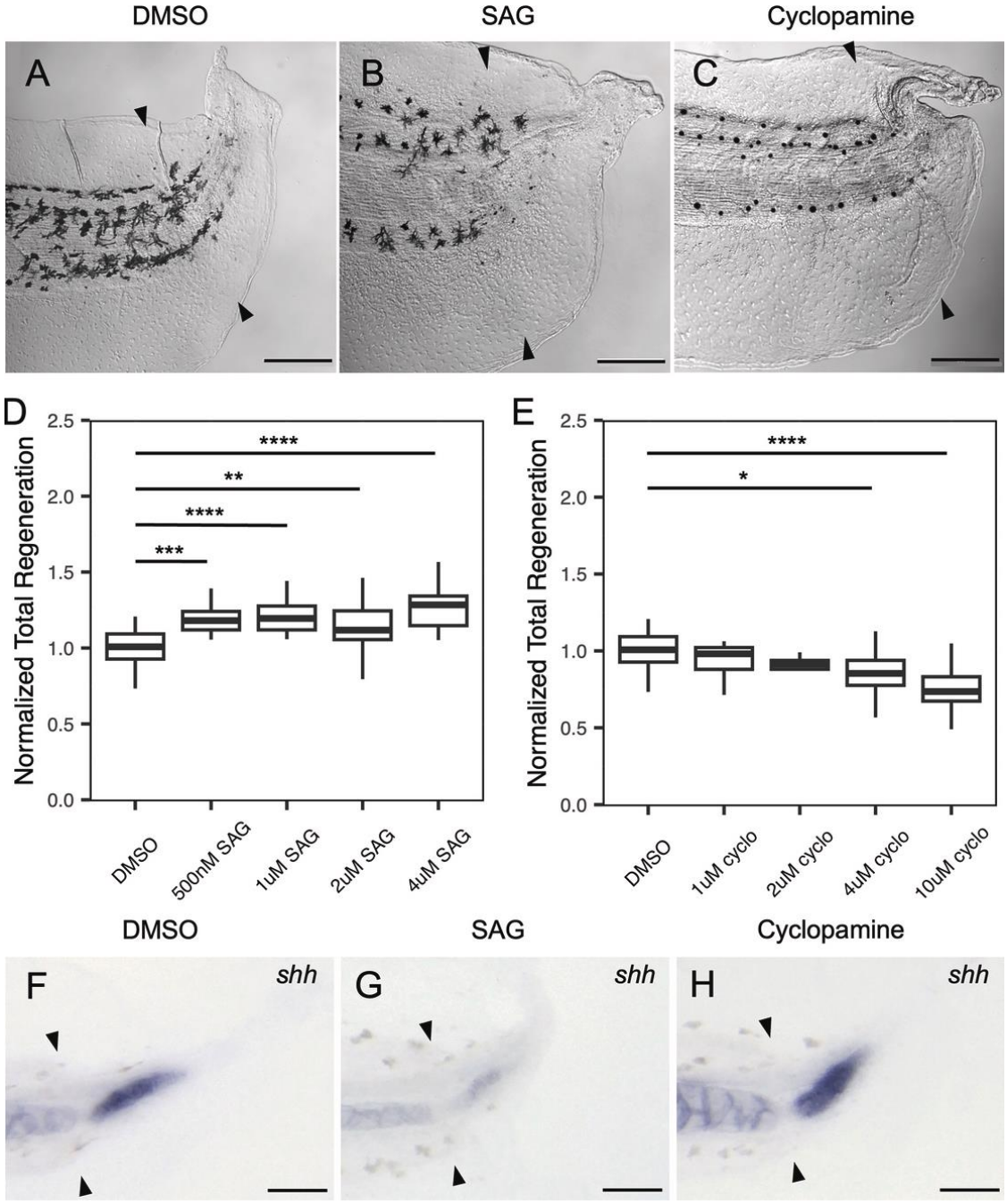

Figure 2.S2. Shh perturbation alters total regeneration. (A-C) DIC images of 3 dpa regenerated tails following treatment with (A) DMSO (B) 4 µM SAG (C) 10 µM cyclopamine. Scale bar = 200 µm. (D-E) Dose curves with total regeneration at 3 dpa normalized to DMSO treated group within respective clutch for (D) SAG and (E) cyclopamine. Significance was determined by one-way ANOVA followed by Tukey's multiple comparisons test ($*p < 0.05$, $**p < 0.01$, $***p < 0.0001$). (F-H) Images of *in situ* hybridization visualizing *shh* expression following treatment with (F) DMSO (G) 4 µM SAG (H) 10 µM cyclopamine. Scale bar = 100 µm. Paired triangles represent amputation plane.

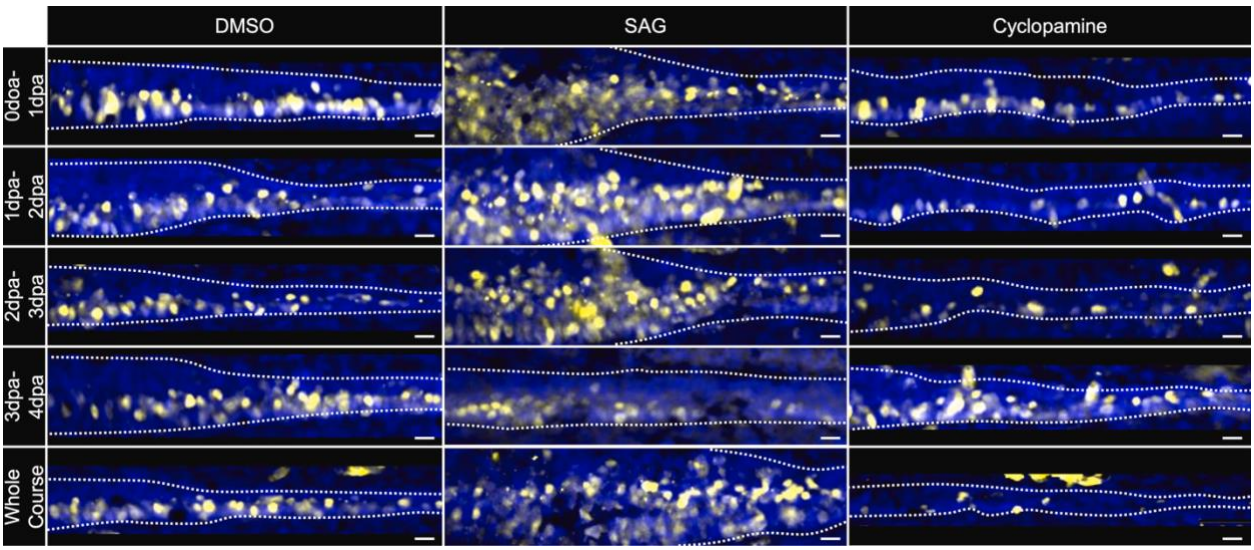

Figure 2.S3. Regenerating NPCs are more sensitive to Shh modulation before 3 dpa. Images of Nkx6.1+ cells after treatment with DMSO, SAG, or cyclopamine during specific regenerative timepoints. Dotted white lines represent spinal cord boundary. Scale bar = 10 μm.

Chapter 3. SPINAL CORD REGENERATION DEPLOYS CELL-TYPE SPECIFIC DEVELOPMENTAL AND NON-DEVELOPMENTAL STRATEGIES TO RESTORE NEURON DIVERSITY

Chapter 3 is adapted with minimal modification from:

Angell Swearer, A., Perkowski, S, Husain, I., Figueiredo, T., McCartney, M., and Wills, A. Spinal cord regeneration deploys cell-type specific developmental and non-developmental strategies to restore neuron diversity. Submitted to Nature Communications November 3, 2025, In Review.

I completed the conceptual design, troubleshooting, experiments, and primary writing for this work. SP designed and completed the BrdU experiments and aided in the scRNAseq analysis and writing. IH and TF designed and helped with the Dendra2 experiments. MM designed and completed the TH+ antibody control. AW led the design and writing for this work.

3.1. Abstract

A major goal of spinal cord injury research is to develop a path to endogenous regeneration. This approach has been heavily informed by animal models of natural regeneration. An unresolved question is whether these models rebuild the spinal cord by exclusively accessing developmental mechanisms of neuron differentiation. To address this question, we contrasted single-cell gene expression during regeneration with stage-matched controls in the conditionally regenerative frog *Xenopus tropicalis*. We generated an expanded atlas of neuronal diversity, annotating several neurons in *Xenopus* for the first time. From this atlas, we found that the neuron composition of the developing and regenerating spinal cord differ. So do the strategies employed, which favor waves of cell-type specific neural plasticity, proliferation, and proliferative neurogenesis during regeneration. Low levels of early neurogenesis are then compensated by movement of post-mitotic neurons. Our work highlights the use of distinct developmental versus regenerative paths to heal post-injury.

3.2. Introduction

Spinal cord injury can cause a permanent and devastating impact to quality of life (NINDS 2019). Naturally occurring models of vertebrate spinal cord regeneration represent the gold standard for understanding how functionality can be restored after major injury. Such models include zebrafish (Cigliola et al. 2020), urodeles (Tazaki et al. 2017), *Xenopus* frogs (Edwards-Faret et al. 2017), lizards (Sun et al. 2018), and more recently, the spiny mouse *Acomys* (Nogueira-Rodrigues et al. 2022). These studies in animal models are complemented by bioengineering efforts that leverage implanted devices or substrates to encourage neural plasticity or neurogenesis, and by stem cell therapeutic efforts focused on either promoting endogenous repair or exogenous transplantation of neural cell types (Clifford et al. 2023; Hu et al. 2023; Yu et al. 2023). All these approaches are heavily informed by our understanding of neurogenesis as it occurs during embryogenesis, where the mechanisms that give rise to spatially distinct neuron domains have been elucidated in beautiful molecular detail.

During embryogenesis, the vertebrate spinal cord is elegantly patterned into distinct neuronal domains from regionally restricted neural progenitor cell (NPC) populations (Leung and Shimeld 2019). Neurogenesis progresses through development in waves, dependent on windows of progenitor specification and differentiation. The spinal cord is thus made up of neurons generated either through primary neurogenesis during neurula stages or ongoing secondary neurogenesis (Henningfeld et al. 2007; Hartenstein 1989). The early spinal cord includes major neuron types such as dorsal primary Rohon-Beard sensory neurons (RBNs) (Bixby and Spitzer 1982), various primary and secondary interneurons (INs), ventrolateral motor neurons (MNs), and ventral secondary Kolmer-Agduhr interneurons (KAs, or cerebrospinal fluid-contacting neurons (CSF-cNs) in mammals) (Dale et al. 1987b; 1987a) (reviewed in

Xenopus in Roberts 2000; Roberts et al. 2012; Roberts and Clarke 1982). In addition, specific cardinal IN types (dI1-6, V0-3) have been documented in zebrafish and mice but have largely not been characterized in *Xenopus* frogs. Overall, the presence and positioning of these neuron types is crucial to forming a complete neural circuit that allows larvae to respond to sensory stimuli via motor movement. The transcriptional regulation of NPC organization and differentiation into INs, KAs, and MNs is highly conserved across vertebrates, although RBNs are only found in fish and larval amphibians and they degenerate during later development to make way for the dorsal root ganglia (Yajima et al. 2014). Despite the plethora of research describing these neurons during development and homeostasis, little is known about how—and if—each of these neuron types regenerate.

Studies of spinal cord regeneration across animal models have made clear two considerations about development and regeneration. First is that the path to regeneration varies by species, both with respect to the completeness of spinal cord regeneration and with respect to how developmental signals are redeployed. An excellent example is the role of Sonic hedgehog (Shh) signaling, which is an indispensable regulator of dorsal versus ventral cell fate in the developing spinal cord (Ulloa and Martí 2010). While anole lizards fail to regenerate dorsal NPC domains due to ubiquitous *shh* expression (Sun et al. 2018), axolotls (Arbanas et al. 2024; Schnapp et al. 2005) and *Xenopus tropicalis* (Angell Swearer, Perkowski, et al. 2025) reactivate Shh signaling in ventral tissues to recapitulate dorsal/ventral patterning post-injury, although *Xenopus* expresses *shh* in the ventral floor plate and notochord and axolotls express *shh* only in the floor plate in a divergence from developmental patterning. Thus, the degree of functional regeneration and extent of developmental recapitulation vary by species, even among regeneratively competent models. The second consideration is that spinal cord regeneration can

employ neurogenic mechanisms that differ from developmental neurogenesis. Examples include dedifferentiation of radial glia into neural progenitors, a process that has been well documented in zebrafish and axolotls (Echeverri and Tanaka 2002; Kroehne et al. 2011); movement of differentiated neurons (Zhang et al. 2003); and generation of regeneration-specific, injury-induced neurons (iNeurons) in zebrafish (Saraswathy et al. 2024). These studies have demonstrated that many processes can contribute to neural regeneration, but the picture of how these mechanisms underlie the repopulation of diverse neuron types is incomplete.

Most animal studies leverage adult spinal cord transection as their injury model, leaving a gap in our understanding of how complete regeneration compares to development. *Xenopus* frogs are a unique model in that they are regenerative during larval stages but lose the ability to undergo spinal cord regeneration during metamorphosis (Beck et al. 2009), suggesting that their regenerative competence at tadpole stages is tied to their access to ongoing developmental mechanisms. *Xenopus tropicalis* is therefore an ideal model in which to compare developmental and regenerative neuron repopulation. Here we used scRNA-seq to establish a molecular atlas of neuron types in the tadpole, then defined how the neuronal cell composition of the spinal cord changes during early, intermediate, and late phases of regeneration. We specifically contrasted the cell composition and organization of the post-injury spinal cord as regeneration progresses with that of the stage-matched developing spinal cord. We then delved more deeply into how the many neurogenic mechanisms that have been described in regeneration are employed by distinct neuronal cell types, using HCR and lineage tracing to elucidate distinct roles of proliferative neurogenesis and post-mitotic neuron movement.

3.3. Results

3.3.1. scRNA-seq shows dynamic changes in cell type abundance over developmental and regenerative time

Our principal goal was to catalog changes in neural cell type composition in the spinal cord during tail regeneration and compare these differences with changes over a corresponding developmental timeline. To this end, we performed single-cell RNA sequencing on injured and stage-matched uninjured tail tissue from 0 to 7 days post amputation (dpa), beginning at stage 41 (3 days post fertilization) (Nieuwkoop et al. 1994). By 7 dpa, tail length in injured tadpoles matched uninjured peers and we considered regeneration complete (Figure 3.S1A, B). To enrich for neural cells we used the transgenic line *Xtr.Tg*(*pax6*:GFP;*cryga*:RFP;*actc1*:RFP), which broadly marks NPCs with GFP in *X. tropicalis* (Kakebeen et al. 2020). At stage 41, we amputated tadpoles and collected the posterior third of the tail as our "tail tip" sample and ~100 microns of tissue proximal to the amputation plane as our "mid-trunk" sample to control for anterior/posterior differences in cell composition (Figure 3.1A). We then split tadpoles into uninjured and regenerating groups and collected tail tissue from both groups at 1 dpa, 3 dpa, and 7 dpa to represent early, intermediate, and late spinal cord regeneration, respectively (Figure 3.1A). Permissive FACS gating conditions were used to enrich for high-expressing *pax6*:GFP+ cells (such as NPCs) as well as low-expressing *pax6*:GFP+ (such as differentiated neurons) and some *pax6*:GFP- cells, allowing us to populate non-neural and non-*pax6* clusters. After quality control filtering, a total of 20,450 uninjured and 15,402 regenerating cells were included for downstream

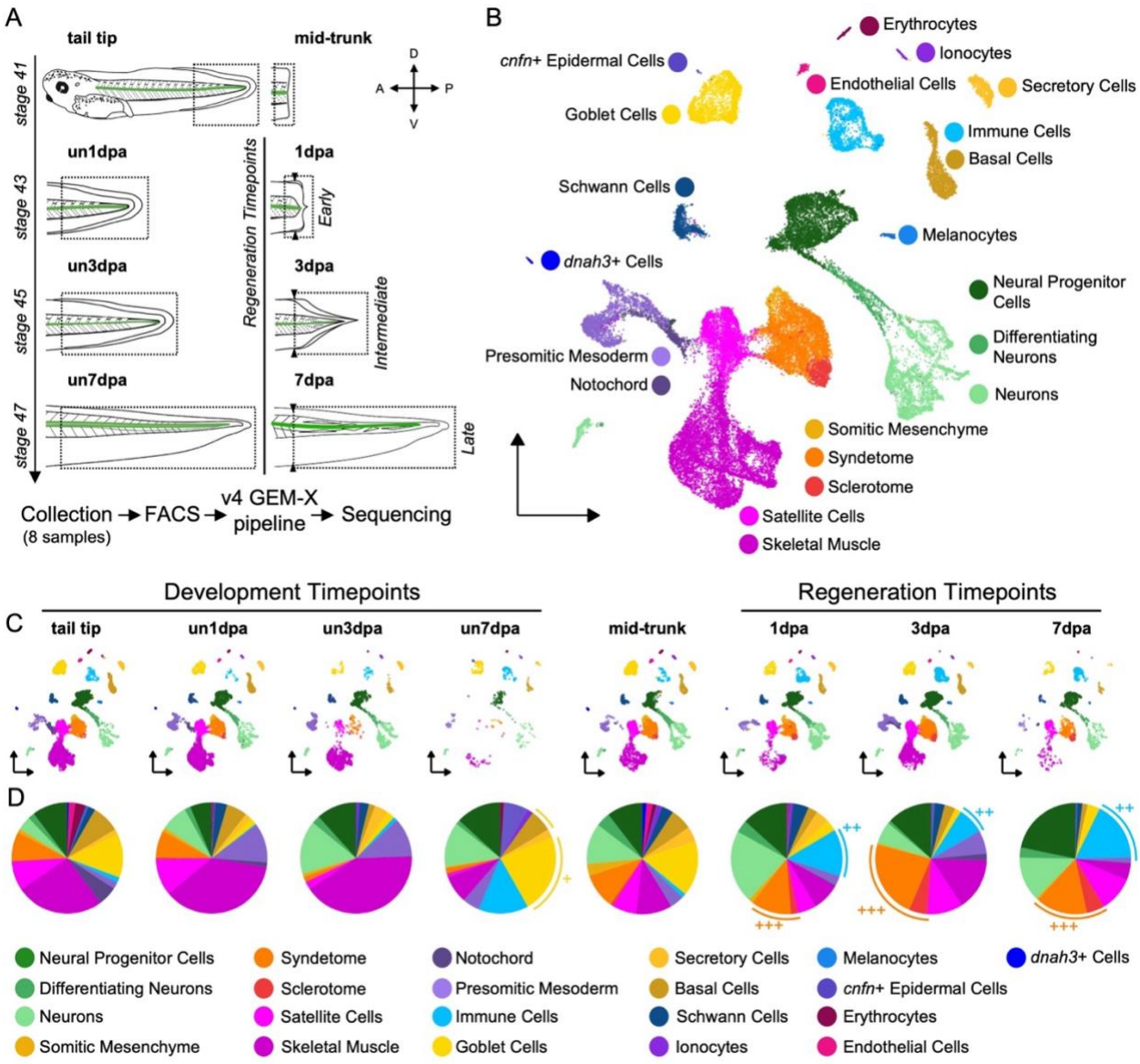

Figure 3.1. Single-cell RNA sequencing reveals dynamic changes in non-neural cell populations during development and regeneration. A) Experimental design of single-cell RNA sequencing experiment, starting with the tail tip (stage 41, posterior third of the tail) and mid-trunk (100 µm proximal tissue to amputation plane) before following up with developmental uninjured (un) or amputated samples at 1, 3, or 7 days post amputation (dpa). Samples were collected and sorted via FACS before processing and sequencing. B) UMAP of 35,852 cells grouped into 21 neural and non-neural cell clusters. C) UMAP of each timepoint, including developmental and regenerating samples. D) Pie chart showing the cluster makeup of each sample. $^{+}$denotes expanded goblet cells and basal cells in development, $^{++}$denotes expanded immune cells in regeneration, and $^{+++}$denotes expanded syndetome and sclerotome in regeneration.

analysis with Seurat (Figure 3.S1C) (Butler et al. 2018; Hao et al. 2021; Satija et al. 2015; Stuart et al. 2019). After dataset integration and UMAP dimensional reduction we identified clusters, to which we assigned unique cell type labels based on previous scRNA-seq analyses in *Xenopus* and other relevant developmental markers (Figure 3.1B, Figure 3.S2) (Aztekin et al. 2019; Segerdell et al. 2013).

We first examined global trends in cell type composition as tail development and regeneration progressed. Many of the patterns we observe for days 1-3 were similar to those observed in *X. laevis* (Aztekin et al. 2019). While the overall cell type composition of tail tips and mid-trunk tissue was similar, we noted several striking changes in cell type abundance between the stage-matched developmental and regenerating timepoints by 7 dpa (Figure 3.1C). Examples include the expansion of goblet cells and basal cells in development but not regeneration (Figure 3.1D+), and the relative enrichment of immune cells (Figure 3.1D++) and immature connective tissue types like sclerotome and syndetome (Figure 3.1D+++) in regeneration.

3.3.2. An expanded atlas of Xenopus *neuron types based on conserved marker genes*

For the remainder of our study, we focused on changes in neural cell types. To interrogate spinal cord regeneration, we selected 7,337 neural cells (3,708 uninjured cells and 3,629 regenerating cells). We then set out to use molecular markers to better define a molecular atlas of neuron types. Previous designations of larval neuron types in *Xenopus* have relied on their morphology and neurotransmitter reactivity. These approaches have enabled the identification of dorsal Rohon Beard Neurons (RBNs) (Bixby and Spitzer 1982), intermediate excitatory and inhibitory Interneurons (INs), ventrolateral motor neurons (MNs), and ventral cerebrospinal fluid contacting Kolmer-Agduhr interneurons (KAs) (Dale et al. 1987b; 1987a) (Figure 3.2A,

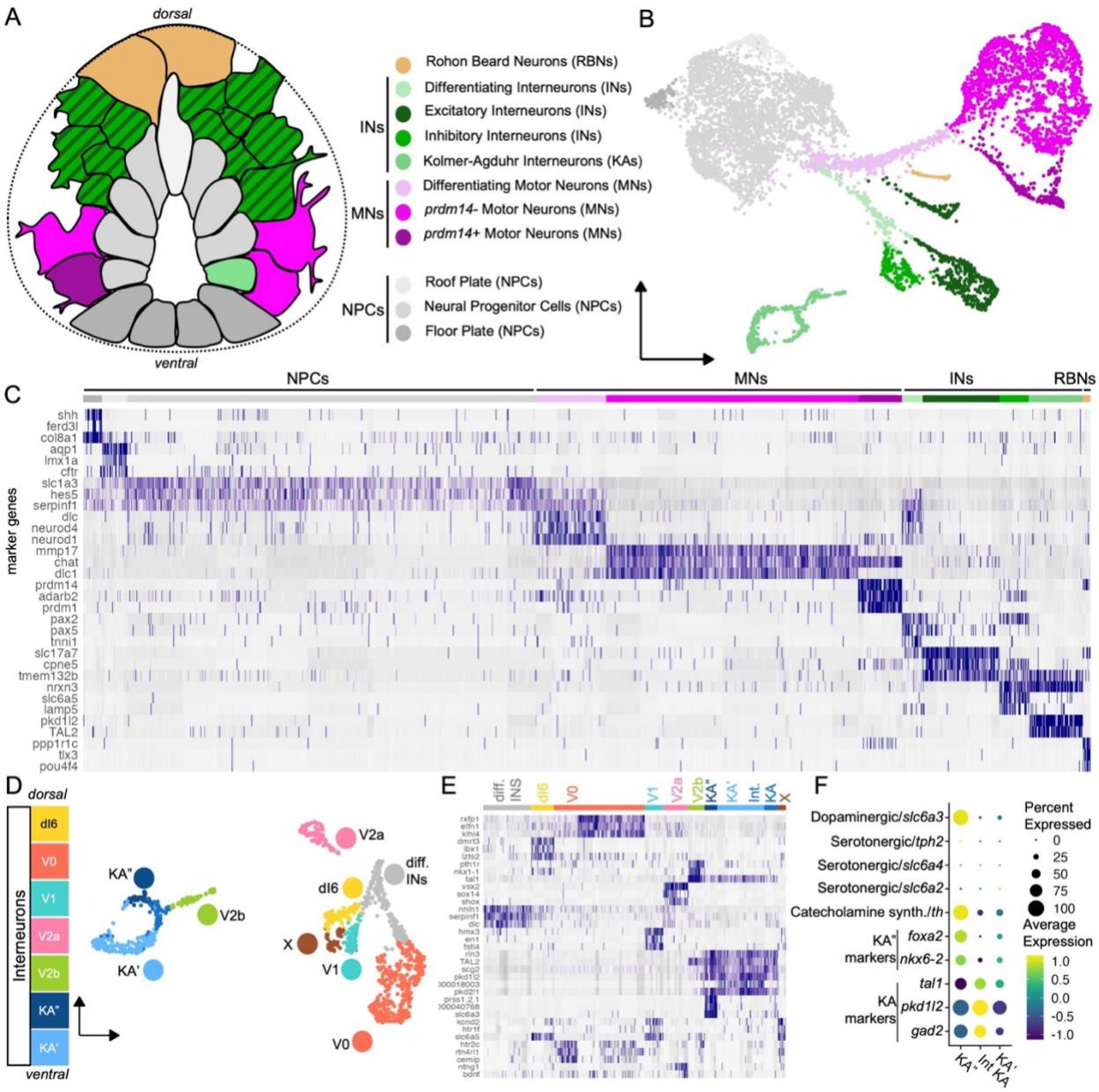

Figure 3.2. Conserved markers identify distinct major and cardinal neurons in the *Xenopus tropicalis* spinal cord. A) Cross-section diagram showing the relative position of major spinal cord cell types in a stage 41 tadpole. B) UMAP of the merged neural subset showing major NPC and neuron cell types. C) Top 3 markers of each cell cluster. D) UMAP and legend of subset cardinal interneuron types in dorsal/ventral order. In addition to differentiating interneurons (diff. INs) Interneuron populations include KA' and KA" clusters, a cluster corresponding to V2b inhibitory interneurons (Ventral Longitudinal Descending or VeLD in zebrafish), a cluster corresponding to V2a Excitatory interneurons (Circumferential Descending (CiD) interneurons in zebrafish), a cluster corresponding to V1 inhibitory interneurons (Circumferential Ascending (CiA) interneurons in zebrafish), a cluster corresponding to V0v excitatory interneurons (Multipolar Commissural Descending and Unipolar Commissural Descending or MCoD/UCoD in zebrafish), and a cluster corresponding to inhibitory dI6 interneurons (Commissural Local or

CoLo in zebrafish). These types were determined by (E) the top 3 gene markers of each interneuron type and marker genes (Table S1). X denotes unidentifiable glycinergic interneuron groups. F) Dot plot showing gene expression between KA", intermediate Interneuron (Int KA), and KA' interneuron groups.

reviewed in Roberts 2000; Roberts et al. 2012; Roberts and Clarke 1982). Three subtypes of interneurons have subsequently been identified based on their expression of *vsx2*, *engrailed1*, or *evx1* (Dale et al. 1987b; Juárez-Morales et al. 2017; Li et al. 2004; Dale et al. 1987a). In our analysis, we first mapped clusters back to *Xenopus* neuron types based on known neurotransmitter types and markers, where available (Figure 3.2B). We then used unique patterns of gene expression from zebrafish and mouse to assign identities to neuron classes that had not previously been molecularly classified (Figure 3.2A-C, Table 3.S1).

Through this combined approach of validation and conservation, we identified RBNs as well as several types of both known and new MNs, INs, and KAs in our merged dataset. We found two main subtypes of MNs in our dataset: a *prdm14*+, *adarb2*+, *prdm1*+ cluster, and *prdm14*-, *dlc1*+, *mmp17*+ cluster (Figure 3.2C). *prdm14* is thought to play a role in primary MN differentiation in zebrafish (Liu et al. 2012) and may represent differences in the birth time or innervation of these MN clusters. Within the IN cluster, we confirmed the presence of *en1*+ inhibitory GABAergic/glycinergic INs, *vsx2*+ excitatory glutamatergic/cholinergic INs, and *evx1*+ excitatory glutamatergic INs as previously identified in *Xenopus laevis* (Dale et al. 1987a; Juárez-Morales et al. 2017; Li et al. 2004; Dale et al. 1987b). These populations likely correspond with V1, V2a, and V0v INs, which have been morphologically identified in *Xenopus laevis* as ascending INs, descending INs, and commissural INs, respectively (Figure 3.2D-E, Table 3.S1). In addition, for the first time in *Xenopus* we found populations of descending INs corresponding to V2b inhibitory INs and dI6 INs that likely represent commissural INs (Figure

3.2D-E, Table 3.S1). While other cardinal classes such as V3 and dI1-5 could not be identified, it is not yet clear if these neuron types are not present in *Xenopus tropicalis* at these stages or if they arise in different temporal or spatial locations than our collection points. Finally, one cluster was identified as differentiating INs, and one cluster of glycinergic INs remained unidentifiable (Figure 3.2D-E).

Interestingly, the inhibitory KA INs split into 2 mature clusters and one intermediate cluster. Two subtypes of KAs, KA' and KA", have been reported in zebrafish, mice, and other species but not previously in *Xenopus* (Yang et al. 2020). In our dataset, both clusters express *gad2* and *pkd1l2*, but only one expresses KA" markers *foxa2*, *nkx6-2*, and *th* (tyrosine hydroxylase). Given that the *th*-expressing cluster did not express other markers of catecholaminergic or serotonergic activity (*slc6a2*, *slc6a4*, *tph2*) and did express *slc6a3*, we provisionally identified these as GABAergic/dopaminergic KA" interneurons (Figure 3.2F).

3.3.3. Major neuron diversity and organization regenerate post injury

Next, we examined how these populations changed over development and regeneration. First, we found that all major neuron types (RBNs, INs, and both MNs) identified in uninjured populations were present during regeneration in our single cell dataset, indicating that neuronal diversity is largely regenerated after amputation (Figure 3.3A). While this confirms the presence of these neurons in the regenerating spinal cord, we next wanted to investigate if the spatial neuron organization found in uninjured tissue also regenerates. We performed Hybridization Chain Reaction (HCR) in situ RNA detection to visualize the expression of marker genes for major cell types (*chat*-/*prdm14*+: RBNs, *lhx1*+: INs, *chat*+/*prdm14*-: MNs, *chat*+/*prdm14*+: MNs) (Figure S3). We then manually mapped neuron borders to visualize segmented cells within the dorsal/ventral axis (Figure 3.3B). At the stage 41 mid-trunk, all cell types could be identified

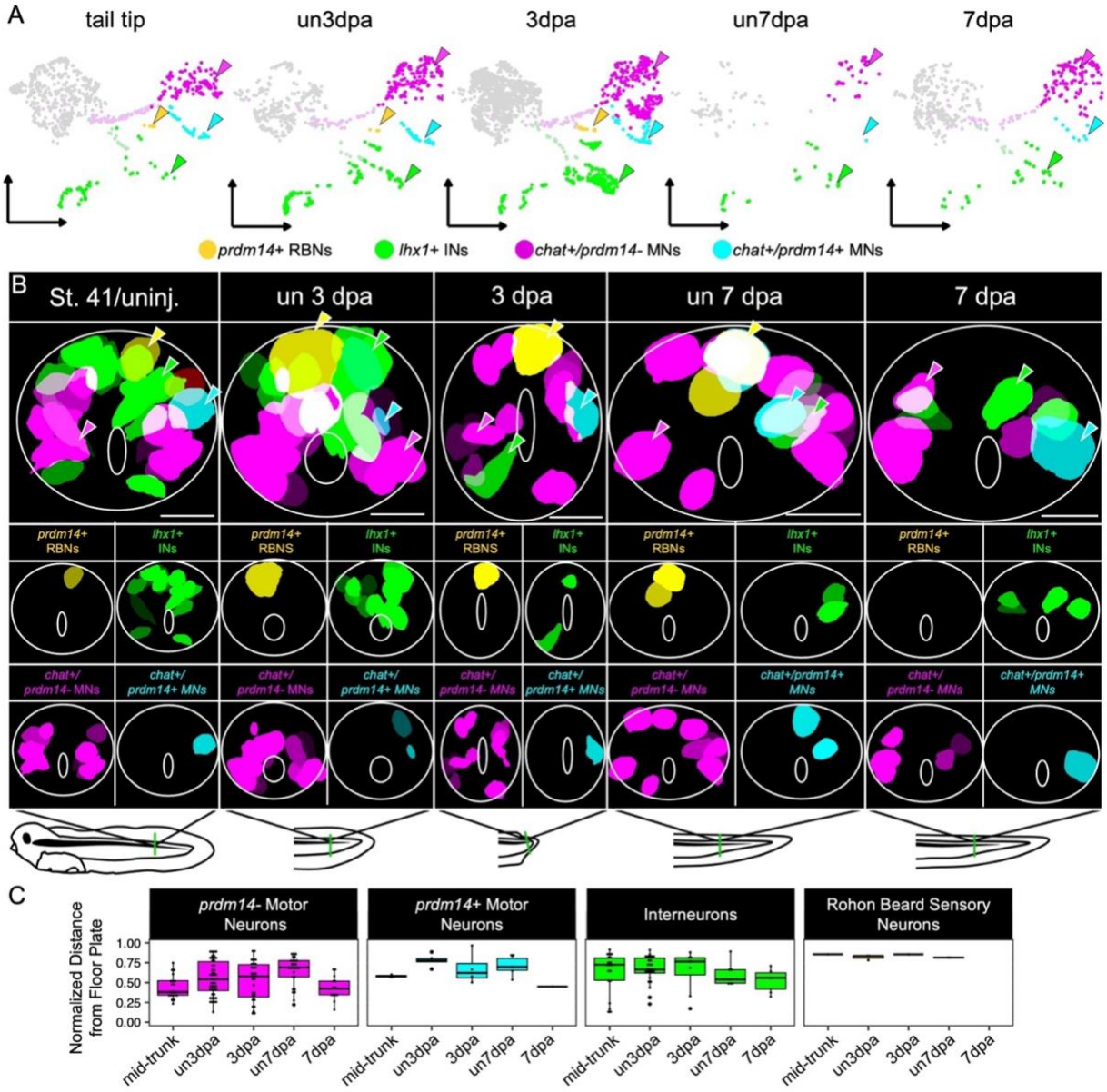

Figure 3.3. Major neuron types occur in spatial domains within regenerating tissue.
A) UMAP showing cell clusters during developmental and regenerating timepoints. B) Cell masks based on HCR fluorescence in cross-sectioned spinal cords in the stage 41 mid-trunk and in uninjured or regenerating tissue at 3 and 7 dpa. White solid line denotes spinal cord boundary (outer) and central canal (inner). Yellow is *prdm14*+ RBNs, green is *lhx1*+ INs, magenta is *chat*+ MNs, and cyan is *chat*+/*prdm14*+ MNs. Example cells of each type are shown with a color matched arrowhead. Bottom diagram shows approximate location of cross-section. All scale bars are 100 µm. C) Bar chart showing normalized distance from the floor plate for each cell type. All samples are not significantly different. St. 41/uninj n = 2 sections; un 3 dpa n = 5 sections; 3 dpa n = 9 sections; un 7 dpa n = 4 sections; 7 dpa n = 3 sections. Positive sections were selected from n = 4 tadpoles per timepoint.

within their expected dorsal/ventral ranges (Figure 3.3B,C) (Roberts and Clarke 1982). After collecting later developmental (un3dpa, un7dpa) and regenerating (3dpa, 7dpa) samples, we found that this dorsal/ventral range did not change significantly based on condition or time, indicating that neuron spatial organization is regenerated post injury. The only exceptions were RBNs, which are known to degrade at later stages and could rarely be found after 3 dpa (Figure 3.3C) (Yajima et al. 2014). We conclude that the spatial domains of RBNs, INs, and MNs are generally re-established during regeneration, as we have previously found for neural progenitors (Angell Swearer, Perkowski, et al. 2025).

3.3.4. Neuron repopulation strength post-injury depends on neuronal birthdate

After confirming the regeneration of major neuron types and their spatial organization, we next wanted to see if neurons made at different times in development regenerate to the same extent in our scRNA-seq dataset. First, we defined neurons by their developmental window of neurogenesis. Spinal cord neurons have been traditionally categorized into two groups based on their time of birth during early primary or later secondary neurogenesis. To factor in additional nuance, we used the terms “early” to indicate neurons established by late neurula, “mid” for secondary neurons arising after neurulation but no longer being generated by stage 41, and “late” for neurons still undergoing neurogenesis by stage 41 (Figure 3.4A). We assigned a preliminary primary or secondary origin to neuron categories based on what is known from *X. laevis* and zebrafish (Figure 3.4B, Table 3.S1) (Bernhardt et al. 1990; Roberts and Clarke 1982; Saint-Amant and Drapeau 2001; Satou et al. 2012; 2009), then confirmed this identity based on the developmental population dynamic data (Figure 3.4C). We found that during our developmental timepoints, primary early neurons decreased in proportion (RBNs, V2b INs), while secondary or late neurons increased in proportion beginning either at day 0 (MNs, V0v INs, KA’s) or day 1

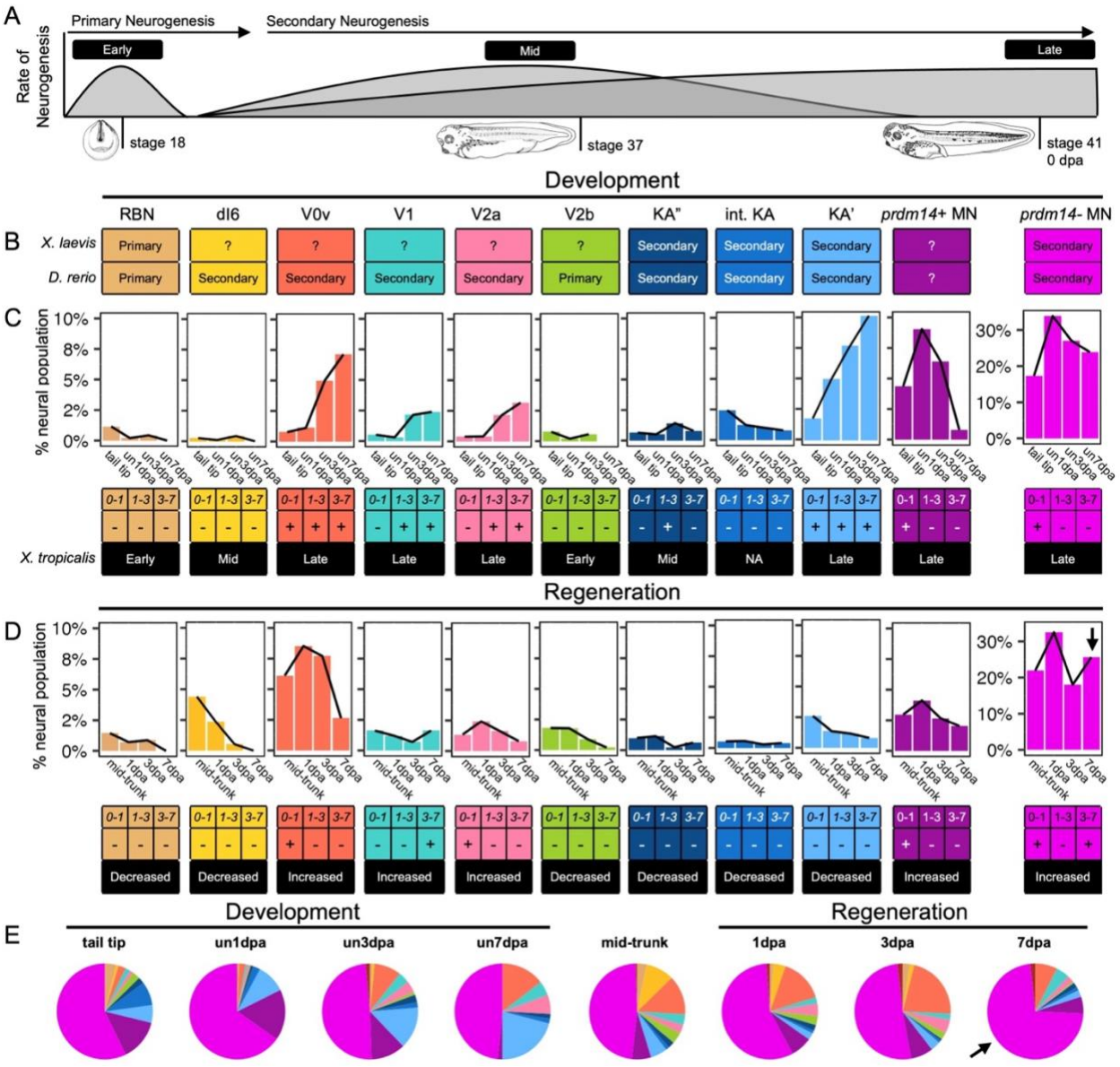

Figure 3.4. Neuron subtype repopulation after injury depends on developmental identity. A) Schematic showing waves of primary and secondary neurogenesis (y axis) over developmental time (developmental stages over x axis), additionally annotated as early neurogenesis (occurring during neurulation), mid neurogenesis (occurring between neurulation and stage 41) and late neurogenesis (occurring during stage 41). B) Literature analysis from *Xenopus laevis* or *Danio rerio* (Table S1). C) Proportional bar charts showing changes in the % neural population over developmental time, as labeled as decreased (-) or increased (+). D) Proportional bar charts per neuron type showing changes in the % neural population over regenerative time, as labeled as decreased (-) or increased (+). Arrow denotes expanded *prdm14*- MN cluster at 7dpa. E) Pie charts showing the proportion of neurons at each time point. Arrow denotes expanded *prdm14*- MN cluster at 7dpa.

(V2a INs, V1 INs) (Figure 3.4C). We identified secondary mid neurons (KA"s, dI6 INs) based on previous evidence indicating a secondary origin (Dale et al. 1987a; 1987a) but a decrease in proportion in our dataset. Interestingly, in comparison to KA", KA' neurons increase during developmental stages, illustrating a novel divergence between the two cell types (Figure 3.4C).

If spinal cord regeneration fully recapitulates development, we would expect all neuron types to be newly generated in parallel from NPCs. Instead, neuron populations changed dynamically during regeneration based on their window of neurogenesis and identity. Most early and mid neurons, which have exited their neurogenic window by the time of amputation, proportionally decreased after injury. Most late neurons, which are still being generated at stage 41, proportionally increased during at least one regenerating timepoint (Figure 3.4D). However, several of these late neuron types diverged from their developmental trajectory over regenerative time. The most striking examples were the late *prdm14*+ MNs, V0v INs, and V2A INs, which expanded immediately after injury but then decreased markedly at later timepoints, and the late KA" neurons, which declined steadily over regenerative time (Figure 3.4D). Only two neuron types (*prdm14*- MNs and V1 INs) increased in proportion from 3-7 dpa. These *prdm14*- MNs undergo a unique and dynamic pattern: first expanding by 1 dpa, then declining at 3 dpa, and expanding again by 7 dpa (Figure 3.4D). To assess if these proportions were differentially affected by changes in the progenitor cluster, we looked at internal neuron proportions (Figure 3.4E), which showed the universal declines seen at 3 dpa is likely due to progenitor growth, but there remains a strong expansion of *prdm14*- MNs at 1 and 7 dpa in both analyses (Figure 3.4D, E arrows). Overall this result indicates that neurons do not universally regenerate, but instead dynamically repopulate the regenerating spinal cord depending on their neurogenic window and identity.

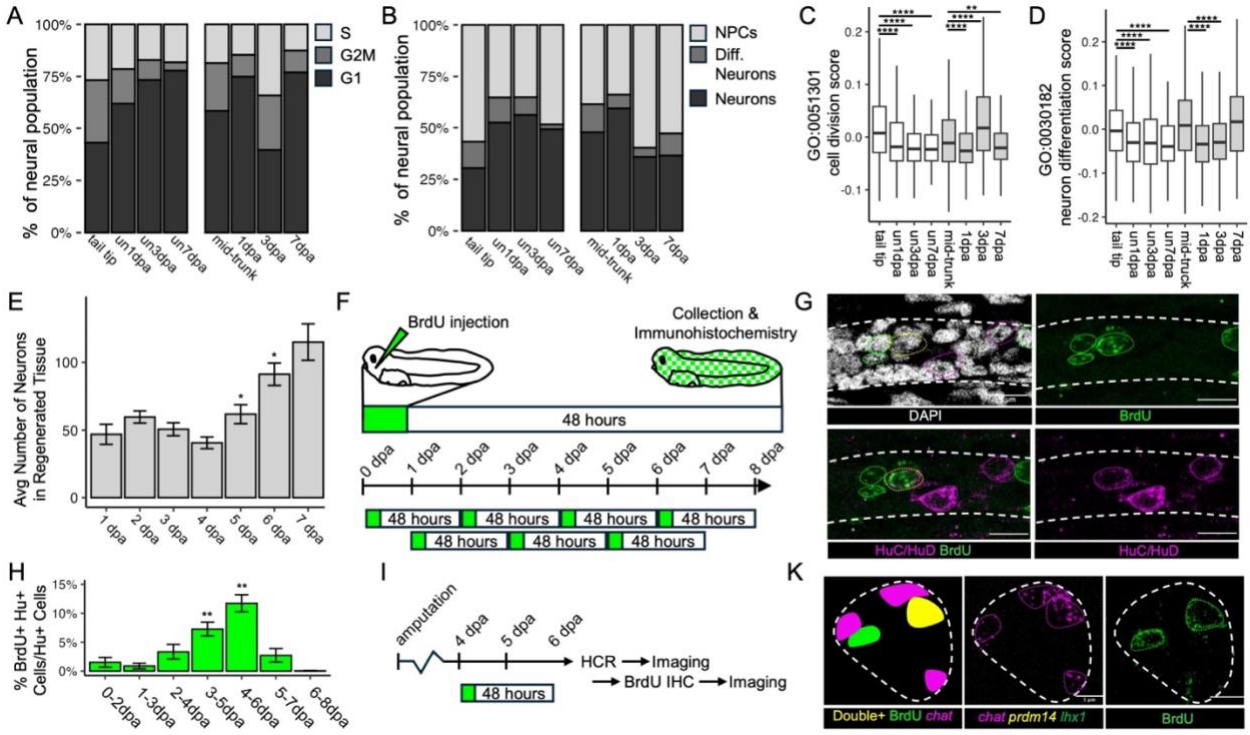

Figure 3.5. Regeneration proceeds via a wave of proliferation and then proliferative neurogenesis. A) Bar chart of G1, G2M and S phase cells as a proportion of entire neural population. B) Bar chart of NPCs, Differentiating (Diff.) Neurons, and Neurons as a proportion of entire neural population. C) GO:0051301 cell division score over developmental and regenerative time. ****p-value < 0.0001, **p-value < 0.01 compared to tail tip for developmental timepoints and mid-trunk for regenerating timepoints. D) GO:0030182 neuron differentiation score over development and regenerative time. ****p-value < 0.0001 compared to tail tip for developmental timepoints and mid-trunk for regenerating timepoints. E) Bar chart of the average number of HuC/HuD+ neurons in regenerated tissue over regeneration. * p-value < 0.05 comparing 1dpa to 1dpa n = 4; 2dpa n = 14; 3dpa n = 11; 4dpa n = 10; 5dpa n = 12; 6dpa n = 12; 7dpa = 14. F) Experimental diagram of BrdU injection and BrdU/HuC/HuD Immunohistochemistry. G) Whole mount image showing double HuC/HuD and BrdU+ cell at 6 dpa after injection of label at 4 dpa. White dashed lines indicate spinal cord border; magenta dotted lines indicate HuC/HuD+ neurons; green dotted lines indicate BrdU+ cells; yellow dotted line indicates double positive cell. Scale bar = 5 μm. H) Plot showing the percent of BrdU/HuC/HuD+ cells within HuC/HuD+ cells 48 hours post injection. ** p-value < 0.01 comparing 0-2 dpa timepoint to 0d-2d n = 6; 1d-3d n = 7; 2d-4d n = 6; 3d-5d n = 5; 4d-6d n = 7; 5d-7d n = 6; 6d-8d n = 7. I) Experimental diagram showing BrdU injection, sample collection and iterative co-staining with HCR and BrdU. K) Cross-section image showing *chat*+/*prdm14*-BrdU+ MN at 6 dpa after injection at 4 dpa. White dashed lines indicate spinal cord border; green dotted lines indicate BrdU+ Neurons; magenta dotted lines indicate chat+/prdm14- cells; yellow dotted line indicates double positive cell. Scale bar = 5 μm. n = 3 *prdm14*+BrdU+ cells from 10 sections generated from 4 tadpoles. All statistical tests done via Wilcoxon test.

3.3.5. Proliferative neurogenesis explains the increase in neurons from 3-7 dpa but not 0-1 dpa

The dynamic and cell-type specific changes in neuronal subtypes we observed suggested waves of neurogenesis might be occurring between 0-1 dpa and 3-7 dpa; we therefore set out to investigate if these waves could be attributed to proliferative neurogenesis by assessing cell cycle and Gene Ontology (GO) term enrichment (Ashburner et al. 2000; The Gene Ontology Consortium et al. 2023). To assess the balance of progenitors and post-mitotic cells, we calculated the percent population of cells in S, G2M, or G1 phase using Seurat-based cell cycle prediction analysis. During development, the proportion of neural cells in G2M declines steadily from 0-7 days. This decline is accompanied by a decrease in NPCs and in GO:0051301 cell division score (Figure 3.5A-C, left panels, Figure S4). By contrast, in regeneration there is a marked increase in G2M cells at 3 dpa accompanied by an expansion of NPCs and an increase in the cell division score at the same timepoint (Figure 3.5A-C, right panels, Figure S4). At 1 dpa, the proportion of NPCs actually decreases, as does the proportion of cells in G2M, in agreement with our previous findings (Figure 3.5A, B) (Kakebeen et al. 2020). To assess if the neuron repopulation that we see from 0-1 dpa and 3-7 dpa is the result of neurogenesis, we looked for top GO terms during regeneration. Unexpectedly, we did not see an enrichment for GO:0030182 neuron differentiation terms at 1 dpa, only at 7 dpa (Figure 3.5D, Figure S4C, D).

This analysis suggested that only the expansion of V1 INs and *prdm14*- MNs we see from 3-7 dpa could be explained by new differentiation of neurons from mitotically active progenitors, or proliferative neurogenesis. To confirm these results in vivo, we tracked neuron repopulation by staining for the pan-neuronal marker HuC/HuD during regeneration. We found that starting at 1 dpa, the average number of neurons per regenerate does not increase until 5 dpa, where it increases until our endpoint at 7 dpa (Figure 3.5E). To see if this increase in neuron population at

5 dpa is due to proliferative neurogenesis, we injected tadpoles with BrdU according to established protocols (Thuret et al. 2015). A 2-day chase was necessary after injection to detect substantial neurogenesis (Figure 3.5F). We found that there is little to no proliferative neurogenesis in the regenerated tissue prior to 3 dpa, as less than 5% of neurons were BrdU+. Instead, there is a peak in neurogenesis at 4-6 dpa, with ~12% double positive cells, before declining to baseline levels (Figure 3.5G, H). We conclude that proliferative neurogenesis begins between 3 dpa and 4 dpa, which is reflected in the increase of NPCs, cells in G2M, and cell division scores at 3dpa (Figure 3.5A, B, C). This mechanism likely fuels the formation of new neurons we observe 5-7 dpa (Figure 3.5E), as well as the increases in Differentiating Neurons and GO neuron differentiation score we observe at 7 dpa (Figure 3.5B, D).

To test which neuron types were being generated by proliferative neurogenesis, we did iterative staining of HCR and BrdU (Figure 3.5I). The only double positive cells we found at 7 dpa were BrdU+ *chat*+/*prdm14*- cells, indicating that the most common BrdU+ HuC/HuD+ neurons generated 5-7 dpa are either V2a INs or prdm14- MNs (Figure 3.5K), which echoes the strong increase in *prdm14*- MNs at 7 dpa compared to most other neuron types (Figure 3.4). However, proliferative neurogenesis cannot explain the increase in neurons observed at 1dpa (Figure 3.5B) or the increase in V0v, V2a, *prdm14*+ and *prdm14*- MNs at that timepoint (Figure 3.4D) (see Discussion).

3.3.6. Emergence of transient population of regeneration-specific neurons at 1dpa

In zebrafish, a transient group of injury induced neurons (iNeurons) arises soon after spinal cord injury and plays a central role in cell-cell signaling and spontaneous neuronal plasticity and thus, in functional recovery. iNeuron markers colocalize with various neuron markers such as *hb9, isl1, pax2, gad1b*, and *vgluta*, indicating they arise from various

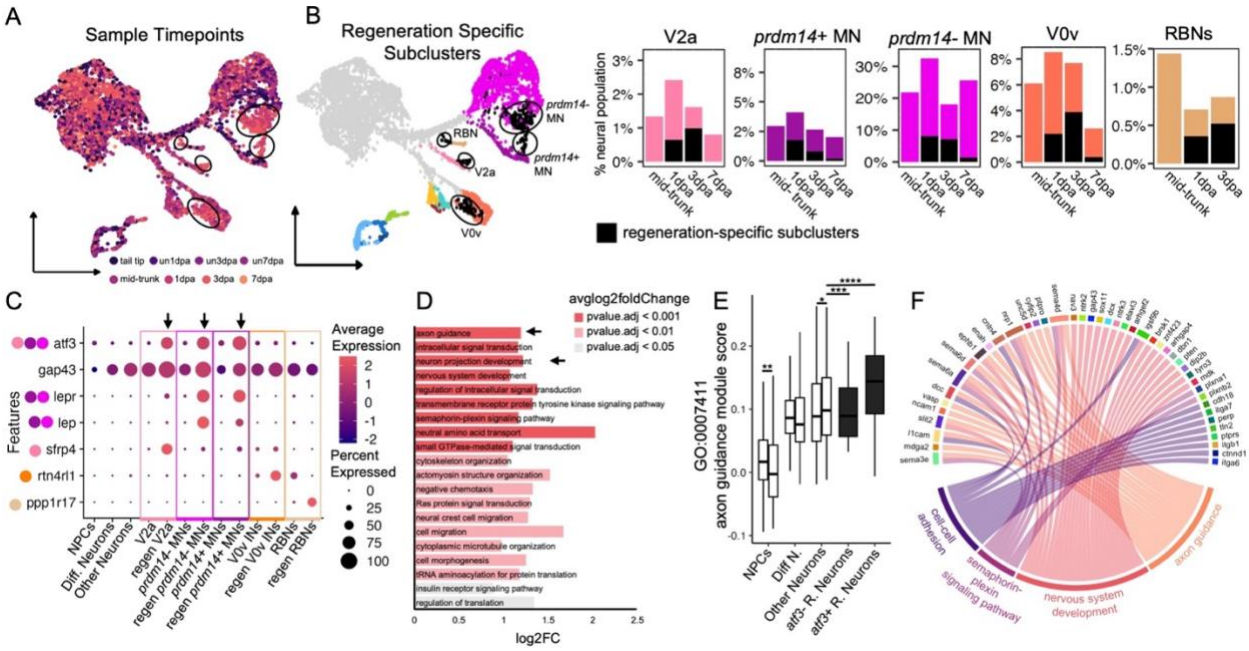

Figure 3.6. Regeneration-specific neuron subclusters arise in specific neuron types and show distinct patterns of gene expression and cell processes. Combined UMAP showing sample distribution; black circles show regeneration-specific subclusters. B) Regeneration specific subclusters (black) appear in V2a INs, *prdm14*+ MNs, *prdm14*- MNs, V0v INs, and RBNs by 1 dpa, as shown by combined UMAP (left) and proportional bar charts (right). C) Gene expression of NPCs, Differentiating (Diff) Neurons, Other Neuron types, and regeneration-specific subclusters. Some subclusters express iNeuron markers (*atf3, gap43*), others express *Xenopus lep*+ MN markers (*lepr, lep*), and others have unique expression patterns (*sfrp4, rtn4rl1, ppp1r17*). Arrows highlight *atf3*+ Regenerating Neurons. Y-axis dots represent clusters gene is expressed in. D) Gene ontology of *atf3*+ Regenerating Neurons compared to other Neuron types at 1dpa. Enriched terms are sorted by strength of adjusted p-value. E) Plot of GO: 0007411 axon guidance score at 1 dpa in different cell clusters in uninjured (left bar) or regenerating (right bar) timepoints. Black denotes regeneration-specific subclusters. *pvalue < 0.05, **pvalue < 0.01, ***pvalue < 0.001, ****pvalue < 0.0001 F) Plot of GO:0007411 axon guidance score and associated modules at 1 dpa (lower half), compared to upregulated genes representing scores (upper half). All statistical tests done via Wilcoxon test.

neuron types after injury (Saraswathy et al. 2024). Given the lack of both proliferation and neurogenesis at 1 dpa as well as previous evidence of a transient class of *lepr*+ regeneration-specific neurons in *Xenopus*, (Aztekin et al. 2019; Kakebeen et al. 2020) we hypothesized that pro-regenerative mechanisms are enacted by a similar population of injury-responsive neurons at this timepoint.

To test this hypothesis, we identified subclusters of neurons that appeared transiently after injury (Figure 3.6A). These transient subclusters arose in V2a INs, *prdm14*+ MNs, *prdm14*- MNs, V0v INs, and RBNs primarily at 1 and 3 dpa (Figure 3.6B). Despite this temporal commonality, each subcluster showed unique patterns of gene expression. In comparison to the RBN and V0v regeneration-specific subclusters, V2a IN, *prdm14*- MN, and *prdm14*+ MN subclusters all strongly expressed *atf3*, a gene previously implicated in neuron regeneration and a marker of zebrafish iNeurons (Figure 3.6C) (Katz et al. 2022; Saraswathy et al. 2024). This observation supports previous work showing that transient regeneration specific neurons do not represent one neuron type, but rather arise within several types (Saraswathy et al., 2024). The *atf3*+ MN subclusters also express leptin receptor (*lepr*), which has been previously identified in a regeneration-specific MN cluster during neuron regeneration in *Xenopus* (Aztekin et al. 2019; Kakebeen et al. 2020; Love et al. 2011), indicating that zebrafish iNeurons and *Xenopus lepr*+ transient MNs may represent a conserved regeneration-specific mechanism (Figure 3.6C).

Previously, zebrafish iNeurons were found to have a role in cell signaling and neural plasticity through cell morphogenetic mechanisms like axon regrowth and migration (Saraswathy et al., 2024). To assess if *atf3*+ subclusters play a similar central signaling role in *Xenopus*, we used CellChat to find top signaling pathways (Jin et al. 2021). Overall, while many top pathways were similar to iNeurons (ex/ L1CAM signaling), the differences in total signaling strength between regenerating neurons and non-regeneration specific clusters were insignificant (Figure S5). To then interrogate if *atf3*+ subclusters drive spontaneous neuronal plasticity, we investigated what GO terms were enriched in *atf3*+ regenerating neurons compared to non-regeneration specific neurons at 1 dpa. Similar to zebrafish iNeurons, the top enriched GO term was axon guidance, with other top terms including intracellular signaling transduction (Figure

S6A, B), neuron projection development (also increased in zebrafish iNeurons), and nervous system development (Figure 3.6D, E, 3.S6). To see what genes were driving this enrichment, we plotted genes associated with nervous system development against axon guidance and other top overlapping associated GO terms. Many nervous system development genes were associated with axon guidance and specifically the semaphorin-plexin signaling pathway and/or cell-cell adhesion (Figure 3.6F), indicating that like iNeurons, *atf3*+ cells prioritize neural plasticity and axon remodeling during early regeneration (Figure S6D-E).

3.3.7. Movement of anterior neurons contributes to repopulation of the regenerating tail

Though all neuron types exist in regenerated tissue, proliferative neurogenesis doesn't occur until 4 dpa (Figure 3.5) and is only clearly identifiable for some neuron types. This timing raises the question of how other neurons appear in new tissue without new neuron differentiation. A possible mechanism is movement of post-mitotic, differentiated neurons from uninjured tissue into new tissue, as has been reported in urodeles (Zhang et al. 2003). We tested for neuron movement via two methods, focusing on KA" INs, because they are present in two ventral columns with well-spaced cell soma and can be visualized with an antibody against TH. First, we quantified the number of dopaminergic/GABAergic KA" INs in pre-amputation, un7dpa, and 7dpa tails to test if the total number of neurons are retained or if more are generated during regeneration. We found that prior to amputation, an average of 61 TH+ KA" INs populate the spinal cord from vent to amputation plane. After 7 days, un7dpa samples have developed on average 125 TH+ KA" INs, likely due to maturation of existing cells. By contrast, regenerating 7dpa samples do not recover lost density and instead retain on average only 70 KA" neurons across the whole spinal cord, with ~12 within the regenerating portion (Figure 3.7A). To confirm that these cells were not a result of proliferative neurogenesis, we injected tadpoles with BrdU at

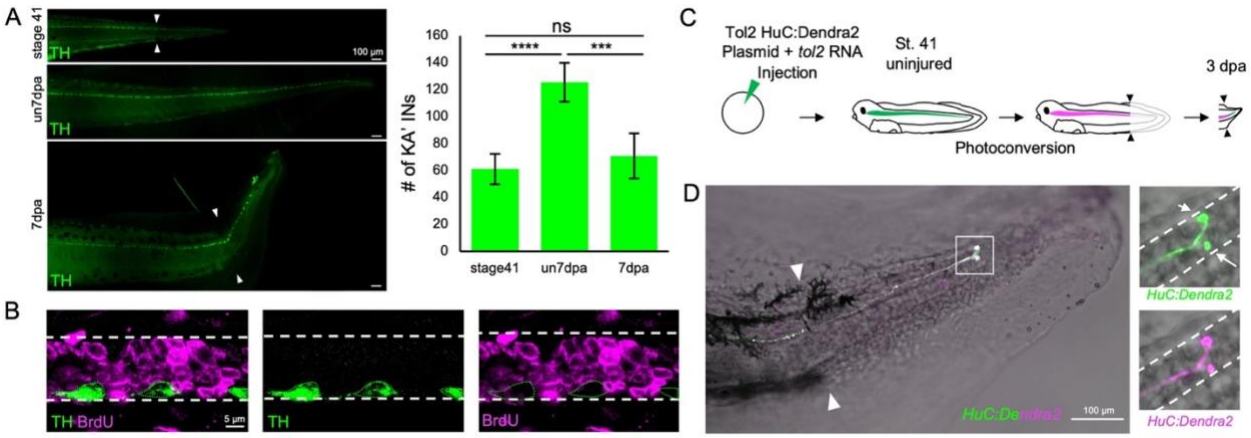

Figure 3.7. Post-mitotic neurons are displaced from uninjured tissue to regenerating tissue. A) TH+ KA" INs in the uninjured stage 41 (0 dpa) or un 7 dpa tadpole tail compared to the 7 dpa regenerate; paired triangles represent amputation plane (left). Bar chart showing the average number of TH+ KA" INs (n = 4 per timepoint) (right). B) Image of 6 dpa tadpole co-stained for TH and BrdU. Green dotted lines represent TH+ KA" INs, white dashed lines show spinal cord border. C) Diagram of experimental design: Tol2 HuC:Dendra2 plasmid and *tol2* RNA was injected into the single-celled embryo. At stage 41, tadpoles were photoconverted and amputated. At 3 dpa, tadpoles were imaged. B) Representative image of double-positive neuron in the regenerated tail. Paired triangles represent amputation plane. White box represents insets of the 488 (top, green) and 594 (bottom, magenta) channels. White dashed lines represent spinal cord border.

4 dpa before collection at 6 dpa and co-staining with TH. All TH+ KA" INs identified were BrdU- (Figure 3.7B). To see what cellular processes were occurring in KA" INs at this time, we looked at GO terms and found enrichment for cell migration in several cells, including KA" INs (Figure S7). To test if we could inhibit neuron movement by blocking cell migration, we inhibited migration factor DCLK and counted TH+ KA" INs, finding a decrease in the number of KA" INs in the regenerating spinal cord (Figure S7).

To directly confirm that mature neurons were displaced from uninjured tissue, we injected 1-cell stage embryos with *tol2* mRNA and a donor plasmid containing sequence for the photoconvertible protein Dendra2 under the control of the mouse Hu promoter. Dendra2 is subsequently expressed mosaically in a small fraction of Hu+ neurons. At stage 41, the entire tail was photoconverted, amputated, and the tadpole allowed to regenerate (Figure 3.7C). Any

neurons present before the injury would thus appear double positive, while neurons generated subsequently would appear green. At 3 dpa, we found double positive Dendra2 cells in the regenerating spinal cord, confirming that neurons move from uninjured tissue into the regenerating spinal cord (Figure 3.7D).

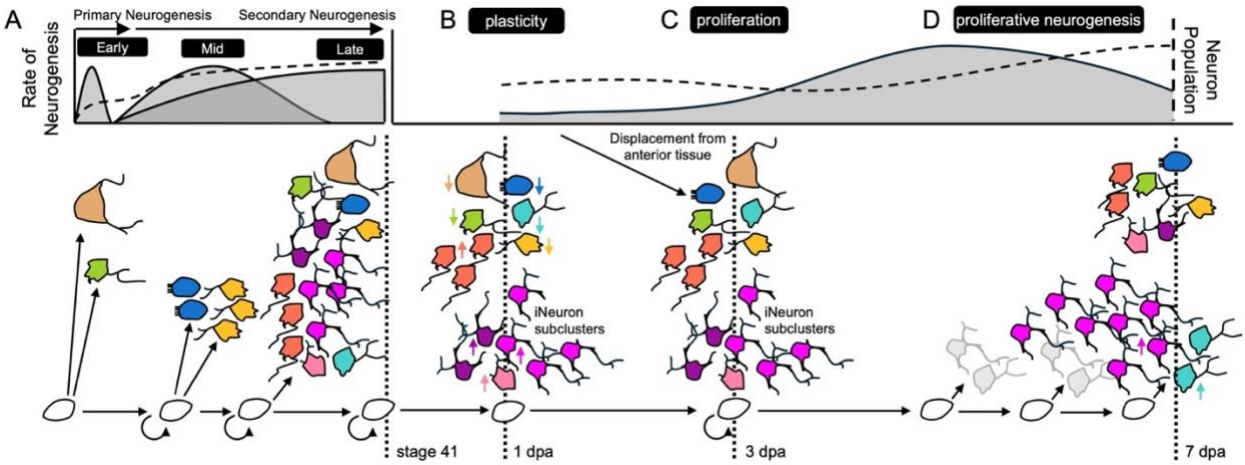

Figure 3.8. The mechanism of neuron regeneration depends on neuron identity. A) During development, primary and secondary neurogenesis gives rise to early, mid, and late neuron types, respectively, resulting in a complex population of neurons by stage 41. B) At 1 dpa, most late neurons increase in proportion in comparison to early and late neurons. Putative iNeuron clusters arise from *prdm14*+ MNs, *prdm14*- MNs, and V2a INs and drive neural plasticity. C) At 3 dpa, NPCs prioritize proliferation, although putative iNeuron clusters remain present. Few new neurons are generated, but neurons from uninjured tissue move into regenerating tissue. D) New neurons—primarily *prdm14*- MNs—are generated by proliferative neurogenesis.

3.4. Discussion

Our study creates a molecular atlas of neurons in the *Xenopus* tadpole, defining marker genes for both known and previously unconfirmed neuronal types. We establish that the overall spatial organization of regeneration largely recapitulates developmental organization, but the cell type composition of the regenerating spinal cord differs in many respects from its uninjured, developing counterpart. Proliferative neurogenesis occurs both less often and later than expected, giving rise principally to *prdm14*- MNs. Some but not all neuron types give rise to a transient

population of neurons that prioritize morphogenetic plasticity as early as 1 dpa. Other neuron types, including KA" INs, repopulate the spinal cord without proliferation, implicating post-mitotic movement (Figure 3.8). These findings have important implications for understanding the mechanisms that may enable plasticity in regenerative conditions or limit repair in non-regenerative conditions.

3.4.1. A molecular atlas of neuronal subtypes in the free-swimming tadpole.

One of our principal goals was to better index the neuron types that exist in the early *Xenopus* free-swimming tadpole. By stage 41, tadpole motor circuits for locomotion and escape must be fully functional, but molecular identifiers for all types of neuron populations were sparse (Roberts et al. 2012). We were able to confirm the presence of and identify markers for each major neuron type and for seven conserved cardinal classes of interneurons that have previously been identified in zebrafish and mouse (Wilson and Sweeney 2023). In addition, we identified several novel subtypes; we were especially interested to find that there are two molecularly distinct populations of Kolmer-Agduhr neurons that could be defined by gene markers and GABAergic/dopaminergic vs GABAergic gene expression. Based on these conserved markers, these populations align to the KA' and KA" populations found in zebrafish and mice (Yang et al. 2020). However, no prior reports of dopaminergic activity in KA interneurons have been reported in *Xenopus* or zebrafish, although serotonin expression has been reported in certain types of KA neurons in fish (Montgomery et al. 2016). In addition, we found two novel subpopulations of MNs (*prdm14*- and *prdm14*+), although the functional distinction between these populations remains unclear. Although patterns of secondary neurogenesis in the tadpole were not previously established for all the cell types we found, our observations agree with what is known in *Xenopus laevis* and show parallels to zebrafish (Bernhardt et al. 1990; Roberts and

Clarke 1982; Saint-Amant and Drapeau 2001; Satou et al. 2012; 2009). Cell types thought to be established through primary neurogenesis, including RBNs and V2b interneurons, remain largely static in number during the 7 days of development we captured (from stage 41-47). By contrast, neuron types that arise through secondary neurogenesis, including V0v, V1, and V2a INs, expand steadily during this time.

3.4.2. Similarities and differences between the uninjured developing spinal cord and regeneration.

A common hypothesis is that regeneration in developing organisms will completely recapitulate developmental mechanisms to replace lost tissue (Aztekin 2024). Our study supports some aspects of this model. We find the spatial organization of the spinal cord is generally restored after injury. We find that all neuron types are present in the regenerating spinal cord, but neurons still undergoing secondary neurogenesis at stage 41 regenerate much more abundantly than those known to be established through primary neurogenesis. This difference may reflect the ability of the larval spinal cord to exploit the same growth and patterning mechanisms already in place before injury to readily replace neurons that are still being generated developmentally at that stage. However, the composition and dynamics of neuron types in the regenerating spinal cord differ in several crucial aspects from their uninjured, developing, counterparts. Among secondary neurogenic cell types, there are notable differences in their dynamics during regeneration versus development. Several cell types that expand during development (V0, V1, V2a, and KA" INs) instead decline in late regeneration, compensated by non-developmental increases in *prdm14*- MNs. Overall, this unique finding indicates that regenerative repopulation depends closely on developmental identity: early primary and mid secondary neurons are no longer able to dynamically repopulate in comparison to late secondary

neurons, which are already undergoing population increases during development at these stages. This discovery illustrates a divergence from the model where development is a complete recapitulation of developmental mechanisms to restore lost tissue complexity.

3.4.3. Neurogenic strategies vary by cell type and temporal window.

Another major motivation for our study was to understand how different classes of neurons are restored over the course of regeneration. Here we found that there are several neurogenic strategies employed that vary by time and cell type, and that some classes of neurons only form after injury. Previously, we had described that NPCs undergo an early cell cycle exit after injury, though we weren't able to answer the question of if and when proliferative neurogenesis occurred (Kakebeen et al. 2020). Here, the increased duration of our study and the inclusion of stage-matched developmental timepoints allowed us to generate a much clearer picture of how neurogenesis proceeds after injury. We find that proliferative neurogenesis certainly does contribute to spinal cord regeneration, but not until intermediate regeneration, with BrdU incorporation into neurons first identifiable at 3 dpa. Proliferative neurogenesis can be tied to the late expansion we see in *prdm14*- MNs, with BrdU detectable in *chat*+ *prdm14*- neurons. We confirmed previous findings showing the emergence of regeneration-specific subclusters that each show unique patterns of gene expression: subclusters arise in both MN groups and V2a INs that express zebrafish iNeuron markers, and the MN subclusters additionally express *lep/lepr* (Saraswathy et al. 2024). Strikingly, we found expression of these markers was found in several but not all neuronal classes, suggesting that some neuron types are primed to adapt post-injury. This observation is only selectively correlated with birth time: no primary neuron classes expressed *atf3* post-injury, but several secondary classes also did not express *atf3*. It is also not clearly correlated with connectivity, although the prioritization of neuronal plasticity at 1 dpa

may indicate these neurons are critical to reinnervation of new tissue. Future research on which neurons are necessary to regeneration could elucidate this connection.

Finally, we addressed what mechanisms, if not proliferative neurogenesis, could underlie neuron repopulation. First we focused on KA" neurons as a representation of postmitotic neurons and found that the average total number of KA" INs in the spinal cord stayed the same post injury, indicating that cells found in the regenerating tissue were from anterior, uninjured tissue. This movement was confirmed by BrdU analysis and photoconversion tracing. Due to the late emergence and small percentage of BrdU+ neurons during regeneration (12% at the peak of proliferative neurogenesis), it's possible that this neuron movement represents a substantial proportion of the neuron repopulation we see at early and intermediate regenerative stages. While some evidence implicates active migration as a mechanism enabling repopulation of these neurons in the spinal cord, we cannot rule out passive movement or direct differentiation from NPCs.

Looking forward, we are especially interested to see how the contributions of *atf3*+ neurons, neuronal migration, and proliferative neurogenesis change as the tadpole progresses through metamorphosis. The stage-specific loss of regenerative competence in the spinal cord is a unique advantage of *Xenopus* for understanding how regeneration becomes limited. While age-specific losses of neural stem cells and changes in the innate immune system are known contributing factors to regenerative loss (Muñoz et al. 2015; Mescher et al. 2013), this study highlights injury-responsive neurons and movement of anterior neurons as other events that are necessary for restoring the full neuronal diversity of the spinal cord and may be differentially lost with maturity.

3.5. Methods:

3.5.1. X. tropicalis *husbandry and use.*

Use of *Xenopus tropicalis* was carried out under the approval and oversight of the IACUC committee at UW, an AALAC-accredited institution. Generation of tadpoles was carried out according to published methods (Kakebeen et al. 2020). In this study we used both wild-type frogs and frogs from the triple transgenic line *Xtr.Tg(pax6*:GFP;*cryga*:RFP;*actc1*:RFP) (RRID:NXR_1.0021 (Hartley et al. 2001; Hirsch et al. 2002)) reared and purchased from the National *Xenopus* Resource (https://www.mbl.edu/xenopus/; RRID:SCR_013731). Pax6 transgenic matings were performed by crossing a heterozygous transgenic frog to a wild-type frog. These matings yielded clutches with 50/50 wt/pax6:GFP+ populations. For amputation assay, NF stage 41 tadpoles were anesthetized with 0.05% MS-222 in 1/9x MR and tested for response to touch prior to amputation surgery. Once fully anesthetized, a sterilized scalpel was used to amputate the posterior third of the tail. Amputated tadpoles were removed from anesthetic media within 10 min of amputation into new 1/9x MR. Tadpoles were kept at a density of no more than 1 tadpoles per 2.5 mL. Tadpoles were fed daily sera Micron (Lane et al. 2022) at ¼ mL per 2.5 L, starting at 3 dpa until final timepoint collection.

To measure regenerated length of tail, samples were mounted and imaged with a Leica M205FA fluorescence Stereomicroscope. Using the Leica imaging software (LasX), measurements were taken from the vent to the most posterior point of the tail. Regenerating measurements were taken based off of morphological identification of amputation plane.

3.5.2. scRNA-sequencing pipeline.

Tadpoles were anesthetized with 0.05% MS-222 in 1/9x MR and tested for response to touch

prior to amputation surgery. Once fully anesthetized, a sterilized scalpel was used to amputate and collect intended tissue (Figure 3.1A). Tail tissues were collected within 30 minutes of amputation and added to a vial with 72 µl trypLE (ThermoFisher Scientific:12604013) and 3 µl 100 mg/mL collagenase P (ROCHE:11213857001) for every 100 tail tissues. Samples were moved to a 28°C water bath for dissociation and triturated with a p200 every 5 minutes until dissociated fully and no chunks were visible (30-60 minutes). To quench the reaction, 150 µl of ice cold 10% FBS was added for every 100 tail tissues. Samples were then spun down for 5 minutes at 1000xg. Supernatant was disposed and cells were resuspended in 300 µl 10% FBS for FACS. For each sample, 22-294 tadpoles were used (tail tip: 294 tadpoles; un1dpa: 222 tadpoles; un3dpa: 133 tadpoles; un7dpa: 22 tadpoles; mid-trunk: 294 tadpoles; 1dpa: 208 tadpoles; 3dpa: 144 tadpoles; 7dpa: 25 tadpoles). Tail tip and mid-trunk tissues were collected from the same specimens.

Cell sorting and collecting were performed as previously described (Kakebeen et al. 2020), except cells were collected into 500 µl solutions of 1x PBS with 1 mg/ml BSA (NEB:B9200S). Single-cell mRNA libraries were prepared using the GEM-X single cell 3' v4 kit (10x Genomics), with a target capture of 10,000 cells. Quality control and quantification assays were performed using a Qubit fluorometer (Thermofisher) and a Screentape Assay (Agilent). Libraries were sequenced on an Illumina NextSeq2000 using a 100 cycle, P4 XLEAP-SBS™ kit. Each sample was sequenced to an average read depth of 226 million total reads, which resulted in an average read depth of ~28,000 reads/cell after normalization.

3.5.3. scRNA-sequencing processing.

RNA sequencing reads were processed using CellRanger v9.01 Count and Aggregate by 10x Genomics. To generate the reference genome, the *Xenopus tropicalis* v10.0 reference genome

and gene models were downloaded from Xenbase. The output from CellRanger was processed using DoubletFinder to detect doublets. The data were then run through the Seurat v3.1 pipeline (Satija et al. 2015) in R Studio v4.4.3 using standard filtering and preprocessing. Cells expressing < 200 genes were removed from downstream analysis, with a mitochondrial RNA read cutoff of 25%. Two poor quality clusters indicated by abnormally low UMI count and high mitochondrial RNA percentage were manually removed. After QC analysis, cells were normalized, scaled by Sample and nFeature_RNA, then integrated with RPCA. Cell cycle was predicted as previously described (Kakebeen et al. 2020).

Go.db (v3.21) was used to evaluate Gene Ontology (Ashburner et al. 2000; The Gene Ontology Consortium et al. 2023) terms during regeneration, and Circlize (v0.6.16) (Gu et al. 2014) was used to generate chord graphs of gene-term connectivity. CellChat (v1.4.0) (Jin et al., 2021) was used to evaluate *atf3*+ regenerating neuron cell-cell interactions. Only *Xenopus* genes with 1-to-1 ortholog mapping, as defined on Xenbase, were mapped to mouse orthologs.

3.5.4. Hybridization Chain Reaction and Sectioning.

For HCR, tadpoles were fixed overnight in 1x MEM with 3.7% formaldehyde at 4C. HCR was done in whole mount from established protocols (Willsey 2021) at a probe concentration of 16 nM. Post HCR protocol, samples were washed 3 x 15 min with 1X PBS, 1 x 15 min with 15% sucrose in 1X PBS, then overnight at 4°C. To identify regenerating tissue post-sectioning, fins were trimmed dorsal and ventrally only posterior to the amputation plane. Samples were then transferred into OCT (Thermofisher 23-750-571) and kept at -80°C until sectioning with a Leica CM3050 S Cryostat. Post sectioning, slides were baked at 37ºC for 20 minutes before imaging using a Leica SP8 Confocal with a 63X objective. They were processed using FIJI image analysis software. For cell masks, Cellpose (Stringer et al. 2021) was manually used to create 3D

cell masks based on HCR and DAPI staining that were then imported into FIJI for downstream processing (Schindelin et al. 2012). To measure Dorsal/Ventral location, the center point of cells was measured from the bottom of the spinal cord floor plate then normalized to spinal cord height, as measured from the bottom of the floor plate to the top of the roof plate.

3.5.5. BrdU Labeling.

In order to assess the level of proliferative neurogenesis during regeneration, we used the DNA-synthesis marker BrdU. Tadpoles at the indicated stage were injected with 16 nL of BrdU (10 mM, Fisher, B23151) in the gills, following the protocol established *Xenopus* for tracking neurogenesis during development (Thuret et al. 2015). After injection, tadpoles were allowed to regenerate for 2 days to allow for detectable differentiation into neurons via HuC/D staining. We found labeling in the spinal cord within 1 hour after injection, and that labeling persisted in progenitors for ~2 days post-injection (data not shown). Staining proceeded as previously described (Angell Swearer, S. Perkowski, et al. 2025), (1° Abs: 1:200 Rb anti-BrdU polyclonal, Fisher, PA5-32256; 1:200 Ms HuC/D monoclonal, Fisher, A21271) with the addition of a 10 minute 2N HCl acid wash following the initial permeabilization in PBS-Triton. Because the BrdU 10 minute 2N HCl wash destroys HCR signal, we iteratively stained for HCR and BrdU. Samples were injected with BrdU as described then run through the HCR protocol, sectioned and imaged as described above. Slides then underwent staining for BrdU and re-imaging using the described protocol, with solution volumes adjusted for slide Immunohistochemistry.

3.5.6. TH Immunohistochemistry.

Tadpoles were stained and imaged as previously described (Angell Swearer, S. Perkowski, et al. 2025), (1° Abs: 1:200 Mouse anti-Tyrosine Hydroxylase monoclonal, Immunostar, 22941). Co-

staining with BrdU was conducted as described above.

3.5.7. Dclk1 inhibitor treatments.

Tadpoles were treated by immersion in 5μM Dclk1-in1 (Tocris cat #7285; 50mM stock solution was made up in DMSO, diluent for immersion was 1/9MR) either immediately following amputation or at the corresponding uninjured timepoint. 0.01% DMSO was used as a vehicle control. Inhibitor solution was refreshed on days 1, 3, and 5.

3.5.8. Dendra2 Photoconversion.

In order to track migration and differentiate between newly generated neuronal cells, we used a pMT-HuC: Dendra2 plasmid on post-mitotic neurons. The tadpoles were injected at the one-cell and two-cell embryo stages with 30 pg of Dendra2 plasmid and 10 pg of tol2 RNA. After injection, *Xenopus tropicalis* tadpoles were grown to stage 41, when we took pictures using the 20X objective on a compound microscope. Then we conducted photoconversions for differentiating between old and new neurons by directing UV light on a posterior section of the tail. Then the distal 1/3 of the tail was amputated using a scalpel. At 3 days post-amputation (dpa), the tails were once again imaged in the 488 nm and 594 nm channels.

3.5.9. Statistics.

All statistics were performed using using R Stats package (v3.6.2).

3.6. Acknowledgements

I thank members of the Wills lab for critical comments during the preparation of this manuscript and support in frog husbandry. I thank the ISCRM Genomics Core and Director Mary Regier for

equipment use and their support during the scRNA-Seq pipeline. Equipment resources and technical assistance for work conducted in the ISCRM Genomics Core were supported by a generous gift from the John H. Tietze Foundation and support from the Washington State Legislature. I thank the UW Cell Analysis Facility for the equipment use and their support for cell sorting. I thank the Ruohola-Baker lab for the use of their equipment for tissue processing during cell dissociation. I thank the Kong lab for access and training on their cryostats. We thank Xenbase for curation of genomic and literature information and the National *Xenopus* Resource for frogs. AAS was supported by the Cellular and Molecular Biology Training Grant NRSA 5T32GM136534-02 from NIGMS. SBP was supported by a Mary Gates Fellowship for Undergraduate Research. This work was supported by NINDS R01NS099124 to AEW.

3.7. Supplemental Figures

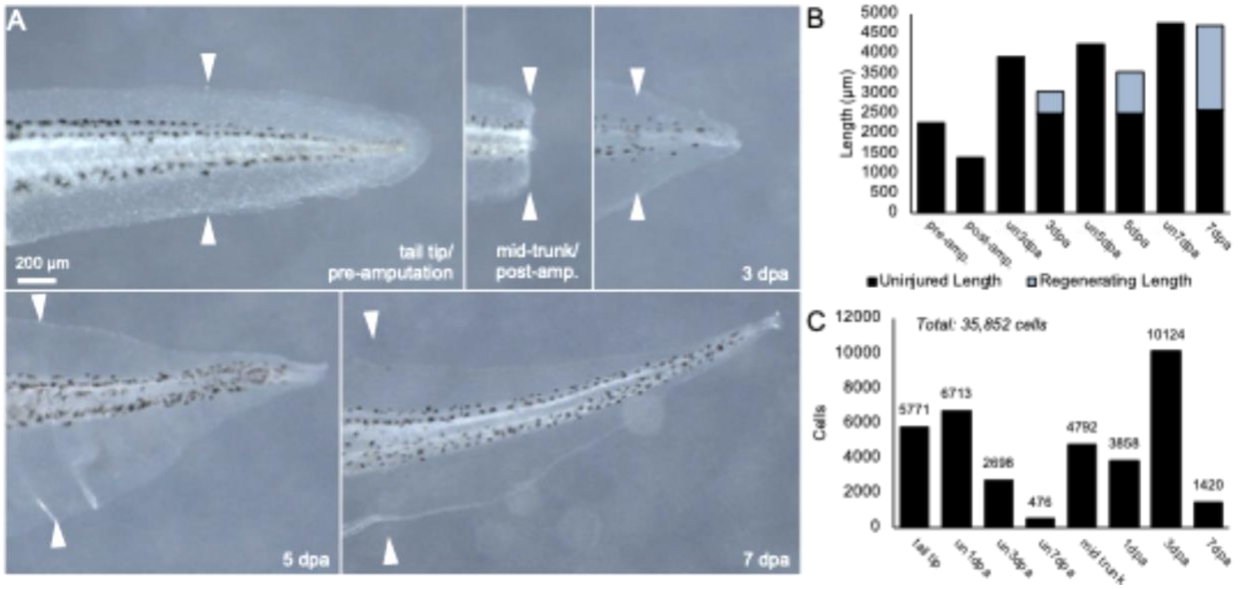

Figure 3.S1. Experimental 7 day time course of regenerating stage 41 tadpoles. Brightfield images of tadpoles at tail tip/pre-amputation (pre-amp.) stage 41, mid-trunk/post-amputation (post-amp.), 3 dpa, 5 dpa, and 7 dpa. B) Bar chart of average vent-to-tip tail length in microns of uninjured (un-) or regenerating tails. Black denotes uninjured tissue, and grey denotes regenerated tissue. C) Bar chart of cells collected by scRNA-seq, post quality control analysis; numbers above bars show cell counts per timepoint; total dataset is 35,852 cells.

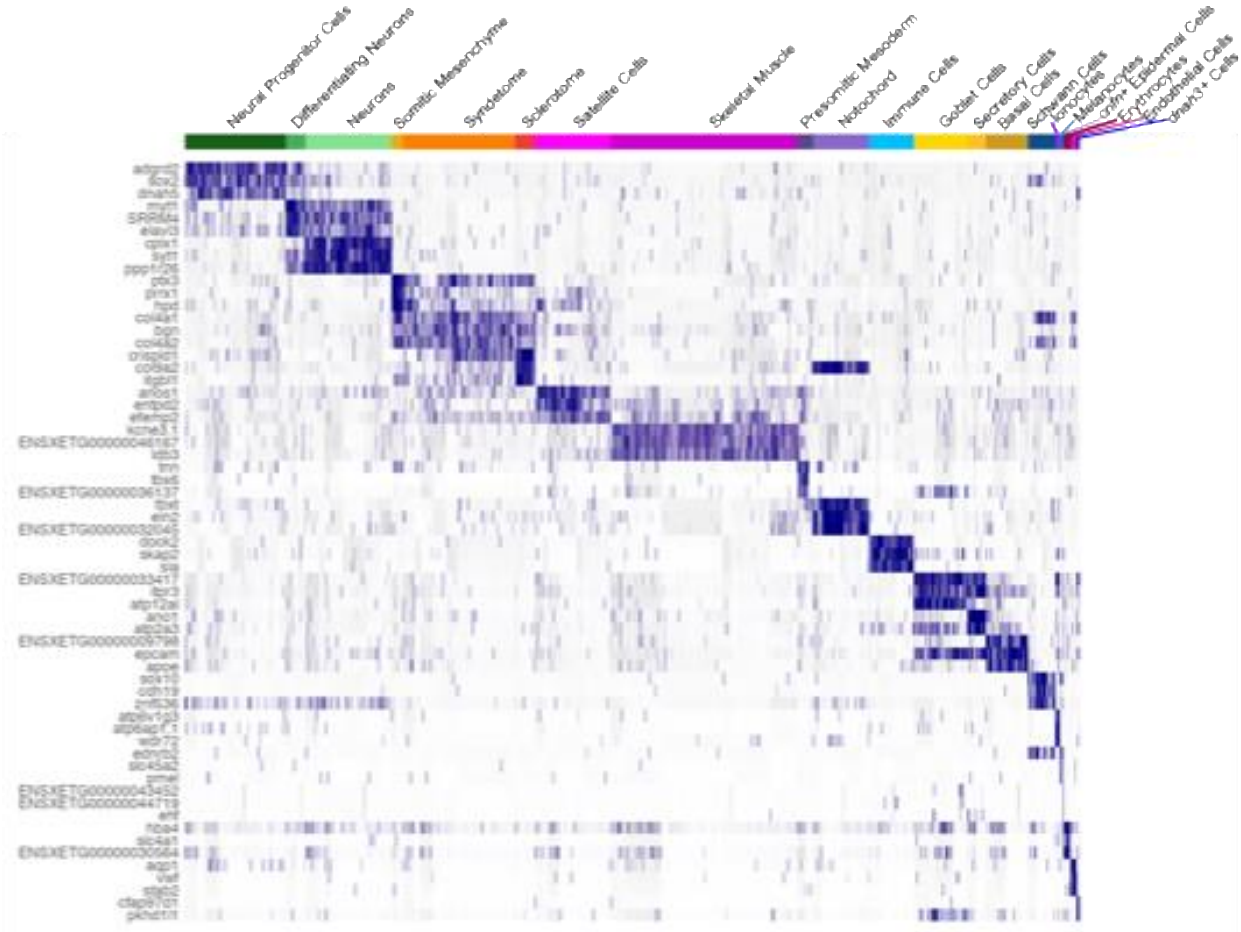

Figure 3.S2. Gene expression patterns identify tail cell types. Heatmap of top three differentially expressed genes for each identified cell type. Purple indicates high expression, white indicates low expression.

Cardinal Classification	Neurotransmitter	Zebrafish	likely *Xenopus* counterpart	Birth Date	Marker Genes	Potential Subcluster Notes
RBN	Glutamatergic	Rohon Beard Neurons - Tuttle et al., 2024.	Rohon Beard Neurons	Primary	*prdm14, isl2, isl1, tlx3*	NA
dI6	Glycinergic	Commissural Local (CoLo) - *Satou et al. 2009, Kelly et al., 2023*	commissural interneurons (cIN)	Secondary - *Satou et al., 2009*	*lhx1, dmrt3, lbx1*	NA
V0v	Glutamatergic	Multipolar Commissural Descending (MCoD) and Unipolar Commissural Descending (UCoD) - *Satou et al., 2012, Bernhardt et al., 1990, Kelly et al., 2023*	Dorsolateral commissural (dlc) and/or excitatory commissural interneurons (eclNs)	Secondary - *Satou et al., 2012*	***evx1***, *lhx1, nrn1,* *developmental **dbx1*** - *Juárez-Morales*	*cbln2+* subcluster
V1	Glycinergic/ GABAergic	Circumferential Ascending (CiA) - *Higashijima et al., 2004, Kelly et al., 2023*	ascending interneurons (aINs) - *Li et al., 2004*	Secondary	***en1,*** *lhx1, pnoc, pax2, sp9, foxd3, gbx2, otp*	NA
V2a	Glutamatergic/ Cholinergic	Circumferential Descending (CiD) - *Kimura et al., 2006, Kelly et al., 2023, Kelly et al., 2023*	descending interneurons (dINs) - *Soffe et al., 2009*	Secondary - *Bernhardt et al., 1990*	***vsx2***, *nrn1, nkx6-2, lhx3*	*chat- sox21+, prdm8+, sox14+* subcluster
V2b	GABAergic	Ventral Longitudinal Descending (VeLD) - *Kimura et al., 2006, Kelly et al., 2023*	descending interneurons (dINs) - *Soffe et al., 2009, Li et al., 2004*	Primary - *Bernhardt et al., 1990*	*gata2, gata3, lhx1, sox1, tal1*	*slc6a5+* subcluster
KA'	GABAergic	Dorsal Kolmer-Agduhr (KA') - *Yang et al., 2020*	Kolmer-Agduhr interneuron - *Roberts and Clarke 1982, Kale et al., 1987, Blinor and Heathcote, 2001*	Secondary	*pkd1l2, kctd8, sox1, tal1*	NA
KA"	GABAergic/ Dopaminergic	Ventral Kolmer-Agduhr (KA") - *Yang et al., 2020*	Kolmer-Agduhr interneuron - *Roberts and Clarke 1982, Kale et al., 1987, Blinor and Heathcote, 2001*	Secondary	*pkd1l2, sox1, nkx6-2, foxa2, tal1*	*chgb, cfap210, sall2, daw1, cdx4*
?	Glycinergic	NA	NA	NA	*meg11+, lhx1*	NA
?	Glycinergic	NA	NA	NA	*foxp2+, pax2+*	NA
Reviewed in:		*Lewis and Eisen 2003, Sengupta and Bagnall, 2023, Wilson and Sweeney, 2023, and Cucun et al., 2024. Reviewed in mouse in Delile et al., 2019*	*Roberts, 2011*	*Saint-Amant and Drapeau 2001*		

Table 3.S1. Conserved markers from zebrafish can be used to identify *Xenopus* neuron counterparts based on literature analysis. Cardinal neurons have been identified in zebrafish literature by their neurotransmitter use, morphological classification, and birth date. These identities can be tied to their likely *Xenopus* counterpart in our scRNA-seq dataset based on cluster Marker Genes. Bold genes indicate marker genes that have been previously identified in *Xenopus*. For some neurons, additional subclusters could be identified for future studies. Two clusters of glycinergic neurons remain unidentified, and V3 and dI1-5 INs could not be found in our dataset.

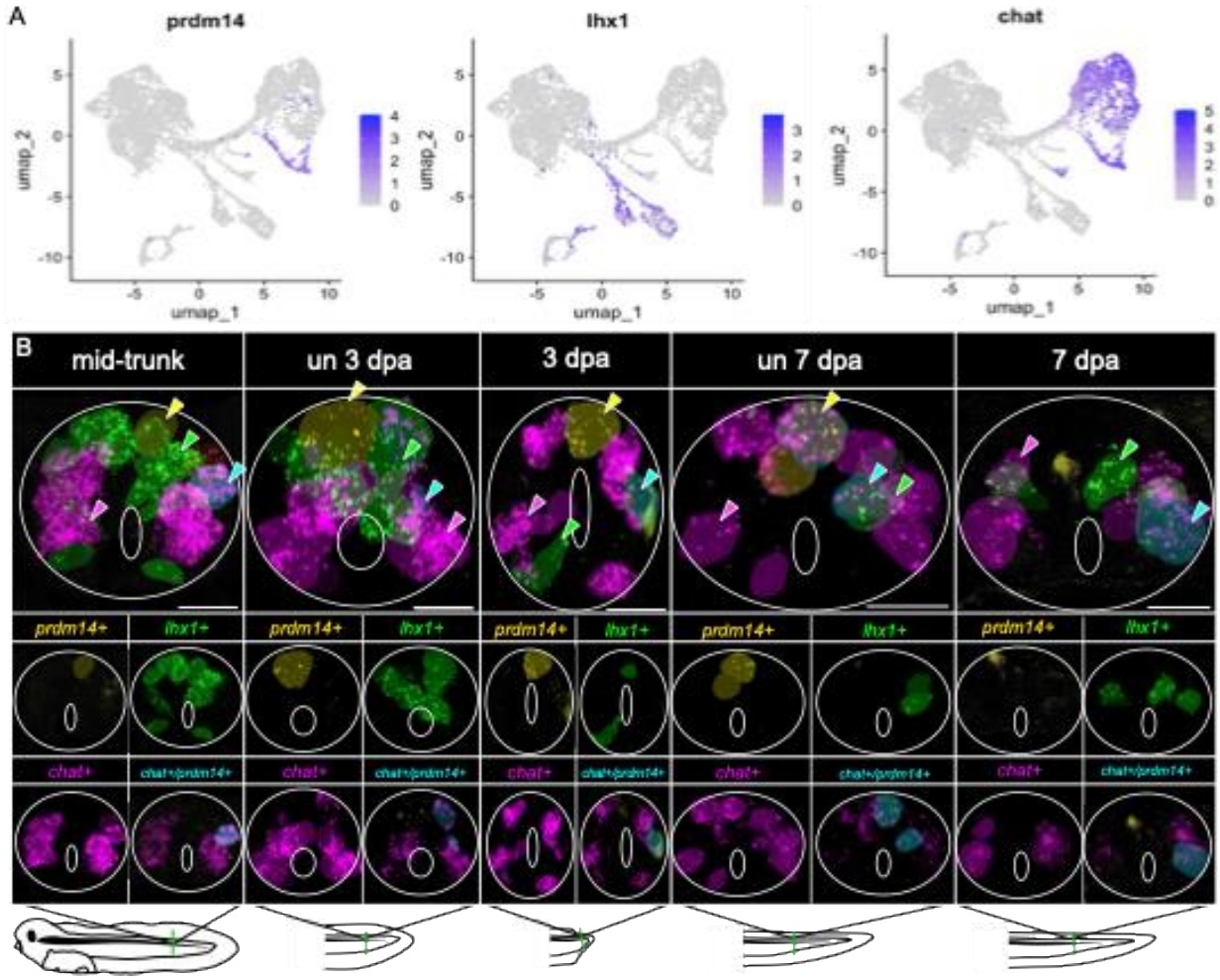

Figure 3.S3. HCR of neuron types within regenerating tissue. A) UMAPs showing chosen HCR probe gene expression of *prdm14, lhx1,* and *chat*. B) Images showing the raw HCR Z-stacks used to generate masks in Figure 3. Segmented cell masks are overlayed. White solid line denotes spinal cord boundary (outer) and central canal (inner). HCR: yellow is *prdm14*, green is *lhx1*, magenta is *chat*. Cells: yellow is *prdm14* + RBNs, green is *lhx1*+ INs, magenta is *prdm14-/chat*+ MNs, cyan is *prdm14+/chat*+ MNs. Example cells of each type are shown with a color matched arrowhead. All scale bars are 100 μm.

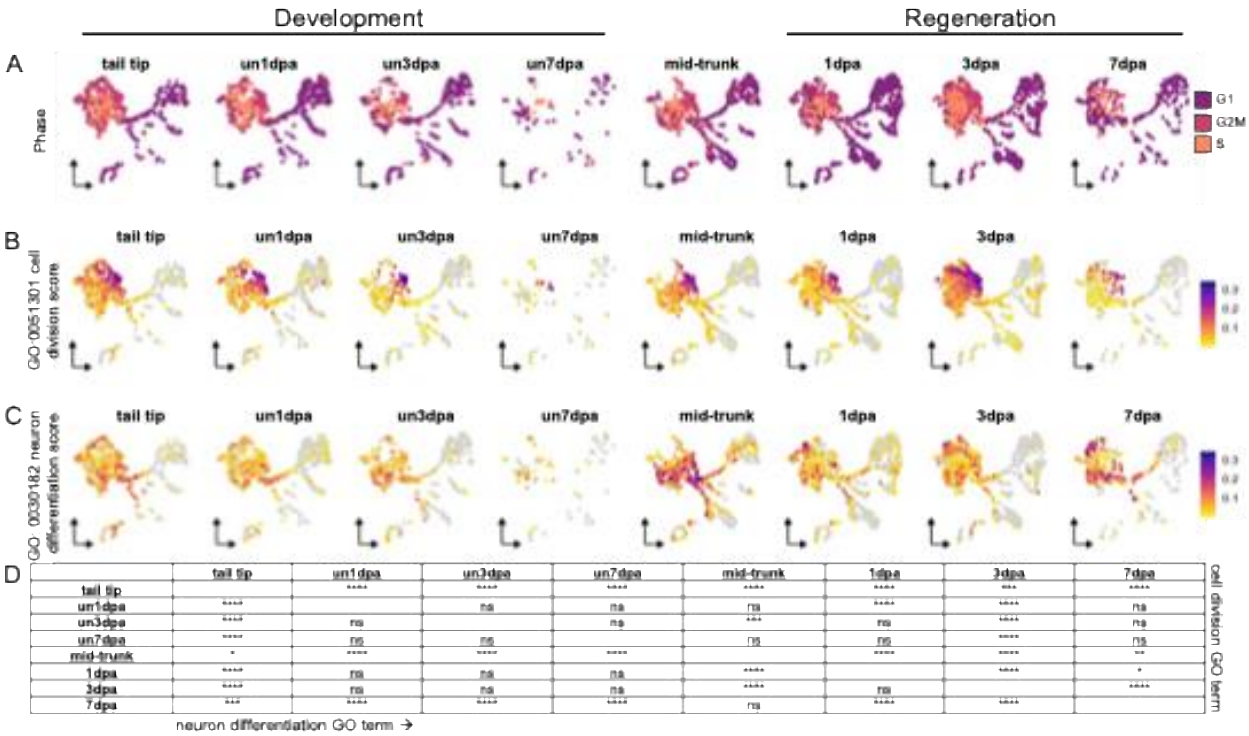

Figure 3.S4. Faceted UMAPs of cell processes throughout development and regeneration. A) Cell cycle phase (G1, G2M, or S) over scRNA-seq timepoints. B) GO:0051301 cell division module score over scRNA-seq timepoints. C) Neuron Differentiation Module Score over scRNA-seq timepoints. D) Comparative adjusted p-values for neuron differentiation GO term (bottom left) and cell division GO term (top right) over developmental and regenerative time.

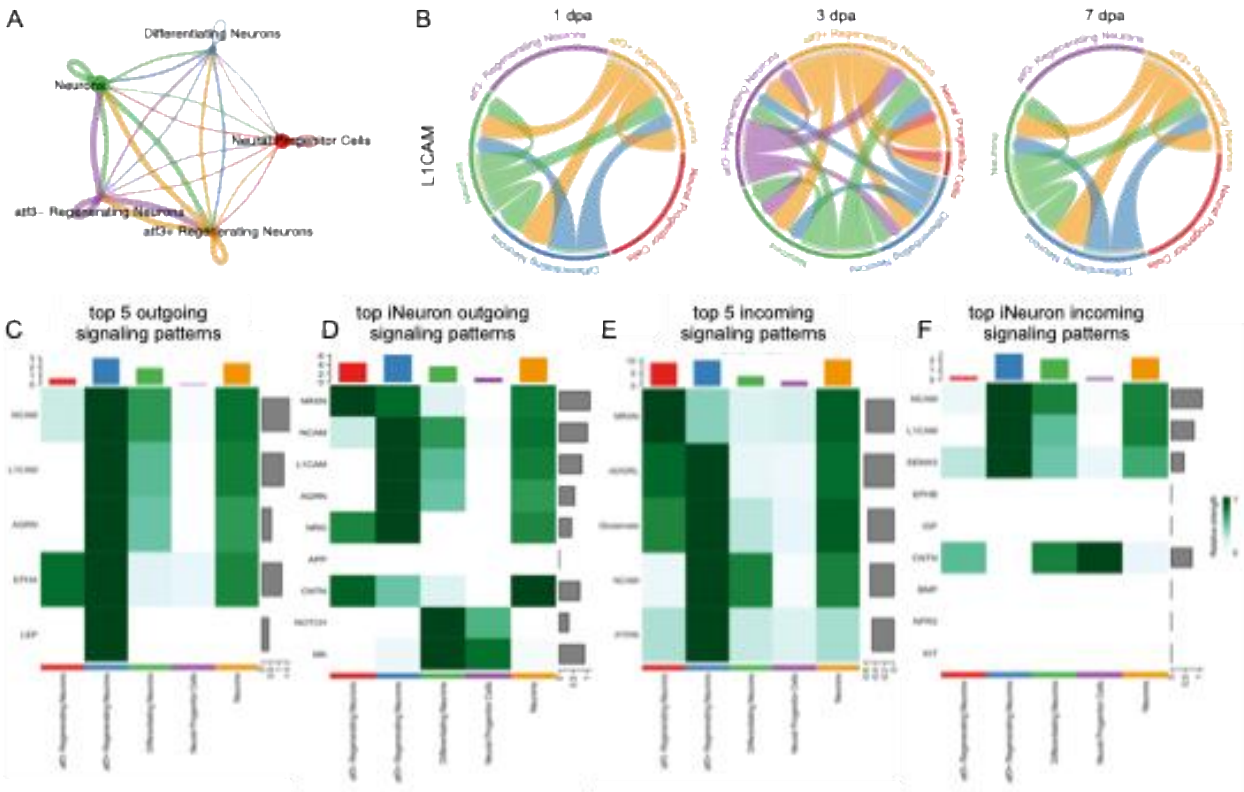

Figure 3.S5. *atf3*+ Regenerating Neurons do not represent a major signaling hub but do show similar top signaling pathways to zebrafish iNeurons. A) Comparative signaling strength of regenerating neurons. B) L1CAM signaling during regeneration. C) Top 5 outgoing signaling patterns at 1 dpa D) Visualization of the top outgoing signaling patterns identified zebrafish iNeurons during regeneration in *Xenopus* regenerating neurons. E) Top 5 incoming signaling patterns at 1dpa F) Visualization of the top incoming signaling patterns identified zebrafish iNeurons during regeneration in *Xenopus* regenerating neurons.

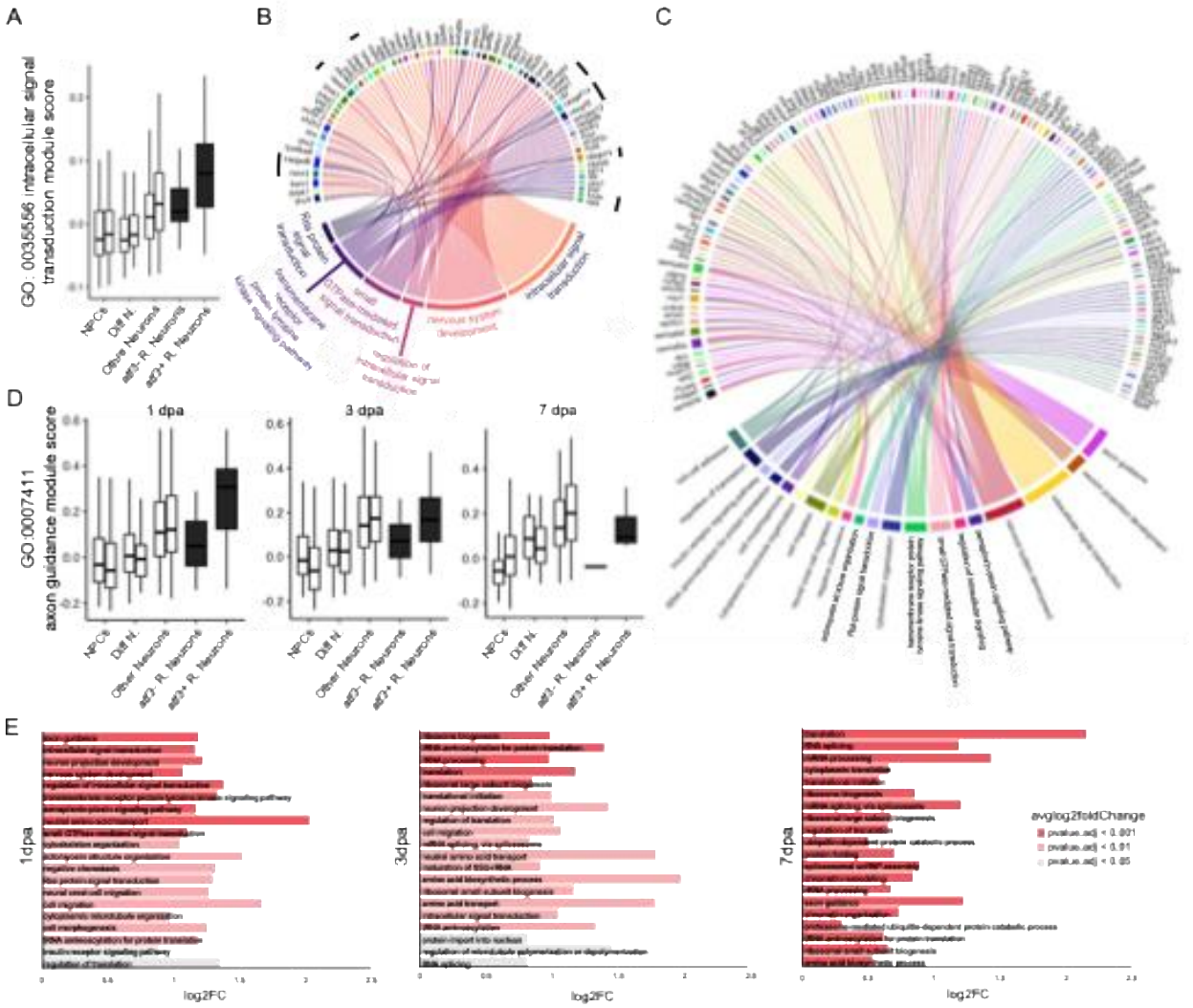

Figure 3.S6. Top 20 GO terms and associated genes in *atf3*+ Regenerating Neurons at 1 dpa compared to 3 dpa and 7 dpa. A) Plot of GO:0035556 intracellular transduction score at 1 dpa in different cell clusters in uninjured (left bar) or regenerating (right bar) timepoints. Black denotes regeneration-specific subclusters. B) Plot of GO:0035556 intracellular transduction score at 1dpaand associated modules at 1 dpa (bottom), compared to upregulated genes representing scores (top). Black bars indicate Ras-associated proteins, which represent one of the top enriched gene families. C) Plot of all top 20 GO terms and associated genes at 1dpa. D) Plot of GO:0035556 intracellular transduction score in different cell clusters in uninjured (left bar) or regenerating (right bar) timepoints at 1 dpa (left), 3 dpa (middle), and 7 dpa (right). Black denotes regeneration-specific subclusters. E) Top 20 GO terms upregulated in *atf3*+ regenerating neurons compared to other Neurons at 1 dpa (left), 3 dpa (middle), and 7 dpa (right).

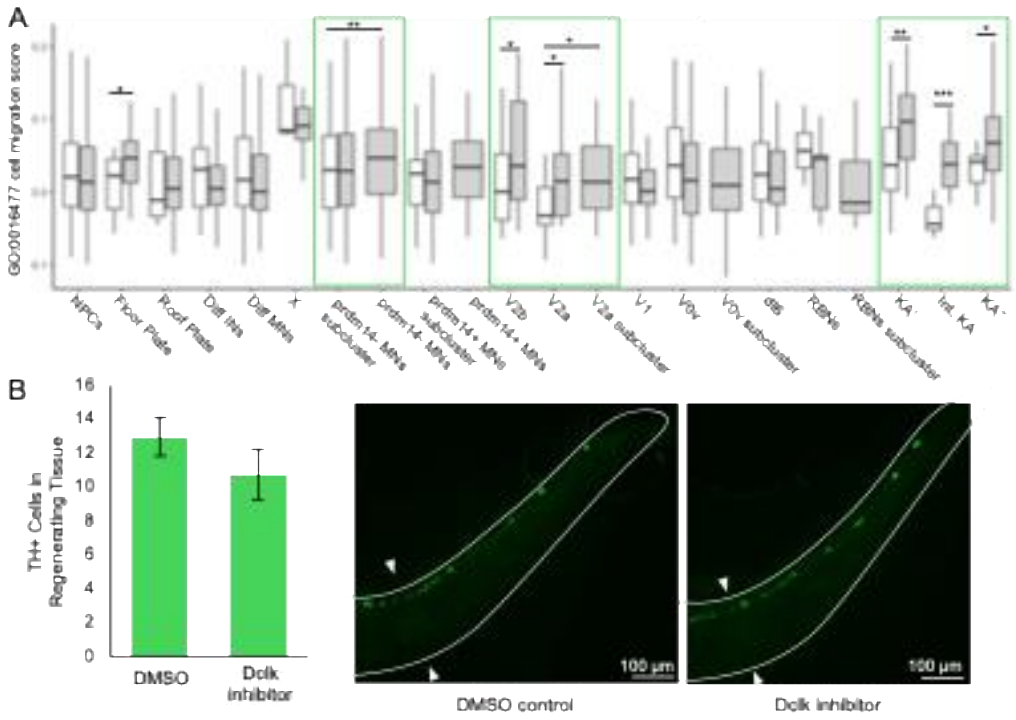

Figure 3.S7. Cell migration may underlie mature neuron displacement. A) GO:0016477 cell migration scores are enriched in regenerating stages in regeneration-specific *prdm14*- MNs, V2bs, V2as, and KA INs (green rectangles). *p-value < 0.05; **p-value < 0.01; ***p-value < 0.001 by Wilcoxon test. B) Dclk inhibition slightly reduces the number of TH+ KA" INs in the regenerating tail (not significant via Wilcoxon test, n = 5 each).

Chapter 4. ADVANCEMENTS IN METHODOLOGY

During my time at UW, I have worked on many techniques both already established and new to the Wills Lab. Among those methods, I have primarily contributed to the protocol for tail vein injection and optimization of hybridization chain reaction (HCR).

4.1. Protocol for tail vein injection in *Xenopus tropicalis* tadpoles

Chapter 4.1 is adapted with minimal modification from:

Jeet H. Patel*, Avery Angell Swearer,* Anneke D. Kakebeen, Lauren Rajchel Loh, Andrea E. Wills. 2024. Protocol for tail vein injection in *Xenopus tropicalis* tadpoles, STAR Protocols, 5, 1, DOI: 10.1016/j.xpro.2024.102895.

Note: Please view online version to see Methods video S1
This work was compiled and written by JP and I, with support from AW. JP, AK and LL performed initial troubleshooting.

4.1.1. Highlights

- An efficient tail vein injection protocol for *Xenopus tadpole* experimentation
- Instructions for screening correctly injected and healthy tadpoles
- Steps for scaling the injection to hundreds of tail veins in a short window

4.1.2. Summary

Functional studies in post-embryonic *Xenopus tadpoles* are challenging because embryonic perturbations often lead to developmental consequences, such as lethality. Here, we describe a high-throughput protocol for tail vein injection to introduce fluorescent tracers into tadpoles, a method that we have previously used to effectively inject morpholinos and molecular antagonists. We describe steps for safely positioning tadpoles onto agarose double-coated plates, draining media, injecting into the ventral tail vein, rehydrating plates, and sorting tadpoles by

fluorescence with minimal injury for high-throughput experiments.

For complete details on the use and execution of this protocol, please refer to Kakebeen et al. 2020; Patel et al. 2022; Shimomura et al. 2015.

Figure 4.1. Graphical Abstract

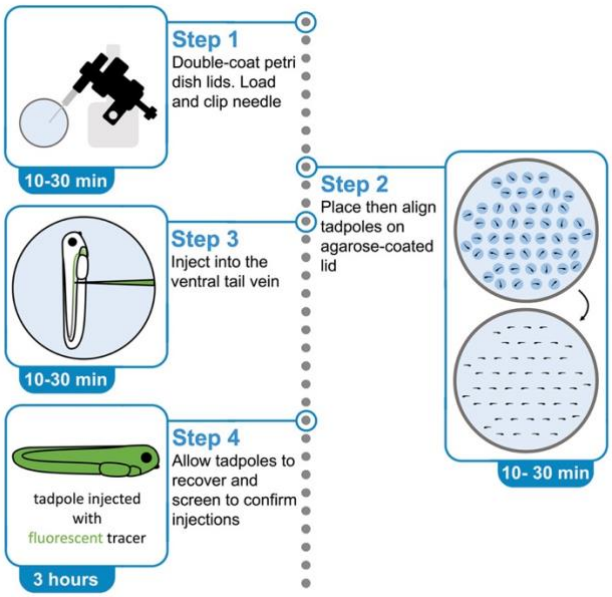

Figure 4.1.1. Before you begin: Timing: 0.5–1 h

The protocol below describes the steps needed to inject the fluorescently labeled glucose analog 2-(N-(7-Nitrobenz-2-oxa-1,3-diazol-4-yl)Amino)-2-Deoxyglucose (2NBDG). We have implemented the same protocol for injection of non-fluorescent reagents such as 2-deoxyglucose and vivo-morpholinos using the labeled dextran, fluoro-Ruby, as a tracer (Patel, Schattinger, et al. 2022; Patel, Ong, et al. 2022; Kakebeen et al. 2020; Morcos et al. 2008). Use of small molecules and vital dyes is beneficial for studying late stage developmental processes and regeneration, as these tools circumvent the need for genetic manipulation and transgenesis, which take years and can have consequences on early development. Temporal control of

experiments is valuable, but has been largely limited to experiments that require introduction of compounds into media. Tail vein injections reduce reagent use and also allow the use of molecules that may be unable to penetrate deep tissues or be taken up from the environment. In comparison to heart injections, tail vein injections are less likely to result in mortality or severe injury. Small molecules have been developed for a range of pathways and allow functional characterization of molecular, cellular, and biochemical processes, which would otherwise result in embryonic lethality. We include images of tadpoles injected with either 2NBDG or with fluoro-Ruby to illustrate distribution differences, both of properly injected tail veins and mis-targeted injections. For other molecules, we recommend testing a variety of concentrations and performing co-injection or parallel injections to confirm effective distribution. This protocol has been optimized for *Xenopus tropicalis* tadpoles ranging from Nieuwkoop-Faber stages 37–45 (Nieuwkoop et al. 1994). We expect this protocol to also work for *Xenopus laevis*, although the 1/9× MR would need to be changed to 1/3× MR and the user may want to adjust needle pulling protocols for greater rigidity.

1. Pull a surplus of glass capillaries.

Note: We suggest pulling two times as many needles as solutions you intend to inject. These needles can be pulled in advance.

Note: We use a Beckman-Coulter needle puller, although users should follow their typical protocol for setting up needles for embryo injection. As an example, we use: Heat = 900; Pull = 40; Velocity = 120; Time = 150; Pressure = 300. However, needles with a long taper (typically 1.2 cm) are recommended to reduce bore size of the clipped needle and size of puncture wound.

2. Prepare 1/9× modified ringers (MR) solution, 1.5% low-melting point (LMP) agarose in 1/9×

MR, and 1.25% MS-222 in 1/9× MR solutions. The 1.5% LMP agarose in 1/9× MR should be melted just before beginning the protocol to prepare injection lids as described below. The lids will quickly dry out and should be made no more than 1–2 h before injecting.

3. Prepare necessary injection mixes.

Note: Depending on the desired injection concentration, you may need to prepare a stock solution and dilute it with deionized (DI) water and/or fluoro-Ruby (or another tracer).

Note: With some compounds, stability at room temperature may be a concern. In this case, prepare mixes on ice or prepare them immediately before injection.

4.1.4. Institutional permissions

All studies in *Xenopus tropicalis* were carried out under the approval and oversight of the IACUC committee at UW, an AALAC-accredited institution, under animal protocol 4374-01. Users will need to acquire approval to work with vertebrate animals at their relevant institution.

4.1.5. Key resources table

REAGENT or RESOURCE	SOURCE	IDENTIFIER
Chemicals, peptides, and recombinant proteins		
Fluoro-Ruby (dextran, tetramethylrhodamine, 10,000 MW, lysine fixable)	Thermo Fisher Scientific	D1817
2-NBDG (2-(*N*-(7-nitrobenz-2-oxa-1,3-diazol-4-yl)amino)-2-deoxyglucose)	Thermo Fisher Scientific	N13195
UltraPure LMP agarose powder	Invitrogen	16520-100
Biological samples		
WT *Xenopus tropicalis*; stages 37–45; sex unsorted	NXR	NXR_1018
Other		
Picospritzer III	Parker	052-0500-900
Narishige MM3 micromanipulator	Narishige	N/A
Beckman Coulter needle puller	N/A	N/A

Thin wall glass capillaries (length = 4″, OD = 1.0 mm, ID = 0.75 mm)	World Precision Instruments	TW100F-4
GJ-8 magnetic stand, for micromanipulator	N/A	N/A
IP iron plate, for micromanipulator	N/A	N/A

Note: alternatives to the microinjection apparatus should not affect protocol success.

4.1.6. Materials and equipment

1× Modified Ringers (MR) Solution (dilute 1:9 before use)∗∗

Reagent	Final concentration	Amount
KCl	2.0 mM	166 mg
$CaCl_2{*}2H_2O$	2.0 mM	363 mg
$MgCl_2{*}6H_2O$	1 mM	251 mg
1 M HEPES, pH 7.6	5 mM	5 mL
5 M NaCl	0.1 M	20 mL
ddH_2O	N/A	to 1 L
Total	**N/A**	**1 L**

∗∗Make 1× MR solution (above). Dilute 1:9 with ddH_2O for 1/9× MR. Can be stored at room temperature (22°C) for up to 1 year as long as no sedimentation or contamination is evident.

1.5% Low Melting Point (LMP) Agarose in 1/9× MR

Reagent	Final concentration	Amount
LMP Agarose Powder	1.5%	1.5 g
1/9× MR	N/A	100 mL

Can be stored at room temperature (22°C) for up to 6 months and remelted as needed.

0.4% MS-222 in 1/9× MR 25× Stock Solution

Reagent	Final concentration	Amount
MS-222	0.4%	4 mg
Tris-HCl pH: 9	N/A	2.1 mL

1/9× MR	N/A	97.9 mL

Can be stored long-term (up to 1 year) at 4°C and brought to room temperature (22°C) for up to 1 month. Working concentration is 0.016%, or a 1:25 dilution. Complete anesthesia should always be confirmed by testing that the escape reflex is absent when the tail of the tadpole is brushed with a pipet tip.

Note: Adjust final pH to 7.5–7.8.

50 mM Stock 2NBDG

Reagent	Final concentration	Amount
2-NBDG (2-(*N*-(7-Nitrobenz-2-oxa-1,3-diazol-4-yl)Amino)-2-Deoxyglucose)	50 mM	5 mg
H_2O	N/A	292.18 µL

Must be stored protected from light. Use at a final concentration of 5 mM in injections mixes. After resuspension, this stock can be stored at -20°C in small, single-use aliquots after resuspension for at least 1 year. In general, refer to manufacturer recommendations for long-term storage.

5 mM Stock Fluoro-Ruby

Reagent	Final concentration	Amount
Fluoro-Ruby (powder)	5 mM	25 mg
Commercial RNase-free H_2O	N/A	500 µL

Keep frozen in a light-protected tube or box at −20°C for up to 5 years. We recommend making a 1 mM working dilution that can be freeze-thawed regularly, to use at 200–500 µM in injections mixes.

4.1.7. Step-by-step method details

Double-coat Petri dish lids

Timing: 5–15 min

Preparation of Petri dish lids by double-coating with agarose is critical for survival and helps to prevent tissue damage. The agarose helps to keep the tails still when attempting to pierce needles into the tail vein and provides a soft base that will keep the tissue moist after the majority of the media is removed. The double-coating progresses quickly to generate an even and consistent agarose base. The use of Petri dish lids is important for this protocol as they have shorter walls, allowing for injections at a shallow angle and more coverage of the plate.

1. Heat 1.5% LMP agarose in 1/9× MR until no solid chunks or small bubbles remain.
2. Line up lids for coating, cleaning out any dust or moisture with a kimwipe.
3. Fill the first lid with melted agarose.
4. Quickly pour excess agarose into the next lid, swirling the residual agarose in the first lid to coat the entire lid and set aside.
5. Repeat step 4 until agarose runs out or the number of desired injection lids are made.
6. Allow plates to cool (usually within 30 s to 1 min).
7. Repeat steps 3–6 to generate a thicker coat of agarose, which will be about 2 mm thick (Figure 4.1.2).
8. Flip lids upside down once they have cooled. This helps to keep the thin agarose from drying out too quickly.

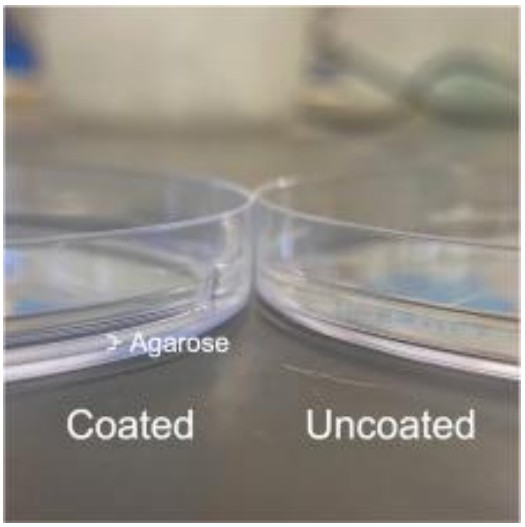

Figure 4.1.2. Agarose coated lid next to an uncoated lid

Load and clip needle

Timing: 5–15 min

Pulled glass capillary needles need to be clipped in order to inject into the tail vein. Injecting 4 nL into the tail vein is standard for this protocol, though up to 8 nL has been tested with similar success. We recommend calibrating capillaries such that each tadpole receives 2 injections in the same location (i.e., 2×2nL injections to achieve a final volume of 4 nL injected). This protocol was developed using a Picospritzer III microinjection system with separate compressed air and the Narishige MM3 micromanipulator, although alternatives to the Picospritzer such as the XenoWorks Digital microinjector, Narishige IM-400, or WPI PV850 should also be effective. Users should follow their typical protocol for embryonic injection.

9. Prepare microinjector rig and turn on compressed air tank (if applicable).
10. Transfer 1–2 μL of injection mix (5 mM 2NBDG or other mix) into a pulled glass capillary and fix into micromanipulator (Figure 4.1.3).
11. Calibrate capillary by breaking the tip with forceps (if applicable) and adjusting injector

settings or clip further until the droplet volume is 2 nL. Prepare tadpoles on agarose plate for injection

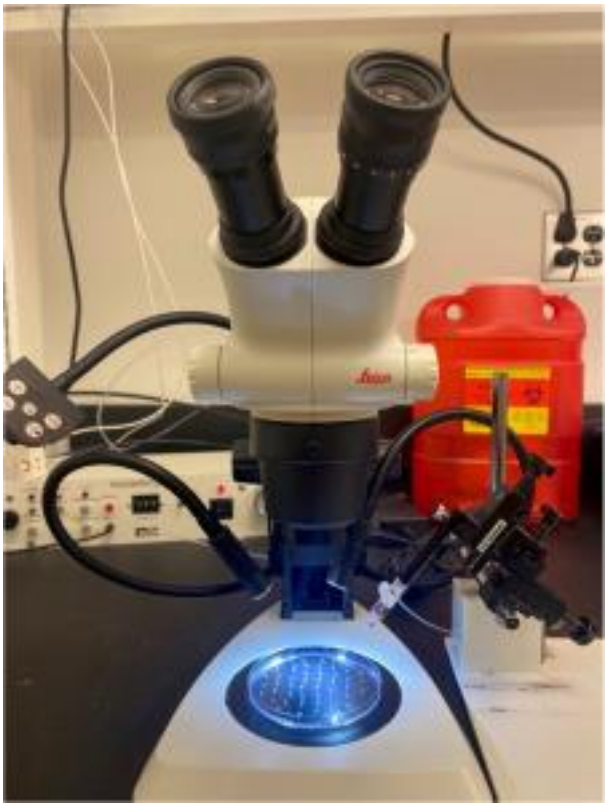

Figure 4.1.3. Microinjection rig setup with loaded capillary and tadpoles oriented for injection

Timing: 10–30 min

Note: Proper plating of tadpoles is critical for performing injections quickly and reducing damage to the tail. We recommend starting with small numbers to get become proficient at proper media removal and tail-vein targeting (in the next step) before scaling up.

12. Add the appropriate amount of 0.4% MS-222 in 1/9× MR (1:25 dilution) to a petri dish with tadpoles to inject. Allow 2–3 min for tadpoles to respond to anesthesia and confirm loss of escape reflex with a gentle poke to the tail.

13. Transfer tadpoles, one at a time, to a double-coated lid.

Note: Each tadpole should be in its own drop of anesthesia supplemented media (Figure 4.1.4). It is best to align the tadpoles in rows as that will allow you to move between tadpoles more easily when injecting. The maximum recommended number of tadpoles per plate is 50 for a 10 cm plate lid.

14. After all tadpoles have been added to the plate, use a P200 pipette to gently remove MOST, but not all, of the media in each droplet (Figure 4.1.4).

Note: During this step, use the tip of the pipette to gently rotate the tadpoles such that the ventral sides are facing the same direction. Fluid flow within the pipette tip can also be manipulated to carefully rotate the tadpoles. Further alignment of tails can be performed while tadpoles are still in a small volume of media. Try to gently nudge the tadpoles by pushing the dorsal side of the head and not the tails, as the tail fins will warp if pushed on.

15. Immediately before starting injections, touch the tip of the P200 to the dorsal side of the head and gently remove as much media as possible from each tadpole (Figure 4.1.4).

Note: It is important to only prepare and inject 1 plate of tadpoles at a time. Droplets of media will eventually lose tension and run into each other if this protocol is paused after step 13; tadpoles could wake up from anesthesia if paused between steps 13–15. Tadpoles will dry out if paused after step 15, and they may dry out if injections take too long, so only set up as many injections as can be performed within roughly 5 min.

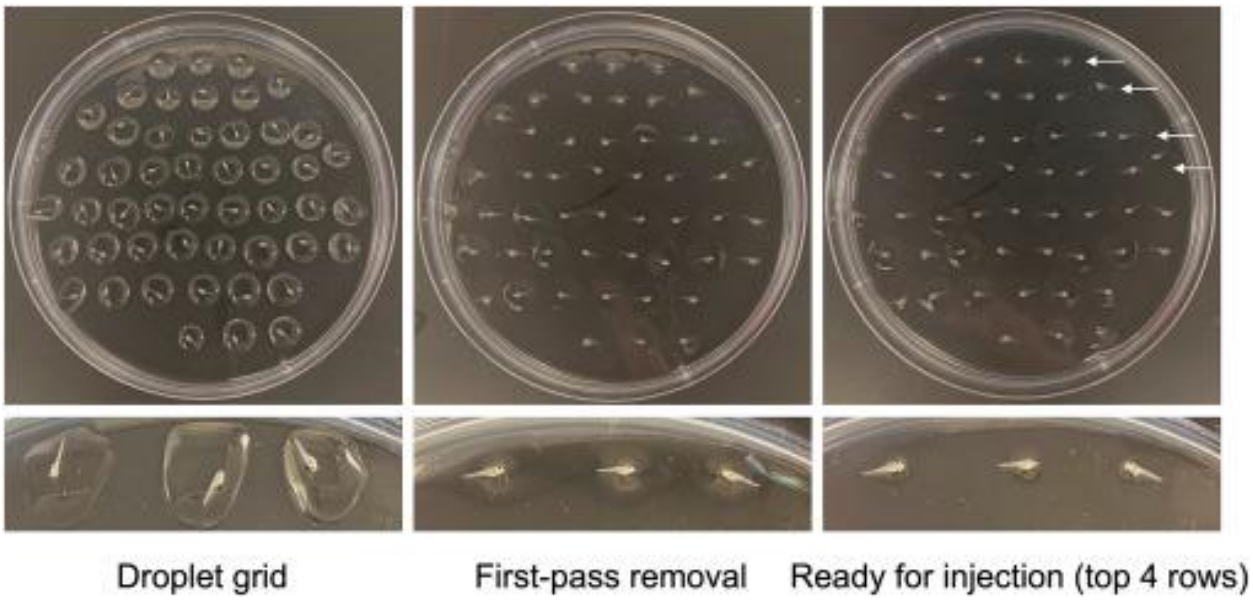

Figure 4.1.4. Plating of tadpoles for injection. Start by plating a grid of tadpoles in individual droplets. Then, orient tadpoles with ventral sides in the same direction while removing most of the media. Anterior/posterior orientation does not matter. Finally, to prevent movement when injecting, remove as much of the media from each tadpole as possible. As an example, the top 4 rows of panel 3 show tadpoles ready for injection, compared to the bottom 4 rows. Top 4 rows are denoted by arrows.

Inject into the ventral tail vein

Timing: 10–30 min

You can identify the tail vein by the movement of blood. Successful injections will fill the ventral tail vein and the displacement may be clearly visible. We recommend 2, 2 nL injections as higher volumes occasionally leak from the vein. 2 injections allow more delivery without creating too much pressure in the vein.

16. Place the plate of "dried" and aligned tadpoles in your injection setup (Figure 4.1.3).

Note: Orient the tadpole such that the needle is able to go into the ventral tail vein from the ventral side. If tadpoles are arranged well, this angle should be sufficient for injecting most of the tadpoles without rotating the plate much. You will need to adjust the lighting and zoom until you are able to identify the tail vein in the bottom left tadpole of your plate.

17. Bring the needle close to the tadpole to inject. To make sure you have found the tail vein, you can gently poke the tadpole (but do not pierce the tail) to see the blood flowing more readily (Methods video S1).
18. Insert the needle into the tail vein and inject 1 or 2 times, depending on your experiment and volume.

Note: Move slowly, being careful to not pierce all the way through the tail.

Note: To minimize injury when injecting 2 times, insert the needle and inject twice in one location without withdrawing the needle between injections.

19. Repeat for each tadpole.

Note: Because of the double coating of agarose, you will likely need to adjust focus between each animal.

Note: Occasionally mucus from the surface of the tadpoles will accumulate on the tip of the needle. This mucus can be removed by gently pulling with forceps or dipping in neighboring agarose. This mucus does not interfere with the needle's ability to pierce the tail vein and may not seem like a problem. However, it may change injection volume if it is not removed, so we recommend removing it when it becomes visible.

Allow tadpoles to recover

Timing: 10–15 min

20. Gently fill the injection lid with 1/9× MR from the edge of the plate, allowing the media to slowly wash over the tadpoles.
21. Most tadpoles, if they did not dry out, should immediately float off the base. If the tail gets stuck, we recommend removing that tadpole as the tail tissue will tear when it begins

swimming.

22. The floating tadpoles will need 5–10 min to recover from the anesthesia.

Screen to confirm injections

Timing: 3–4 h

Confirmation of proper injection is critical for downstream analysis. While signal can be screened after a few minutes, we find it best to wait until a few hours have passed to confirm the tail vein injection and allow circulation of the injection mix before any further experimentation.

23. Allow tadpoles to recover in a light protected environment (under a box or in a dark incubator) to preserve fluorescence.
24. After tadpoles have recovered for 3 h, anesthetize as before and screen for tracer using a fluorescent microscope. Tadpoles that have been correctly injected should be easy to identify, as shown in the "expected outcomes."

4.1.8. Expected outcomes

Successful injections can be screened around 3 h post injection. You can also screen immediately after injection, but you will see more consistent distribution of fluorescent tracers after 3 h (Figures 4.1.5 and 4.1.6). If the tail vein is missed and the axial tissue is instead targeted, the tracers will accumulate in the region that was injected, as shown (Figures 4.1.5 and 4.1.6). The injection success usually is within 90–100%.

Typically, successful control injections with tracers do not result in mortality and tails will appear normal. Rarely, tails will be damaged or torn, and we recommend removing these animals from subsequent analysis (Figure 4.1.7). Tadpoles should be healthy for at least 3 days post injection,

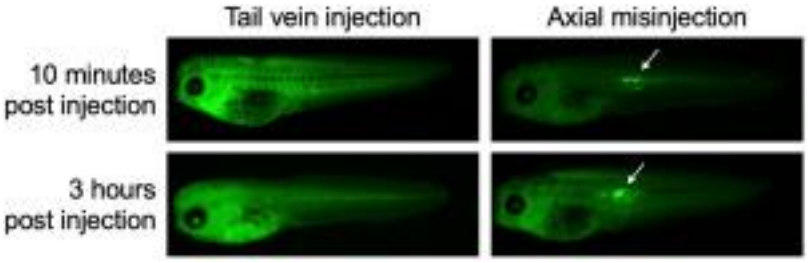

Figure 4.1.5. Expected results after injection with 2NBDG. Stage 41 tadpoles after injection with 4 nL of 5 mM 2NBDG. At 10 min, the signal is clearly seen in the vasculature between somites if injected into the tail vein. Signal is more uniformly distributed throughout most tissues by 3 h post injection. If misinjected, the fluorescent dye accumulates strongly at 10 min and 3 h post injection, seen by a much stronger signal in the notochord or somites. Each column is the same tadpole imaged at each time point. Arrows denote misinjection site.

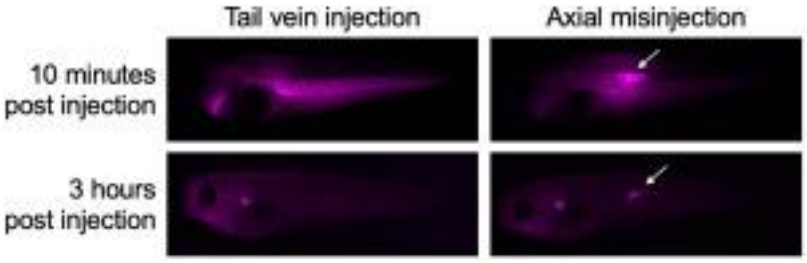

Figure 4.1.6. Expected results after injection with fluoro-Ruby. Stage 41 tadpoles after injection with 4 nL of 500 μM fluoro-Ruby. At 10 min, the signal is seen in the vasculature between somites if injected into the tail vein. By 3 h post injection, the signal is largely accumulated in the kidney. If misinjected, the fluorescent dye accumulates strongly at 10 min and 3 h post injection. At 3 h post injection, some of the dextran will end up in the circulatory system and in the kidney, but the mis-targeted injection is still clearly visible. Arrows denote misinjection site.

allowing additional experimentation. This protocol can be used for molecular or biochemical perturbation of tadpoles for tail regeneration assays as previously described (Patel, Schattinger, et al. 2022; 2022; Kakebeen et al. 2020; Aztekin et al. 2020) and could be implemented for studies of developmentally vital pathways at older stages, circumventing embryonic phenotypes. Similar strategies have been implemented for targeted delivery of vivo-morpholinos to the retina (Liu et al. 2012) and algae to the blood vessels of the brain (Özugur et al. 2022) Our tail vein protocol allows for systematic delivery throughout the tadpole, as shown with our 2NBDG

experiments, and is adaptable for quickly and efficiently scaling up experiments to acquire enough animals for downstream studies.

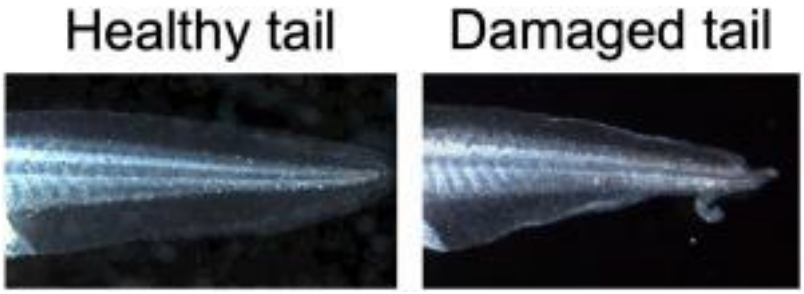

Figure 4.1.7. Tadpoles after recovery from injection. After completing this protocol, tadpoles should appear as on the left with minimal injury to the tail. If the tadpoles dry to the plate or injections take too long, the tail will be damaged as on the right. Lengthy injection time or poor handling most often leads to tearing of the fin tissue at the posterior of the tail.

4.1.9. Limitations

The use of tracers to confirm efficient injection is important, but tracers can interfere with downstream applications, particularly fluorescent-based assays such as fluorescence *in situ* hybridization or immunohistochemistry.

4.1.10. Troubleshooting

Problem 1: Tail fins are missing or torn after injections (steps 20–24).

Potential solution: It is likely the tails are drying too much during the injection process. This problem either means that the agarose is not sufficiently thick or that the injections are taking too long. We first recommend scaling back on the number of tadpoles plated on the dish to get comfortable with finding and injecting the tail veins. If the agarose is too thin, make sure you are using at least 1.5% agarose.

Problem 2: The tip of the needle becomes hard to see/develops a film (steps 17–18).

Potential solution: After several injections, you may see some residue accumulate on the tip of the needle. This residue is normal and is likely from mucus on the skin or agarose from the plate. This material can be removed by either gently nudging it with forceps or by poking the tip into a thicker patch of agarose on the plate, followed by several mock injections to confirm clearing of the tip. This process is important to ensure no errors in injection volume. If the issue persists, we suggest recovering successfully injected tadpoles and clipping a fresh needle for further experiments.

Problem 3: Many injections are not circulating or are mistargeted after protocol completion.
Potential solution: Identifying the tail vein can be challenging, so prior to piercing the skin gently poke the tadpole at the desired injection site. The flow of blood should be visible, though may require adjusting light settings on the scope to see clearly. Once blood flow is confirmed, you should position the needle and insert until the bore is just inside the tail vein. If positioned currently, injection mix should fill the vein and visible displacement will be seen. If the needle inserts too close to organs, they could be damaged. Injections should always be posterior to the major organs, but if damage is a concern, we have successfully injected roughly halfway down the tail, though the vein can be harder to find.

Problem 4: Most of the injected tadpoles die after protocol completion.
Potential solution: Tadpoles may be dying from the injections because the injected compounds are lethal, in which case we suggest performing careful dose curves to confirm lethality. It is also possible that the injection needle is too wide, which would be visible by blood flowing from the injection site. In this case, we recommend pulling longer tapers such that the clipped needle has a

thinner bore.

Problem 5: Tadpoles are becoming bloated/turning white after protocol completion (usually the following day).

Potential solution: Bloating or whitening likely means the tadpoles are becoming infected. While antibiotics could be used to reduce the likelihood of infection, they may also have other effects on the tadpoles that could influence findings (Chapman et al. 2022; Bishop and Beck 2021). We recommend replacing all media used in the experiment and making sure that the plates are sterile to rule out contamination. Additionally, all plastic and tips should be clean; we do not recommend reusing plastic lids or needles after an experiment is completed.

4.1.11. Acknowledgments

We would like to acknowledge past lab members of the Wills Lab for helping to establish and optimize early versions of the protocol presented here. This work was supported by the National Science Foundation Graduate Research Fellowship Program under grant no. DGE-1762114 to J.H.P., CMB Training Grant NIGMS NRSA T32GM007270 to A.A.S., NIH grants 2R01NS099124 and R01GM148490, and an award from the University of Washington Research Royalty Fund to A.E.W.

4.1.12. Author contributions

J.H.P. and A.A.S. coordinated the study, designed and conducted the experiments, and wrote the manuscript draft. A.E.W. supervised study design and experimentation and provided funding. J.H.P., A.A.S., A.D.K., L.R.L., and A.E.W. edited the manuscript.

4.2. Optimizing hybridization chain reaction (HCR) for the Wills Lab

During the last two years of my PhD, I sought to find a way to visualize neuron types without using antibodies. While immunohistochemistry provides valuable data about protein localization, many times commercial antibody options do not work in *Xenopus* or require long troubleshooting periods. As such, I decided to implement hybridization chain reaction (HCR), which uses amplifying RNA probes to label RNA targets. This process is not as expensive as testing commercial antibodies and probes can be generated to target any *Xenopus tropicalis* RNA of interest.

I originally tested a previously published protocol in *Xenopus laevis* (Willsey 2021) then made several adaptations to optimize the protocol in *X. tropicalis*. The most crucial changes were the increase in probe pool size to at least 40 probes per target and the increase to probe concentration from 4 nM to 16 nM; these changes allowed us to visualize RNA from low-expressing targets such as *prdm14*. Amplifiers were used that fluoresced in the 564, 594, and 637 nm wavelengths, since 488 does not seem to work in *Xenopus tropicalis*, a phenomenon confirmed by the Willsey Lab that seems to be *Xenopus* specific.

These probes were generated using the insitu_probe_generator from the Özpolat Lab (Kuehn et al. 2022), an algorithm that enables custom HCR probe generation (Table 4.2.1). This work was done with consultation from Kourtnie Whitfield from the Crespi Lab (WSU), Erik Black from the Rasmussen Lab (UW), and Sydney Sattler from the Abitua Lab (UW).

Table 4.2.1. HCR Probe Sequences:

B2_prdm14_32_Dla100	CCTCGTAAATCCTCATCAaaTAATAAATTAAAATTGGCACAGTCC
B2_prdm14_32_Dla100	TATAAATAAGCATCTTCTTAAAAACaaATCATCCAGTAAACCGCC
B2_prdm14_32_Dla100	CCTCGTAAATCCTCATCAaaAAGGCCGGAGTGGATTTGCATGTGA
B2_prdm14_32_Dla100	GGGGGTGCAACTGCAGAGAACTTGCaaATCATCCAGTAAACCGCC
B2_prdm14_32_Dla100	CCTCGTAAATCCTCATCAaaTTGCCACACAGGGAGCAGATGTAGC
B2_prdm14_32_Dla100	CGAAACTCCTCCATTTCCAGAAAGGaaATCATCCAGTAAACCGCC
B2_prdm14_32_Dla100	CCTCGTAAATCCTCATCAaaGGCTGTCGTGGGCGGCGTGTGATGC
B2_prdm14_32_Dla100	TTTCCTTGGTATGAGTGCGCCGTACaaATCATCCAGTAAACCGCC
B2_prdm14_32_Dla100	CCTCGTAAATCCTCATCAaaAGGCTTCTCGCCCGAGTGCTGCCGG
B2_prdm14_32_Dla100	GGCCTTGCCACAGTGTTTGCATTTGaaATCATCCAGTAAACCGCC

B2_prdm14_32_Dla100	CCTCGTAAATCCTCATCAaaAATGCCTTGTTGCAGTAGACGCACT
B2_prdm14_32_Dla100	TGTGTGCGAAGGATGCTTGATGCAGaaATCATCCAGTAAACCGCC
B2_prdm14_32_Dla100	CCTCGTAAATCCTCATCAaaTGTGCTTGTTCAGGCTGGAAGACTG
B2_prdm14_32_Dla100	ATGGTCTCTCTCCCGAGTGGACCCTaaATCATCCAGTAAACCGCC
B2_prdm14_32_Dla100	CCTCGTAAATCCTCATCAaaGTGGGGCCGGTGCTTCTCATGTACA
B2_prdm14_32_Dla100	AAAGCTTTTGCCACAGACAGTGCACaaATCATCCAGTAAACCGCC
B2_prdm14_32_Dla100	CCTCGTAAATCCTCATCAaaTTCTCAAACGACCTGTTGCACAGAT
B2_prdm14_32_Dla100	AGGATGTGGATCCGCAGCCTGTCCCaaATCATCCAGTAAACCGCC
B2_prdm14_32_Dla100	CCTCGTAAATCCTCATCAaaCACAGCGCGTATACTTCAGGTGCTT
B2_prdm14_32_Dla100	ACGGAAACTTTCTGTCCCCTTGGTCaaATCATCCAGTAAACCGCC
B2_prdm14_32_Dla100	CCTCGTAAATCCTCATCAaaGCCGCAGCGCTCGCACTTATATCCC
B2_prdm14_32_Dla100	CCGGTAGTACCGGTACGCGAACACTaaATCATCCAGTAAACCGCC
B2_prdm14_32_Dla100	CCTCGTAAATCCTCATCAaaAGGCTGAGTGGGATGCCGAGGAATT
B2_prdm14_32_Dla100	GGGGGCCTTCCTTCCCCTAGGCCCTaaATCATCCAGTAAACCGCC
B2_prdm14_32_Dla100	CCTCGTAAATCCTCATCAaaGCTCCTGCCCGGGGAGAATCTCTTT
B2_prdm14_32_Dla100	GGTAGGAGTCCCCGTACCAGACGAGaaATCATCCAGTAAACCGCC
B2_prdm14_32_Dla100	CCTCGTAAATCCTCATCAaaCTGCAGCGCAATCAGGTTCTGCTCC
B2_prdm14_32_Dla100	CGACTCATAGTAAATCTCCCCCTCGaaATCATCCAGTAAACCGCC
B2_prdm14_32_Dla100	CCTCGTAAATCCTCATCAaaATCCAGTTCCCTGCGGCCCCTTTCC
B2_prdm14_32_Dla100	GGGAACCGCGCACAATTCACCCGGGaaATCATCCAGTAAACCGCC
B2_prdm14_32_Dla100	CCTCGTAAATCCTCATCAaaCAAAGATCTCCCACATAAGAGAGTT
B2_prdm14_32_Dla100	CTATAAAGTGACTGAGCCGCCCCTCaaATCATCCAGTAAACCGCC
B2_prdm14_32_Dla100	CCTCGTAAATCCTCATCAaaCACCACTTTGCCTTGGAATGGGCCG
B2_prdm14_32_Dla100	CCCATAAGTCTTTATCTCGCTGGGGaaATCATCCAGTAAACCGCC
B2_prdm14_32_Dla100	CCTCGTAAATCCTCATCAaaCAGAAGACCCCAGCTTTGGGCAAGG
B2_prdm14_32_Dla100	TTGGCTCCTTTAGGGATGAGGTTCTaaATCATCCAGTAAACCGCC
B2_prdm14_32_Dla100	CCTCGTAAATCCTCATCAaaCTTCTGGCAACTGCAACGAATCTCT
B2_prdm14_32_Dla100	CATAGGAAGTGTCCAGCACTGTCAGaaATCATCCAGTAAACCGCC
B2_prdm14_32_Dla100	CCTCGTAAATCCTCATCAaaGCAGGCAGTAGGAATCCGCAGGCCA
B2_prdm14_32_Dla100	CAATATGTGTGAATCCAGTCCTGTAaaATCATCCAGTAAACCGCC
B2_prdm14_32_Dla100	CCTCGTAAATCCTCATCAaaCTCCTGGAGTCGCTGCCGCAGGTGT
B2_prdm14_32_Dla100	AGGGCATGAGTGACAGTCTGTTGGCaaATCATCCAGTAAACCGCC
B2_prdm14_32_Dla100	CCTCGTAAATCCTCATCAaaCTGTGAAATGGTAAGTGCGGGAGGG
B2_prdm14_32_Dla100	CGTACAGAACTGTCTGTAGATCTTCaaATCATCCAGTAAACCGCC
B2_prdm14_32_Dla100	CCTCGTAAATCCTCATCAaaCGCGCTTTTGCACTTCTTTGGGACA
B2_prdm14_32_Dla100	CACCTCCAGGCTGGGGAGGCTCAGGaaATCATCCAGTAAACCGCC
B2_prdm14_32_Dla100	CCTCGTAAATCCTCATCAaaGGGTGGGAGGCTCGGATAGCGCTGA
B2_prdm14_32_Dla100	GGAGACTTGAGTTTCTCCGGGCTGCaaATCATCCAGTAAACCGCC
B2_prdm14_32_Dla100	CCTCGTAAATCCTCATCAaaGCTGCACCTTAGTGAGGATGGAATA
B2_prdm14_32_Dla100	AGTCCTGCTGGCTGTAGGGGACAGGaaATCATCCAGTAAACCGCC
B2_prdm14_32_Dla100	CCTCGTAAATCCTCATCAaaATTTGGGGGCAAACTCTGGGTCAGT
B2_prdm14_32_Dla100	GCCCAATAGCGGGTTCACTTGCGCAaaATCATCCAGTAAACCGCC
B2_prdm14_32_Dla100	CCTCGTAAATCCTCATCAaaCCCAAGTGAGAGGAGTTGGTGACCA
B2_prdm14_32_Dla100	GCAGGGAGGTCTCGGAAGTTAAAGGaaATCATCCAGTAAACCGCC
B2_prdm14_32_Dla100	CCTCGTAAATCCTCATCAaaTCTCATGAGGAGTGGCCAGTATGTT
B2_prdm14_32_Dla100	TGCCCAGGGATTTCAGCGGGTTAAAaaATCATCCAGTAAACCGCC
B2_prdm14_32_Dla100	CCTCGTAAATCCTCATCAaaGGCTGATATGAAGTGGGTCACAAGG
B2_prdm14_32_Dla100	GGGGGAAATAAGGGCCAACAGCTGAaaATCATCCAGTAAACCGCC
B2_prdm14_32_Dla100	CCTCGTAAATCCTCATCAaaTAGAGCCATGATCATGGGCTTTGCA
B2_prdm14_32_Dla100	AGGCCTGTCATTCGGGCTGGGAACAaaATCATCCAGTAAACCGCC
B2_prdm14_32_Dla100	CCTCGTAAATCCTCATCAaaACTGTTATGACTGAACCCTCGCTAA
B2_prdm14_32_Dla100	ACAGAACAGGCAGAAGGTCAGTCCCaaATCATCCAGTAAACCGCC
B2_prdm14_32_Dla100	CCTCGTAAATCCTCATCAaaGGCCCCGGCTCATCCCGTACTAATG
B2_prdm14_32_Dla100	CAGATAATCCTCCAAGTAGAATCCTaaATCATCCAGTAAACCGCC
B2_lepr_49_Dla100	CCTCGTAAATCCTCATCAaaTCAAAGAGGAATGGAGAACCATTTG
B2_lepr_49_Dla100	CTCAGGTCTTCAAAAACTGCTTCAGaaATCATCCAGTAAACCGCC
B2_lepr_49_Dla100	CCTCGTAAATCCTCATCAaaTTTGGCACATCTTTCCAAAATAATT
B2_lepr_49_Dla100	CCCTGAGCCCAAGAGCAGTGCTTTGaaATCATCCAGTAAACCGCC
B2_lepr_49_Dla100	CCTCGTAAATCCTCATCAaaTTCCCATAAGCAAGAAGACTGAAAA
B2_lepr_49_Dla100	TCATCCTTTGGTGAGATATTAGTATaaATCATCCAGTAAACCGCC
B2_lepr_49_Dla100	CCTCGTAAATCCTCATCAaaGGCATCCTTTGGTGCTTCAGTCAAT
B2_lepr_49_Dla100	AATAACTGGCAGTATAACATACAAGaaATCATCCAGTAAACCGCC
B2_lepr_49_Dla100	CCTCGTAAATCCTCATCAaaGAACGACCAACTCCTTCTGGAAATA
B2_lepr_49_Dla100	ACTGTAGAAAAGCCATTTACAACTTaaATCATCCAGTAAACCGCC
B2_lepr_49_Dla100	CCTCGTAAATCCTCATCAaaTCATGTTTCGAGGGATATTCATCCA
B2_lepr_49_Dla100	AAAAATTGTCTTCAATATAACACCTaaATCATCCAGTAAACCGCC

B2_lepr_49_Dla100	CCTCGTAAATCCTCATCAaaCCATTCAACAATAAATTCCAATGGC
B2_lepr_49_Dla100	TACCTTTTCTTCATTCCCAAGATTCaaATCATCCAGTAAACCGCC
B2_lepr_49_Dla100	CCTCGTAAATCCTCATCAaaGCCACTGCACAAGTGTTGTTCATAT
B2_lepr_49_Dla100	TCACTTTTGGGCAACATAGTCCACAaaATCATCCAGTAAACCGCC
B2_lepr_49_Dla100	CCTCGTAAATCCTCATCAaaCTGTACTCATTTCACAGGAAAATGT
B2_lepr_49_Dla100	AAACTCTGAAGGACTCCACAGATGTaaATCATCCAGTAAACCGCC
B2_lepr_49_Dla100	CCTCGTAAATCCTCATCAaaGGAGTTGACAGCTAGAAGTGTAACT
B2_lepr_49_Dla100	CTTGCTGTTTGTCAGAGAGTATCCAaaATCATCCAGTAAACCGCC
B2_lepr_49_Dla100	CCTCGTAAATCCTCATCAaaTGCTTTGTTGTGTTTCCTACATATT
B2_lepr_49_Dla100	ACAGCGTTATCCGATAAAGTGAAAGaaATCATCCAGTAAACCGCC
B2_lepr_49_Dla100	CCTCGTAAATCCTCATCAaaGAATGACTTCATATCCTTGAATAGA
B2_lepr_49_Dla100	ACCAGGTGACATTTTTAGAATTCAGaaATCATCCAGTAAACCGCC
B2_lepr_49_Dla100	CCTCGTAAATCCTCATCAaaCCAAATAATGGAAATATTGTCCCCT
B2_lepr_49_Dla100	CAGTGAGTGCTCTGATGGTAGGGGCaaATCATCCAGTAAACCGCC
B2_lepr_49_Dla100	CCTCGTAAATCCTCATCAaaCAGAAAGTTGGTCCTTGCAAAGGAA
B2_lepr_49_Dla100	TGCATGGGATTATTGTGAGTAGTTCaaATCATCCAGTAAACCGCC
B2_lepr_49_Dla100	CCTCGTAAATCCTCATCAaaGTTGGCTCCAATCACTCCAGTATCC
B2_lepr_49_Dla100	TAATGTCTCTTACAACAGTGTGCACaaATCATCCAGTAAACCGCC
B2_lepr_49_Dla100	CCTCGTAAATCCTCATCAaaGACAGTGTATGAGGCACAGACATCT
B2_lepr_49_Dla100	TCCATCAGTTCTTCTAGAACGTACTaaATCATCCAGTAAACCGCC
B2_lepr_49_Dla100	CCTCGTAAATCCTCATCAaaAAAATATCCAGCACCTTCCATATTA
B2_lepr_49_Dla100	ACCTGTATACTGACAAATTCTTCTTaaATCATCCAGTAAACCGCC
B2_lepr_49_Dla100	CCTCGTAAATCCTCATCAaaGGAACTGAAGATCAGTAGATGGAAG
B2_lepr_49_Dla100	CTTGCCCTTGCAAACAGTAACGGACaaATCATCCAGTAAACCGCC
B2_lepr_49_Dla100	CCTCGTAAATCCTCATCAaaTCCTGAACCCTTAGTCATTTCAGCT
B2_lepr_49_Dla100	AGGCCTTTTCCAACTCACATATAAAaaATCATCCAGTAAACCGCC
B2_lepr_49_Dla100	CCTCGTAAATCCTCATCAaaGTATTTATGGGAAGGATGCAAACAG
B2_lepr_49_Dla100	ACTCTTGATGGAGCAAGTGGTTTTAaaATCATCCAGTAAACCGCC
B2_lepr_49_Dla100	CCTCGTAAATCCTCATCAaaGTATCTCAATCCACATAATATAGCC
B2_lepr_49_Dla100	GCGAATTAAGTGCTCCTAAATGGTGaaATCATCCAGTAAACCGCC
B2_lepr_49_Dla100	CCTCGTAAATCCTCATCAaaTTCATAGAATCCATCCATTTGTAAC
B2_lepr_49_Dla100	GACAAGGTGAACAGGCTCAAATGTGaaATCATCCAGTAAACCGCC
B2_lepr_49_Dla100	CCTCGTAAATCCTCATCAaaTTTAAATCTTTATCTAAGCAATAAA
B2_lepr_49_Dla100	CAATCTTTTGAAATCGGCACATTGCaaATCATCCAGTAAACCGCC
B2_lepr_49_Dla100	CCTCGTAAATCCTCATCAaaCACTTCCTTCAGGTAGTGTCATATT
B2_lepr_49_Dla100	TGTTTCTATAATACTTGAACTGTAAaaATCATCCAGTAAACCGCC
B2_lepr_49_Dla100	CCTCGTAAATCCTCATCAaaAATACTGATGTTGACATCTAAAACA
B2_lepr_49_Dla100	TTTTTGATTCCCATCAGTTTCACATaaATCATCCAGTAAACCGCC
B2_lepr_49_Dla100	CCTCGTAAATCCTCATCAaaTTATGGTTAATACAGCAATGTAAGG
B2_lepr_49_Dla100	ATTTCTGCATACCGATGATGACATTaaATCATCCAGTAAACCGCC
B2_lepr_49_Dla100	CCTCGTAAATCCTCATCAaaTTGTATTGAGGTGAGTCAGGAACAC
B2_lepr_49_Dla100	CATATCGGAACTTTCCCTTTGGTTTaaATCATCCAGTAAACCGCC
B2_lepr_49_Dla100	CCTCGTAAATCCTCATCAaaCTGATGCTTTGGTATCTTCTCCCCA
B2_lepr_49_Dla100	GCTAAAATAATCACTGGTCATTCTGaaATCATCCAGTAAACCGCC
B2_lepr_49_Dla100	CCTCGTAAATCCTCATCAaaGGAACTTTCTTGCCATTGTCACAAA
B2_lepr_49_Dla100	TTTAGCCACCATGTGATATTACTGGaaATCATCCAGTAAACCGCC
B2_lepr_49_Dla100	CCTCGTAAATCCTCATCAaaTACTAACCAATACTTTTTGGGGGAA
B2_lepr_49_Dla100	AGCAGGAGACAGAAGTGCTGGAGCCaaATCATCCAGTAAACCGCC
B2_lepr_49_Dla100	CCTCGTAAATCCTCATCAaaGGTTTTACTCCAGTCACTCCAGAGT
B2_lepr_49_Dla100	GAATACATCTTGTGAATTTAAAACCaaATCATCCAGTAAACCGCC
B2_lepr_49_Dla100	CCTCGTAAATCCTCATCAaaTCTATTACCATTTCTGTACAAGGCT
B2_lepr_49_Dla100	GATTTGTGTAAGTTTATACATCTGAaaATCATCCAGTAAACCGCC
B2_lepr_49_Dla100	CCTCGTAAATCCTCATCAaaTGACCAGCAGATAAACCTGTGAGTT
B2_lepr_49_Dla100	TATCACTGATGATCACTGATGTTTCaaATCATCCAGTAAACCGCC
B2_lepr_49_Dla100	CCTCGTAAATCCTCATCAaaTTGATACTGGAGCTCATAAGCAGCA
B2_lepr_49_Dla100	CTCTGCTGCTTTCACTGTATATCTTaaATCATCCAGTAAACCGCC
B2_lepr_49_Dla100	CCTCGTAAATCCTCATCAaaGTGCCTTGTTCCATTATTTCCGCTC
B2_lepr_49_Dla100	ATGGGTTTCAACCAAAACACCTTTAaaATCATCCAGTAAACCGCC
B2_lepr_49_Dla100	CCTCGTAAATCCTCATCAaaTATGGTAAGGTACAACAGACATAGG
B2_lepr_49_Dla100	AGTCATCAGGAGGATCAGGCTTGACaaATCATCCAGTAAACCGCC
B2_lepr_49_Dla100	CCTCGTAAATCCTCATCAaaGATTTCAATCCATAGGATGTAGGTA
B2_lepr_49_Dla100	GGAGTGAAGAAGTGCTGTGATATTCaaATCATCCAGTAAACCGCC
B2_lepr_49_Dla100	CCTCGTAAATCCTCATCAaaTCACATTTCTCATATCCAAAGCATC
B2_lepr_49_Dla100	TTGAATTTTACAGACGGTACAATGCaaATCATCCAGTAAACCGCC
B2_lepr_49_Dla100	CCTCGTAAATCCTCATCAaaTTGCAACCAAAGAATAATGAAGACT
B2_lepr_49_Dla100	ATTCAGCTGTGCCTTTCAGCTCACTaaATCATCCAGTAAACCGCC

B2_lepr_49_Dla100	CCTCGTAAATCCTCATCAaaTTCTGGTAATAACTGCAGGTCACAA
B2_lepr_49_Dla100	TTGATAATCTGTTACAATGTGCTTTaaATCATCCAGTAAACCGCC
B2_lepr_49_Dla100	CCTCGTAAATCCTCATCAaaCACTGTACTTTCCAGCTGAAATCTT
B2_lepr_49_Dla100	AGTGTATTTGCTTTTTCCTCAAATGaaATCATCCAGTAAACCGCC
B2_lepr_49_Dla100	CCTCGTAAATCCTCATCAaaAAAGCATTTCCTTTAACTCTGCAAC
B2_lepr_49_Dla100	GTTGGATATCTGATGCAAAGCTTGCaaATCATCCAGTAAACCGCC
B2_lepr_49_Dla100	CCTCGTAAATCCTCATCAaaATGATCCCATAGGCAACATGAAACA
B2_lepr_49_Dla100	GTTCTGACTTGAAAAGTTTGTATTTaaATCATCCAGTAAACCGCC
B2_lepr_49_Dla100	CCTCGTAAATCCTCATCAaaGTACATCTAAAATCCGACCTGCCCT
B2_lepr_49_Dla100	CCTTGTGATTTTAAATCAGCTAAATaaATCATCCAGTAAACCGCC
B2_lepr_49_Dla100	CCTCGTAAATCCTCATCAaaACTTATTCTGTAAAATTCCAGCCAG
B2_lepr_49_Dla100	AAGTATCATACTTCCCTGAGATATCaaATCATCCAGTAAACCGCC
B2_lepr_49_Dla100	CCTCGTAAATCCTCATCAaaAATGCAAGTCAGAAAGAAATCGGAA
B2_lepr_49_Dla100	TGGATAATTTACTGACTTGTTGGTCaaATCATCCAGTAAACCGCC
B2_lepr_49_Dla100	CCTCGTAAATCCTCATCAaaGCTGTTATTTGCATATATCTTAAGA
B2_lepr_49_Dla100	GGAGTCCAGTACATCTCTGAATAAGaaATCATCCAGTAAACCGCC
B2_lepr_49_Dla100	CCTCGTAAATCCTCATCAaaACATATCTTGCTTTGGGTAGTTTAC
B2_lepr_49_Dla100	GAAAGAATGGCAATATCCAGTGCCAaaATCATCCAGTAAACCGCC
B2_lepr_49_Dla100	CCTCGTAAATCCTCATCAaaGAGTGTGAGAAGTTGCTGCCTTCTG
B2_lepr_49_Dla100	CTTCTGGACCCCTCAGCAATAGCCGaaATCATCCAGTAAACCGCC
B1_lhx1_42_Dla100	GAGGAGGGCAGCAAACGGaaGGATTATTACTAAAACATTAGGCTC
B1_lhx1_42_Dla100	TTTTTGAACAAAGAGGTTTCTAAAAtaGAAGAGTCTTCCTTTACG
B1_lhx1_42_Dla100	GAGGAGGGCAGCAAACGGaaCTGCTTATAGTTCCATAGTCATTTT
B1_lhx1_42_Dla100	AATTTGACGTCAGACGTAAACAGTTtaGAAGAGTCTTCCTTTACG
B1_lhx1_42_Dla100	GAGGAGGGCAGCAAACGGaaTTCCAACAGACCTTCATAATGAGGA
B1_lhx1_42_Dla100	TTTTTGTTTCAAGTCTCCTTCCAGGtaGAAGAGTCTTCCTTTACG
B1_lhx1_42_Dla100	GAGGAGGGCAGCAAACGGaaTAGAATAGTTGATGCTGAGGGGTTT
B1_lhx1_42_Dla100	TTTTTCGTGTGAGTAGCTTTGTGAAtaGAAGAGTCTTCCTTTACG
B1_lhx1_42_Dla100	GAGGAGGGCAGCAAACGGaaGTTGTGTCGCACCTGAATATACAGG
B1_lhx1_42_Dla100	TTGTTGTATTTTGTTATTTTGGCAAtaGAAGAGTCTTCCTTTACG
B1_lhx1_42_Dla100	GAGGAGGGCAGCAAACGGaaCAGTACATTTCTCCAAGGAAGAGAA
B1_lhx1_42_Dla100	GTGTCTGAAGCTAAAACAGTCTGGCtaGAAGAGTCTTCCTTTACG
B1_lhx1_42_Dla100	GAGGAGGGCAGCAAACGGaaTAGGCAATTCTTGATAAGGTATTTT
B1_lhx1_42_Dla100	TCAACATTCTAGACAGACTCAACATtaGAAGAGTCTTCCTTTACG
B1_lhx1_42_Dla100	GAGGAGGGCAGCAAACGGaaTTGCACTTAGGTGTACTGTGTGTAC
B1_lhx1_42_Dla100	TCCTATGGAGTCCTTCAAGATTATCtaGAAGAGTCTTCCTTTACG
B1_lhx1_42_Dla100	GAGGAGGGCAGCAAACGGaaTACCACCTACCAGGCTATTCTTTTC
B1_lhx1_42_Dla100	GAAAGCAGATTTATATTGTGTCCTGtaGAAGAGTCTTCCTTTACG
B1_lhx1_42_Dla100	GAGGAGGGCAGCAAACGGaaCAGCGTCACCAGTTTGATTTTTCTG
B1_lhx1_42_Dla100	CCCCTAGCATGACAAAACTCTACTTtaGAAGAGTCTTCCTTTACG
B1_lhx1_42_Dla100	GAGGAGGGCAGCAAACGGaaTTAGGACAGAATATAATTTTATTTA
B1_lhx1_42_Dla100	TTTTTCCATCCAAAACTGTACACACtaGAAGAGTCTTCCTTTACG
B1_lhx1_42_Dla100	GAGGAGGGCAGCAAACGGaaGAAACGTTGACATGGTAGCCCATTG
B1_lhx1_42_Dla100	GTTCTGTACACCACGTTATTTTCATtaGAAGAGTCTTCCTTTACG
B1_lhx1_42_Dla100	GAGGAGGGCAGCAAACGGaaGGCTACCACACTGCAGTTTCGTTCA
B1_lhx1_42_Dla100	TTTTTGTTTCTGTTTTTGTCCAACTtaGAAGAGTCTTCCTTTACG
B1_lhx1_42_Dla100	GAGGAGGGCAGCAAACGGaaAACCTGCTGCTCCATTGACCGATAG
B1_lhx1_42_Dla100	CTGGCGGGTGTGACAAATGGTTGCCtaGAAGAGTCTTCCTTTACG
B1_lhx1_42_Dla100	GAGGAGGGCAGCAAACGGaaGACATAGAGTGCATGGAACCTGGTA
B1_lhx1_42_Dla100	GGGGGACTTTGACCAAACACTTCTGtaGAAGAGTCTTCCTTTACG
B1_lhx1_42_Dla100	GAGGAGGGCAGCAAACGGaaGTGGGTGGGACATTATGTCAGTAAA
B1_lhx1_42_Dla100	TGGGCTCTGGGCTTGGAGAGTCTCCtaGAAGAGTCTTCCTTTACG
B1_lhx1_42_Dla100	GAGGAGGGCAGCAAACGGaaAGGGATTGGGTGATCCATTGCACCA
B1_lhx1_42_Dla100	CTGAGCGTCACTAGATGGGTGGTGTtaGAAGAGTCTTCCTTTACG
B1_lhx1_42_Dla100	GAGGAGGGCAGCAAACGGaaACAAATGGCAAATCTACAGGAGTCT
B1_lhx1_42_Dla100	GGAGTTCCTGCAGGCCCAGAAGAAGtaGAAGAGTCTTCCTTTACG
B1_lhx1_42_Dla100	GAGGAGGGCAGCAAACGGaaAAAAGTCATAGTTGCTGCCAGGGCC
B1_lhx1_42_Dla100	CTTGAGATGATGGGGGTCCTTGTGGtaGAAGAGTCTTCCTTTACG
B1_lhx1_42_Dla100	GAGGAGGGCAGCAAACGGaaGGAGAAGGGTCCATTGGGGATGAGT
B1_lhx1_42_Dla100	ATACTCACTCTGATAATCTCCATAGtaGAAGAGTCTTCCTTTACG
B1_lhx1_42_Dla100	GAGGAGGGCAGCAAACGGaaCTCATCCTTCGGGGGCTGCGGAAGA
B1_lhx1_42_Dla100	CCCGGCTCTAACCTGTCCACCAGCGtaGAAGAGTCTTCCTTTACG
B1_lhx1_42_Dla100	GAGGAGGGCAGCAAACGGaaGCTGTTTCATTCTTCTCTCTTTGGA
B1_lhx1_42_Dla100	CGTGTCTGCGGGCCCCCAGAGCGCTtaGAAGAGTCTTCCTTTACG
B1_lhx1_42_Dla100	GAGGAGGGCAGCAAACGGaaTCGCATGTTGAGACCAGTCTCCTGT
B1_lhx1_42_Dla100	TCGGTTCTGGAACCAGACCTGGATGtaGAAGAGTCTTCCTTTACG

B1_lhx1_42_Dla100	GAGGAGGGCAGCAAACGGaaTTTGGTGTAGCTGCAAAAGCTGCTT
B1_lhx1_42_Dla100	AGCTGCTCCCTTATGTGCCGGGTCGtaGAAGAGTCTTCCTTTACG
B1_lhx1_42_Dla100	GAGGAGGGCAGCAAACGGaaTGGTCCTAGGTCCCCTTCTTTTCGC
B1_lhx1_42_Dla100	GGGTCTCCAGCTGTTTGGCTTTGATtaGAAGAGTCTTCCTTTACG
B1_lhx1_42_Dla100	GAGGAGGGCAGCAAACGGaaCCCAGCCTCCTTATCAGAGATATTG
B1_lhx1_42_Dla100	AAGGTTTTGGTCGTCGTTTTCATTAtaGAAGAGTCTTCCTTTACG
B1_lhx1_42_Dla100	GAGGAGGGCAGCAAACGGaaAGCGGGTCTTGAGATTCAGGAGATA
B1_lhx1_42_Dla100	CTTTCAGAGTCTTTAGCGTCATCTTtaGAAGAGTCTTCCTTTACG
B1_lhx1_42_Dla100	GAGGAGGGCAGCAAACGGaaAGCTGTTTTCTTTGGCAGCGTTGTT
B1_lhx1_42_Dla100	TGGGGTCACTGCCTGTTACTGAGATtaGAAGAGTCTTCCTTTACG
B1_lhx1_42_Dla100	GAGGAGGGCAGCAAACGGaaTTTGCAGACAAACTTATTCTCATCG
B1_lhx1_42_Dla100	GTTGTTGTTGTTGTTTAAGTAATCTtaGAAGAGTCTTCCTTTACG
B1_lhx1_42_Dla100	GAGGAGGGCAGCAAACGGaaTGTTTGTTACACATCATACAGGTGA
B1_lhx1_42_Dla100	ATATAAAGTTCCTCTCCAGTGGAGAtaGAAGAGTCTTCCTTTACG
B1_lhx1_42_Dla100	GAGGAGGGCAGCAAACGGaaCCCTCCTGACTAGGTCACTGGGGGA
B1_lhx1_42_Dla100	AGTTCAAGTGAAACACTTTGCTCCTtaGAAGAGTCTTCCTTTACG
B1_lhx1_42_Dla100	GAGGAGGGCAGCAAACGGaaAAGCCCTGTCCAGCACATTCAACAA
B1_lhx1_42_Dla100	CGCAGCACTGCACGCATTTCACATGtaGAAGAGTCTTCCTTTACG
B1_lhx1_42_Dla100	GAGGAGGGCAGCAAACGGaaAGCACAGTGAACCATTGTCTTTGGT
B1_lhx1_42_Dla100	ACGATCCAGAATGGGCCTTTCGCATtaGAAGAGTCTTCCTTTACG
B1_lhx1_42_Dla100	GAGGAGGGCAGCAAACGGaaTAGGAGGACAGAAGGCAGACACTAT
B1_lhx1_42_Dla100	TTGGGATTTTAAAGGAAGGGGACGGtaGAAGAGTCTTCCTTTACG
B1_lhx1_42_Dla100	GAGGAGGGCAGCAAACGGaaGGAGATCCCCAAGCCAAGGTAGCAG
B1_lhx1_42_Dla100	CCAGAAAGACAAGCAGACGGAGCTGtaGAAGAGTCTTCCTTTACG
B1_lhx1_42_Dla100	GAGGAGGGCAGCAAACGGaaTCAGTTGCCTTCTGGCTCTGAGGTA
B1_lhx1_42_Dla100	GTAGGAGAGGGCAGAGATGTGGGGCtaGAAGAGTCTTCCTTTACG
B1_lhx1_42_Dla100	GAGGAGGGCAGCAAACGGaaGGCTATAGAAATTACAAGCCAAGGG
B1_lhx1_42_Dla100	CAGTCAATGCTGAAAGTGCATCTGTtaGAAGAGTCTTCCTTTACG
B1_lhx1_42_Dla100	GAGGAGGGCAGCAAACGGaaCCACGGACAGGCTCCACAAACACAC
B1_lhx1_42_Dla100	TTAGGTTGCCCGGCATCACGTCCAGtaGAAGAGTCTTCCTTTACG
B1_lhx1_42_Dla100	GAGGAGGGCAGCAAACGGaaTAATTTTCCTTTTCTTCCCACTCCT
B1_lhx1_42_Dla100	GGGCCGTTGGTTCGGCTTGCAGTTAtaGAAGAGTCTTCCTTTACG
B1_lhx1_42_Dla100	GAGGAGGGCAGCAAACGGaaCGTTCTCACTTAACGTCACCAAGGA
B1_lhx1_42_Dla100	GGTATCCCGGGGGCTGATTCCTTTGtaGAAGAGTCTTCCTTTACG
B1_lhx1_42_Dla100	GAGGAGGGCAGCAAACGGaaCTGGCTTTATTGTCCAAATCCCACT
B1_lhx1_42_Dla100	CCCCTAGCCCATCAACAACTTCTGCtaGAAGAGTCTTCCTTTACG
B1_lhx1_42_Dla100	GAGGAGGGCAGCAAACGGaaATCCCCCGTGAGCATCTACGGTGCC
B1_lhx1_42_Dla100	TGCTGAACAAAGTCGATGAATGAAGtaGAAGAGTCTTCCTTTACG
B3_chat_44_Dla100	GTCCCTGCCTCTATATCTttGAATTTTGCCCAAACCGGATCCTGC
B3_chat_44_Dla100	CGAATCTGAATCCTGCGGAAAAAGGttCCACTCAACTTTAACCCG
B3_chat_44_Dla100	GTCCCTGCCTCTATATCTttCTCCCAAAATGCCCAGCAGAAAAAG
B3_chat_44_Dla100	CGGTGCATCCCTAATTTTTATAAACttCCACTCAACTTTAACCCG
B3_chat_44_Dla100	GTCCCTGCCTCTATATCTttGGAGCAAATAATATATGTAAATGCA
B3_chat_44_Dla100	TAATGCCAATTTTTGAAAAGTGCAGttCCACTCAACTTTAACCCG
B3_chat_44_Dla100	GTCCCTGCCTCTATATCTttAGGGCATATTTTCATATTTTCATGA
B3_chat_44_Dla100	AGGGTATTTATTTGTCATTTTTCTAttCCACTCAACTTTAACCCG
B3_chat_44_Dla100	GTCCCTGCCTCTATATCTttACCCCATGCTGAGATCACACGCATC
B3_chat_44_Dla100	GTTAAATTATTGTAATTTCTAAAATttCCACTCAACTTTAACCCG
B3_chat_44_Dla100	GTCCCTGCCTCTATATCTttTTCAGGCACTGCAGCAAAGTTTAAT
B3_chat_44_Dla100	AAAAATTTCAATAGAGGGCGTTGGAttCCACTCAACTTTAACCCG
B3_chat_44_Dla100	GTCCCTGCCTCTATATCTttAAACAAGTGGGCCTGATGTTGATTT
B3_chat_44_Dla100	AAAAATGAAATATGTGTTATATAAAttCCACTCAACTTTAACCCG
B3_chat_44_Dla100	GTCCCTGCCTCTATATCTttCCTAAAATCCGTCATCTGCACATTA
B3_chat_44_Dla100	TACTAACTGGCTCGTTCCTCGAGTTttCCACTCAACTTTAACCCG
B3_chat_44_Dla100	GTCCCTGCCTCTATATCTttAAAATATAATTAAAGAAAATACTTT
B3_chat_44_Dla100	CAAAAATAAGCAAAGATAACAGTCAttCCACTCAACTTTAACCCG
B3_chat_44_Dla100	GTCCCTGCCTCTATATCTttAAGCATTTATGGCTTGTGCCTGTTT
B3_chat_44_Dla100	TATCCTATATTTTTGCATAGCAAAAttCCACTCAACTTTAACCCG
B3_chat_44_Dla100	GTCCCTGCCTCTATATCTttGCAATTACATTTTAAGCATAAGTCC
B3_chat_44_Dla100	TTTTTCCTTGACTGGTGTTTGGACCttCCACTCAACTTTAACCCG
B3_chat_44_Dla100	GTCCCTGCCTCTATATCTttTTGGCAAATTTACTTGAGGATGTGT
B3_chat_44_Dla100	ATGGCAAGGAGACTTTCTTCTACAGttCCACTCAACTTTAACCCG
B3_chat_44_Dla100	GTCCCTGCCTCTATATCTttAGAGGATGTGTTCTGGCTGTGGATT
B3_chat_44_Dla100	TGCAGTCATGAAAGCTTGAGACGCAttCCACTCAACTTTAACCCG
B3_chat_44_Dla100	GTCCCTGCCTCTATATCTttAGGGCCATAGCAGCAGAACATTTCC
B3_chat_44_Dla100	ACAACACCCATACCCATTTGGGACAttCCACTCAACTTTAACCCG

B3_chat_44_Dla100	GTCCCTGCCTCTATATCTttATGAATCGATTGCTAGTTAAGTACA
B3_chat_44_Dla100	GTTGTTGGAACCTGACTGGTAGAGAttCCACTCAACTTTAACCCG
B3_chat_44_Dla100	GTCCCTGCCTCTATATCTttTGAAATGCTCTTGTGCTAACTCCCT
B3_chat_44_Dla100	CATCTCGAAAGAGCTCAGGAAGTTCttCCACTCAACTTTAACCCG
B3_chat_44_Dla100	GTCCCTGCCTCTATATCTttCCCAGTAATAGCTTGAATTGTATAT
B3_chat_44_Dla100	TGCGAGTAAGTGGTTGTCTATTGCCttCCACTCAACTTTAACCCG
B3_chat_44_Dla100	GTCCCTGCCTCTATATCTttTACTCCATCTTCTCTATATTCGTTA
B3_chat_44_Dla100	GTCTGAGACTTTATTGCAGCCCTAAttCCACTCAACTTTAACCCG
B3_chat_44_Dla100	GTCCCTGCCTCTATATCTttCAAATGCTAGTGCTTCTGCAGTTGA
B3_chat_44_Dla100	TTGTTTCCCCATCAACCATTGCATTttCCACTCAACTTTAACCCG
B3_chat_44_Dla100	GTCCCTGCCTCTATATCTttAAATCGCCGAATAGAAGCGCTCTCA
B3_chat_44_Dla100	CCTTATGTTATCAACACGTCCCATTttCCACTCAACTTTAACCCG
B3_chat_44_Dla100	GTCCCTGCCTCTATATCTttTAAAAAGCAAGTTGAAGTGCTACTT
B3_chat_44_Dla100	GTTGGCACAAGTTTTCTGTGACAGCttCCACTCAACTTTAACCCG
B3_chat_44_Dla100	GTCCCTGCCTCTATATCTttTCTTGATAAACTCTTTCCCGTAGTT
B3_chat_44_Dla100	TGAAAGCATCAGGACTCATTCTTTGttCCACTCAACTTTAACCCG
B3_chat_44_Dla100	GTCCCTGCCTCTATATCTttGTTCACAATTCTTTGCAGTTTGTTT
B3_chat_44_Dla100	AAACTTATAAACAATGAAATCAAGAttCCACTCAACTTTAACCCG
B3_chat_44_Dla100	GTCCCTGCCTCTATATCTttGGAGAACATTTCCACCGAAGTCTTC
B3_chat_44_Dla100	GAGGACGCTAAGTGCCCCTGAATTTttCCACTCAACTTTAACCCG
B3_chat_44_Dla100	GTCCCTGCCTCTATATCTttAGGAGGTGTTCTGTACATTGTACAA
B3_chat_44_Dla100	TTTTTGGGACTATTTTTCATATATTttCCACTCAACTTTAACCCG
B3_chat_44_Dla100	GTCCCTGCCTCTATATCTttAAATTGTACCGCAGACTCCATCGCT
B3_chat_44_Dla100	CGATTCCATCAAATGGAGAATGCTCttCCACTCAACTTTAACCCG
B3_chat_44_Dla100	GTCCCTGCCTCTATATCTttCCACCGGTTGCCTCCATTCCTACCA
B3_chat_44_Dla100	CACGACAAACTGCATGGGTTTATCAttCCACTCAACTTTAACCCG
B3_chat_44_Dla100	GTCCCTGCCTCTATATCTttCTGTTGGTGTCATTTAACTCCATCT
B3_chat_44_Dla100	CCTCCTCCATGAAGTAACTGCAAAGttCCACTCAACTTTAACCCG
B3_chat_44_Dla100	GTCCCTGCCTCTATATCTttTGCACCGTTCAATCATATCCAAAGA
B3_chat_44_Dla100	TTGGAGCATCCAAACACACTATGCAttCCACTCAACTTTAACCCG
B3_chat_44_Dla100	GTCCCTGCCTCTATATCTttTTCTCGTGCATGGGCCCACTCAGCT
B3_chat_44_Dla100	TCGGTTTGTTGAATCTTTCATGAGGttCCACTCAACTTTAACCCG
B3_chat_44_Dla100	GTCCCTGCCTCTATATCTttGGAAGCATCTCTTCTTCATTCTTTG
B3_chat_44_Dla100	CCATCTGATGTTAATAAGCCTATTGttCCACTCAACTTTAACCCG
B3_chat_44_Dla100	GTCCCTGCCTCTATATCTttACAGATCCCCCTCACTAAGACGACG
B3_chat_44_Dla100	TTCTGTCAATTTTACACAGCTGGGTttCCACTCAACTTTAACCCG
B3_chat_44_Dla100	GTCCCTGCCTCTATATCTttCTGATTGTTACATGCAACAATAATG
B3_chat_44_Dla100	ATTAATGACAACATCTAGTACAAAGttCCACTCAACTTTAACCCG
B3_chat_44_Dla100	GTCCCTGCCTCTATATCTttTGTGCCACCAAAGTGTCTTTGATGG
B3_chat_44_Dla100	TCAGGCTCTGGCATAATGGTGCTTTttCCACTCAACTTTAACCCG
B3_chat_44_Dla100	GTCCCTGCCTCTATATCTttCATAGTACTGTTTCATACACATAGG
B3_chat_44_Dla100	CTGGAAGGCGGTATGAAGAAAAGAGttCCACTCAACTTTAACCCG
B3_chat_44_Dla100	GTCCCTGCCTCTATATCTttTACAGGCAGAGCCTGCGAATCCAAC
B3_chat_44_Dla100	TCCTGAAAGCTGACCCCGAGCAAAAttCCACTCAACTTTAACCCG
B3_chat_44_Dla100	GTCCCTGCCTCTATATCTttAGGTTGGCAGCAAACCTCAACTGGT
B3_chat_44_Dla100	GTTTTGTAATCCAGCACTCCAGAGAttCCACTCAACTTTAACCCG
B3_chat_44_Dla100	GTCCCTGCCTCTATATCTttATATAACGGCGGGACTGGAATTTAC
B3_chat_44_Dla100	TGGTATCCCTAAAGTTATGCCTGGCttCCACTCAACTTTAACCCG
B3_chat_44_Dla100	GTCCCTGCCTCTATATCTttATCATCCAGCCAGTAAAGGTGTATC
B3_chat_44_Dla100	AAGAGGCAAACGATTGTTCAAATACttCCACTCAACTTTAACCCG
B3_chat_44_Dla100	GTCCCTGCCTCTATATCTttCGGCCTTGCTTTTCTGGTACTGTTC
B3_chat_44_Dla100	CCCCCGGCATCATAAATGCATCTACttCCACTCAACTTTAACCCG
B3_chat_44_Dla100	GTCCCTGCCTCTATATCTttATATGTGTCCATAGTTTGCTTAAGA
B3_chat_44_Dla100	TGTTACCAAGTGTTTCATGCACTTAttCCACTCAACTTTAACCCG
B3_chat_44_Dla100	GTCCCTGCCTCTATATCTttGCATCTTCACAGCTTTTGCCCTCTG
B3_chat_44_Dla100	GGCACAGGTAACTTTGGCAGCATCTttCCACTCAACTTTAACCCG
B3_chat_44_Dla100	GTCCCTGCCTCTATATCTttGCATTTTTAGTTCCTCAATGAGTAC
B3_chat_44_Dla100	TTCCCAAGGTGGATTTCTTTAGAACttCCACTCAACTTTAACCCG
B3_chat_44_Dla100	GTCCCTGCCTCTATATCTttTTACACGGTATCCTCATTAGTTCCC
B3_chat_44_Dla100	CCTGTTTTACTTCACAAAGTCGAGGttCCACTCAACTTTAACCCG

Chapter 5. CONCLUDING REMARKS AND LINGERING QUESTIONS

During my PhD, I investigated neural diversity and organization in the regenerating *X. tropicalis* spinal cord. First, I used immunohistochemistry and small molecule inhibitors to show that neural progenitor cell (NPC) dorsal/ventral organization is restored during spinal cord regeneration by a ventral morphogen gradient of Shh signaling, in a process parallel to development. This restoration is driven by an increase in Shh expression in the notochord and floor plate after injury and an increased sensitivity of NPCs to Shh signaling within the first three days post injury (Angell Swearer, Perkowski, et al. 2025). Next, I generated a single cell RNA-sequencing dataset to create a foundational atlas of neuron diversity in the uninjured and regenerating spinal cord. I used this dataset and HCR to show that major neuron diversity and organization regenerates, but specific neuron types repopulate at different proportions post injury. This regeneration is accompanied by cell-type specific waves of developmental and non-developmental mechanisms of recovery, including proliferative neurogenesis, transient regeneration-specific neurons, and neuron migration (Angell Swearer et al. 2025).

5.1. Is Xenopus tropicalis spinal cord regeneration "good enough" for functional recovery?

Overall these results indicate that while regeneration recapitulates development to drive NPC repatterning and basic cell organization, neuron regeneration represents a complicated mix of mechanisms. These findings prompt an interesting question in spinal cord regeneration, that is, what is necessary for functional regeneration? My research indicates for the first time that the *X. tropicalis* spinal cord does not completely restore the uninjured spinal cord, and instead certain neuron populations, such as *prdm14*- Motor Neurons, repopulate more robustly. This result leads one to ask whether *X. tropicalis* regeneration is simply "good enough": the extent of neuron repopulation that we see provides enough motor recovery for the tadpole to function during

larval development and is thus evolutionarily valued. This question holds value for the broader community as we use these regeneratively-competent animals to guide human therapeutics. How is neuron repopulation prioritized, both in terms of neurogenesis and re-innervation? How do regenerated neurons accommodate losses in connectivity? Previous research in zebrafish also identified differences in the balance of excitatory and inhibitory neurons over weeks of regeneration (Saraswathy et al. 2024)—so how is neurotransmitter balance and connectivity managed over this time period?

During my PhD, technical limitations prevented me from testing how neural circuitry regenerates in lab. In the future, paired patch clamping in mounted tadpoles during regeneration would enable us to track the connectivity of specific neurons in order to identify how neural circuitry adapts during regeneration, as has been done during development (Roberts et al. 2012). Paired with further investigation into the changes in gene expression that underlie the start of regeneration via my single cell dataset, this work could identify why different signals prompt specific neuron death or survival, neural plasticity, and proliferative neurogenesis to promote recovery. Overall, learning what aspects of regeneration are necessary for the incomplete but functional recovery that we see in *X. tropicalis* may provide an efficient method of troubleshooting stem cell therapy or *in vivo* neuronal reprogramming in humans and is a promising topic of future research.

5.2. What role do progenitor domains have during spinal cord regeneration?

It remains unclear how important the specification of NPC domains is during regeneration. While we were able to identify different NPC domains (ventral, intermediate, and dorsal) via immunohistochemistry, technical limitations prevent us from tracking individual cells over time in order to determine if these domains give rise to restricted neuron lineages. It is

likely that these domains are necessary for neuron repopulation, however, it is also possible that this organization guides other processes that rely on dorsal/ventral signaling such as cell migration or axon innervation (Yam and Charron 2013). Together, this data indicates that Shh is likely important for full functional recovery, although the lack of optimized motor assays in tadpoles prevented me from assaying sensory and motor recovery during Shh modulation. Currently, the intertwined nature of sensory and motor responses prevents us from testing this hypothesis easily (i.e. to test either sensory response we would observe motor movement or to prompt motor movement we would need sensory responsiveness).

Overall, these limitations prevented me from further questioning the necessity of these domains in recovery, but future research investigating neuron regeneration and connectivity after treatment with cyclopamine and SAG could help determine the role of these domains after injury. In addition to patch clamping, retrograde labeling could help identify changes in the motor and sensory innervation in various conditions. Additionally, it would be interesting to compare the effects of domain regeneration in the *X. tropicalis* tadpoles versus the green anole lizard, which only generates a ventralized ependymal tube. In the green anole, do we see different patterns of tail innervation than in the tadpole? How does this lack of patterning change sensory and motor recovery in a behavioral assay?

5.3. Intertwined questions of sensory system development and regeneration

Since *Xenopus* spinal cord research was previously confined to early histology and neural circuitry, many questions remain about when certain neuron types arise during development. Of particular interest is the degeneration of Rohon Beard Sensory Neurons (RBNs) and development of the neural crest-derived Dorsal Root Ganglia (DRG), processes that occur

around stage 46 in *Xenopus* (Yajima et al. 2014). In my dataset, I saw that RBNs decrease until they are lost before stage 47 during development and regeneration. We have seen the emergence of DRG in whole-mount tissues (HuC/HuD staining, data not shown) but have not been able to identify these neurons in this and other single-cell datasets. Thus, essential questions about the sensory system during this time period remain unanswered. Does the regeneration of the sensory system change over time, e.g., if you amputate during earlier stages do RBNs more robustly regenerate? Do the DRG regenerate? If so, how? In the future, investigation into marker genes used in other species paired with deeper co-analysis of single cell data and *in situ* visualization of potential cell targets should help track DRG cells in *Xenopus*. We could then track the regeneration of these cells at different time points during development, especially during metamorphosis, in order to identify the mechanisms behind their recovery. Since these cells are homologous to the mammalian system, understanding their regeneration post injury would contribute to human spinal cord injury responses.

5.3. How much does proliferative neurogenesis contribute to neuron repopulation?

Going into these experiments, I thought that proliferative neurogenesis substantially contributes to neuron repopulation. This assumption was based off of developmental neurogenesis, when most neurons arise from progenitors via asymmetrical cell division and differentiate in place in the spinal cord. Cell migration does contribute to neuron populations, but it occurs mostly via the migration of immature neuroblasts before neuron differentiation (Valiente and Marín 2010). In my research I identified not only proliferative neurogenesis, but also post-mitotic neurons moving into the regenerating spinal cord by 3 dpa, indicating that mature neuron migration contributes to neuron repopulation. If this is driven by inactive transport via the symmetrical division of progenitors or by active transport driven by cell-

intrinsic mechanisms remains to be seen. While I found that proliferative neurogenesis certainly contributes to neuron populations by 7 dpa via BrdU labeling, this 2-day labeling study showed that 12% of local neurons result from proliferative neurogenesis, indicating that post-mitotic neuron migration or other mechanisms such as direct differentiation play a substantial role in neuron repopulation. To determine exact proportions, high throughput lineage tracing is necessary to track individual cells over time in a transgenic line such as the *X. laevis* neuronal brainbow line (*BrainbowL, Xla.Tg(CMV:Brainbow1.0L)NXR*; Livet et al. 2007); image analyses would then suggest what mechanisms are most common during these timepoints. I hope to see such studies in the future to elucidate exactly how many of these neurons are repopulated via developmental or regenerative specific mechanisms.

5.4. Why do certain neuron populations give rise to regeneration-specific subclusters?

Based on my research, neuron response post-injury is correlated with neuron birthdate (i.e. secondary *prdm14*- Motor Neurons repopulate robustly while primary Rohon Beard Neurons repopulate at lower proportions), but even within secondary "Late" neurons there is variability in how neurons respond to injury. Some regeneration-specific "Late" subclusters express regeneration-associated genes such as *atf3* in parallel to zebrafish iNeurons, a transient neuron population that expresses regeneration-specific genes after injury. However, some do not express these genes and instead prioritize different processes. It is unclear why these differences exist, even after controlling for differences in axon connectivity and spatial origin.

The origins of regeneration-specific neurons in other animals similarly remains unclear. In humans, two types of neurons give rise to cells with regeneration specific signatures: spinocerebellar neurons and V2a neurons (Khavandegar et al. 2025; Matson et al. 2022). In

zebrafish, the origin of iNeurons remains unclear, although co-staining shows that they are made up of several neuron types. Future research could not only further define if the same neuron types conserved throughout vertebrates tend to give rise to these transient *atf3*+ cells, but also why these different neuron types respond this way. ATAC-sequencing could provide the context to show what transcriptional pathways activate these gene response signatures, and *in vivo* testing could show why the injury-response of certain neurons may be crucial to recovery. It's likely that neurons uniquely respond to different cell-cell signaling cues.

Since these transient neuron types seem to be driving neural plasticity, I predict that these neuron types are critically important to restoring basic neural connectivity post injury. For example, V2a neurons are known to receive descending and peripheral sensory input and excite motor neurons. This connectivity contrasts with other neurons involved in muscle control, which often influence swimming control and speed more than basic function. Given the strong motor neuron repopulation that we also seen within these timepoints, this pattern may represent the importance of regenerating centralized muscle control soon after injury. However, more research is needed to define this correlation.

5.4. Why does regeneration fail post-metamorphosis?

I found that neuron repopulation depends on their developmental status of the cell; those cells undergoing neurogenesis repopulate more robustly than those past their neurogenic window. This observation raises the question of how these findings might change at different developmental stages, given that these neurogenic windows vary over time. At earlier stages, do different neurons repopulate robustly? Does regeneration decline as neurogenesis declines during older stages? How much does this potential loss of neuronal repopulation underlie the loss of

regeneration with metamorphosis?

Regenerative capacity is known to decline during metamorphosis until froglet stages, when *Xenopus* frogs become incapable of functional spinal cord regeneration. Previous research has shown the importance of Sox2 expressing NPCs in driving this regeneration, and Sox2 expression in these cells declines over metamorphosis (Muñoz et al. 2015). It's clear that these cells are crucial to successful regeneration but unclear if these changes in NPCs alone drive the decline of regenerative competence or if other mechanisms come into play. It is possible that this pool of Sox2+ NPCs no longer responds to injury signals by metamorphosis and thus are unable to repopulate lost tissue. It is also possible that the regenerative-specific mechanisms of neuron plasticity and migration cannot be activated. Further research on tracking changes in cell response over time in comparison to cell signaling would test these options. Overall this failure mirrors the failure of the mammalian spinal cord to regenerate and poses a promising comparison to answering complex questions about how these mechanisms change. Overall, future research needs to explore how these distinct mechanisms contribute to true functional recovery.

Chapter 6: MATERIALS USED/GENERATED

Transgenic Animals		
Xtr.Tg(pax6:*GFP*;cryga:*RFP*;actc1:*RFP*)		RRID:NXR_1.0021
Xtr.Tg(tubb2b:GFP)Amaya		RRID:NXR_1092
Injectables		
pMT-HuC:Dendra2	Addgene Plasmid #80904	Inj: 30 pg / embryo
pCS107:Pbx3:FH	Generated in Lab	Inj: 125-2000 pg / embryo
pCS-TP (Tol2)	Khoka Lab	Inj: 10 pg / embryo
HCR Probes		
chat	See chapter 4.2 for sequence	16 nM
prdm14	See chapter 4.2 for sequence	16 nM
lhx1/lim1	See chapter 4.2 for sequence	16 nM
lepr	See chapter 4.2 for sequence	16 nM
***in situ* hybridization probes**		
shh	forward – gctttctacacctgccttgc,	reverse – taatacgactcactatagggtgagtcatgagtcggtctgc
foxa2	forward – aactgcagcagctttggaa,	reverse – taatacgactcactatagggcccgtttaagagtaagaactgagg
Antibodies		
Msx1/2	DSHB: 4G1	Works at 1:50
Nkx6.1	DSHB: F55A10	Works at 1:50
Nkx2.2	DSHB: 74-5A5	Works at 1:50
Lim1	DSHB: 4F2	Works at 1:50
Isl1	DSHB: 40.2D6	Works at 1:50

Isl1/2	DSHB: 39.4D5	Works at 1:50
Ecad	DSHB: 5D3-s	Did not work at 1:100
Elav4	DSHB: Elav-9F8A9	Did not work at 1:50
Pax7	DSHB: PAX7	Did not work at 1:50
Ache	DSHB: tor23	Did not work at 1:50
Prdm1	DSHB: PCRP-PRDM1-2C5	Did not work at 1:50
Shh	DSHB: 5E1-s	Did not work
Gli1	Thermo-Fisher: MA5:38530	Did not work
Sox2 (Rabbit)	Cell Signaling Technology: 2748S	Did not work
Sox2 (Rabbit)	Abcam: ab97959	Works at 1:100, sometimes
Sox2 (Mouse)	Cell Signaling Technology: 4900S	Did not work at 1:100
Sox2 (Rabbit)	Aviva Systems Biology: ARP31737_P050	Did not work at 1:100
Sox2 (Rabbit)	Genetex: N1C3	Did not work at 1:100
Sox2 (Mouse)	Abcam: AB79351	Works at 1:300
Sox2 (Goat)	R&D Systems: AF2018	Did not work
NeuN	Cell Signaling Technology: D5B10	Did not work
BrdU (Rabbit)	Fisher: PA5-32256	Works at 1:200, after 10 minute acid wash
BrdU (Mouse)	Sigma Life: B2531	Did not work
Msx1	Biorbyt: orb2059	Did not work
Msx2	ProSci: 57-906	Did not work at 1:150
Runx1	ProSci: 5149	Did not work at 1:150
Nkx2-2	ProSci: 6743	Did not work at 1:150
Dbx1	Biorbyt: orb156546	Did not work
Dbx2	DSHB: PCRP	Did not work
Neurofilament	DSHB: 3A10	Works at 1:50
TH	Immunostar: 22941	Works at 1:200

HuC/HuD	Invitrogen: A21271, 16A11	Works at 1:200
Dcx	Abcam: Ab18723	Works
Meis1	Abcam: Ab19867	Works at 1:100
Meis1	Abcam: Ab229962	Works at 1:100
Pbx3	Abcam: Ab109173	Works at 1:100, sometimes
Anti-choline acetyltransferase	Millipore: Ab144P	Did not work
NeuN	Millipore: MAB377	Did not work

Chapter 7: WORKS CITED

Alaynick, William A., Thomas M. Jessell, and Samuel L. Pfaff. 2011. “SnapShot: Spinal Cord Development.” *Cell* 146 (1): 178-178.e1. https://doi.org/10.1016/j.cell.2011.06.038.

Angell Swearer, Avery, Samuel B Perkowski, Iba Husain, Thiago A Figueiredo, Morgan McCartney, and Andrea Elizabeth Wills. 2025. “Spinal Cord Regeneration Deploys Cell-Type Specific Developmental and Non-Developmental Strategies to Restore Neuron Diversity.” Preprint, Developmental Biology, November 12. https://doi.org/10.1101/2025.11.10.687703.

Angell Swearer, Avery, Samuel Perkowski, and Andrea Wills. 2025. “Shh Signaling Directs Dorsal Ventral Patterning in the Regenerating X. Tropicalis Spinal Cord.” *Developmental Biology* 520 (April): 191–99. https://doi.org/10.1016/j.ydbio.2025.01.015.

Arbanas, Laura I., Emanuel Cura Costa, Osvaldo Chara, Leo Otsuki, and Elly M. Tanaka. 2024. “Lineage Tracing of *Shh*+ Floor Plate Cells and Dynamics of Dorsal-Ventral Gene Expression in the Regenerating Axolotl Spinal Cord.” Preprint, June 14. https://doi.org/10.1101/2024.06.14.599012.

Ashburner, Michael, Catherine A. Ball, Judith A. Blake, et al. 2000. “Gene Ontology: Tool for the Unification of Biology.” *Nature Genetics* 25 (1): 25–29. https://doi.org/10.1038/75556.

Aztekin, C., T. W. Hiscock, R. Butler, et al. 2020. “The Myeloid Lineage Is Required for the Emergence of a Regeneration Permissive Environment Following *Xenopus* Tail Amputation.” *Development*, January 1, dev.185496. https://doi.org/10.1242/dev.185496.

Aztekin, C., T. W. Hiscock, J. C. Marioni, J. B. Gurdon, B. D. Simons, and J. Jullien. 2019. “Identification of a Regeneration-Organizing Cell in the Xenopus Tail.” *Science* 364 (6441): 653–58. https://doi.org/10.1126/science.aav9996.

Aztekin, Can. 2024. “Mechanisms of Regeneration: To What Extent Do They Recapitulate Development?” *Development* 151 (14): dev202541. https://doi.org/10.1242/dev.202541.

Barth, K. Anukampa, Yasuyuki Kishimoto, Klaus B. Rohr, Catrin Seydler, Stefan Schulte-Merker, and Stephen W. Wilson. 1999. “Bmp Activity Establishes a Gradient of Positional Information throughout the Entire Neural Plate.” *Development* 126 (22): 4977–87. https://doi.org/10.1242/dev.126.22.4977.

Beck, Caroline W., Juan Carlos Izpisúa Belmonte, and Bea Christen. 2009. “Beyond Early Development: *Xenopus* as an Emerging Model for the Study of Regenerative Mechanisms.” *Developmental Dynamics* 238 (6): 1226–48. https://doi.org/10.1002/dvdy.21890.

Bernhardt, Robert R., Ajay B. Chitnis, Laurie Lindamer, and John Y. Kuwada. 1990. “Identification of Spinal Neurons in the Embryonic and Larval Zebrafish.” *Journal of*

Comparative Neurology 302 (3): 603–16. https://doi.org/10.1002/cne.903020315.

Bishop, Thomas F., and Caroline W. Beck. 2021. "Bacterial Lipopolysaccharides Can Initiate Regeneration of the Xenopus Tadpole Tail." *iScience* 24 (11): 103281. https://doi.org/10.1016/j.isci.2021.103281.

Bixby, John L., and Nicholas C. Spitzer. 1982. "The Appearance and Development of Chemosensitivity in Rohon-Beard Neurones of the *Xenopus* Spinal Cord." *The Journal of Physiology* 330 (1): 513–36. https://doi.org/10.1113/jphysiol.1982.sp014356.

Briscoe, James, and Johan Ericson. 1999. "The Specification of Neuronal Identity by Graded Sonic Hedgehog Signalling." *Seminars in Cell & Developmental Biology* 10 (3): 353–62. https://doi.org/10.1006/scdb.1999.0295.

Briscoe, James, Alessandra Pierani, Thomas M Jessell, and Johan Ericson. 2000. "A Homeodomain Protein Code Specifies Progenitor Cell Identity and Neuronal Fate in the Ventral Neural Tube." *Cell* 101 (4): 435–45. https://doi.org/10.1016/S0092-8674(00)80853-3.

Briscoe, James, and Pascal P. Thérond. 2013. "The Mechanisms of Hedgehog Signalling and Its Roles in Development and Disease." *Nature Reviews Molecular Cell Biology* 14 (7): 416–29. https://doi.org/10.1038/nrm3598.

Butler, Andrew, Paul Hoffman, Peter Smibert, Efthymia Papalexi, and Rahul Satija. 2018. "Integrating Single-Cell Transcriptomic Data across Different Conditions, Technologies, and Species." *Nature Biotechnology* 36 (5): 411–20. https://doi.org/10.1038/nbt.4096.

Cañizares, Marco A., Aida Rodrigo Albors, Gail Singer, et al. 2020. "Multiple Steps Characterise Ventricular Layer Attrition to Form the Ependymal Cell Lining of the Adult Mouse Spinal Cord Central Canal." *Journal of Anatomy* 236 (2): 334–50. https://doi.org/10.1111/joa.13094.

Chapman, Phoebe A., Campbell B. Gilbert, Thomas J. Devine, et al. 2022. "Manipulating the Microbiome Alters Regenerative Outcomes in *Xenopus Laevis* Tadpoles via Lipopolysaccharide Signalling." *Wound Repair and Regeneration* 30 (6): 636–51. https://doi.org/10.1111/wrr.13003.

Chen, Wenbiao, Shawn Burgess, and Nancy Hopkins. 2001. "Analysis of the Zebrafish Smoothened Mutant Reveals Conserved and Divergent Functions of Hedgehog Activity." *Development* 128 (12): 2385–96. https://doi.org/10.1242/dev.128.12.2385.

Chen, Xuanyu, and Hedong Li. 2022. "Neuronal Reprogramming in Treating Spinal Cord Injury." *Neural Regeneration Research* 17 (7): 1440. https://doi.org/10.4103/1673-5374.330590.

Chiang, Chin, Ying Litingtung, Eric Lee, et al. 1996. "Cyclopia and Defective Axial Patterning in Mice Lacking Sonic Hedgehog Gene Function." *Nature* 383 (6599): 407–13. https://doi.org/10.1038/383407a0.

Cigliola, Valentina, Clayton J. Becker, and Kenneth D. Poss. 2020. “Building Bridges, Not Walls: Spinal Cord Regeneration in Zebrafish.” *Disease Models & Mechanisms* 13 (5): dmm044131. https://doi.org/10.1242/dmm.044131.

Clifford, Tanner, Zachary Finkel, Brianna Rodriguez, Adelina Joseph, and Li Cai. 2023. “Current Advancements in Spinal Cord Injury Research—Glial Scar Formation and Neural Regeneration.” *Cells* 12 (6): 853. https://doi.org/10.3390/cells12060853.

Cohen, Michael, Anna Kicheva, Ana Ribeiro, et al. 2015. “Ptch1 and Gli Regulate Shh Signalling Dynamics via Multiple Mechanisms.” *Nature Communications* 6 (1): 6709. https://doi.org/10.1038/ncomms7709.

Dale, N., A. Roberts, O. P. Ottersen, and J. Storm-Mathisen. 1987a. “The Development of a Population of Spinal Cord Neurons and Their Axonal Projections Revealed by GABA Immunocytochemistry in Frog Embryos.” *Proceedings of the Royal Society of London* B (232): 205–15.

Dale, N., A. Roberts, O. P. Ottersen, and J. Storm-Mathisen. 1987b. “The Morphology and Distribution of ‘Kolmer-Agduhr Cells’, a Class of Cererospinal-Fluid-Contacting Neurons Revealed in the Frog Embryo Spinal Cord by GABA Immunocytochemistry.” *Proceedings of the Royal Society of London* B (232): 193–203.

Dasari, Venkata Ramesh. 2014. “Mesenchymal Stem Cells in the Treatment of Spinal Cord Injuries: A Review.” *World Journal of Stem Cells* 6 (2): 120. https://doi.org/10.4252/wjsc.v6.i2.120.

Dessaud, Eric, Lin Lin Yang, Katy Hill, et al. 2007. “Interpretation of the Sonic Hedgehog Morphogen Gradient by a Temporal Adaptation Mechanism.” *Nature* 450 (7170): 717–20. https://doi.org/10.1038/nature06347.

Echeverri, Karen, and Elly M. Tanaka. 2002. “Ectoderm to Mesoderm Lineage Switching During Axolotl Tail Regeneration.” *Science* 298 (5600): 1993–96. https://doi.org/10.1126/science.1077804.

Edwards-Faret, Gabriela, Rosana Muñoz, Emilio E Méndez-Olivos, Dasfne Lee-Liu, Victor S Tapia, and Juan Larraín. 2017. “Spinal Cord Regeneration in Xenopus Laevis.” *Nature Protocols* 12 (2): 372–89. https://doi.org/10.1038/nprot.2016.177.

Feijóo, Carmen G., Maritza G. Oñate, Luis A. Milla, and Verónica A. Palma. 2011. “Sonic Hedgehog (Shh)-Gli Signaling Controls Neural Progenitor Cell Division in the Developing Tectum in Zebrafish.” *European Journal of Neuroscience* 33 (4): 589–98. https://doi.org/10.1111/j.1460-9568.2010.07560.x.

Fisher, Malcolm, Christina James-Zorn, Virgilio Ponferrada, et al. 2023. “Xenbase: Key Features and Resources of the Xenopus Model Organism Knowledgebase.” *Genetics* 224 (1): iyad018. https://doi.org/10.1093/genetics/iyad018.

Fu, Hui, Yingchuan Qi, Min Tan, et al. 2003. “Molecular Mapping of the Origin of Postnatal

Spinal Cord Ependymal Cells: Evidence That Adult Ependymal Cells Are Derived from Nkx6.1+ Ventral Neural Progenitor Cells." *Journal of Comparative Neurology* 456 (3): 237–44. https://doi.org/10.1002/cne.10481.

Gu, Zuguang, Lei Gu, Roland Eils, Matthias Schlesner, and Benedikt Brors. 2014. "*Circlize* Implements and Enhances Circular Visualization in R." *Bioinformatics* 30 (19): 2811–12. https://doi.org/10.1093/bioinformatics/btu393.

Hamilton, Andrew M, Olga A Balashova, and Laura N Borodinsky. 2021. "Non-Canonical Hedgehog Signaling Regulates Spinal Cord and Muscle Regeneration in Xenopus Laevis Larvae." *eLife* 10 (May): e61804. https://doi.org/10.7554/eLife.61804.

Hao, Yuhan, Stephanie Hao, Erica Andersen-Nissen, et al. 2021. "Integrated Analysis of Multimodal Single-Cell Data." *Cell* 184 (13): 3573-3587.e29. https://doi.org/10.1016/j.cell.2021.04.048.

Hartenstein, Volker. 1989. *Early Neurogenesis in Xenopus: The Spatiotemporal Pattern of Proliferation and Cell Lineages in the Embryonic Spinal Cord*.

Hartley, Katharine O., Zöe Hardcastle, Rosalind V. Friday, Enrique Amaya, and Nancy Papalopulu. 2001. "Transgenic Xenopus Embryos Reveal That Anterior Neural Development Requires Continued Suppression of BMP Signaling after Gastrulation." *Developmental Biology* 238 (1): 168–84. https://doi.org/10.1006/dbio.2001.0398.

Henningfeld, Kristine A., Morgane Locker, and Muriel Perron. 2007. "Xenopus Primary Neurogenesis and Retinogenesis." In *Functional Development and Embryology*, vol. 1. 1. Global Science Books.

Hirsch, Nicolas, Lyle B. Zimmerman, Jessica Gray, et al. 2002. "*Xenopus Tropicalis* Transgenic Lines and Their Use in the Study of Embryonic Induction." *Developmental Dynamics* 225 (4): 522–35. https://doi.org/10.1002/dvdy.10188.

Hu, Xiao, Wei Xu, Yilong Ren, et al. 2023. "Spinal Cord Injury: Molecular Mechanisms and Therapeutic Interventions." *Signal Transduction and Targeted Therapy* 8 (1): 245. https://doi.org/10.1038/s41392-023-01477-6.

Jin, Suoqin, Christian F. Guerrero-Juarez, Lihua Zhang, et al. 2021. "Inference and Analysis of Cell-Cell Communication Using CellChat." *Nature Communications* 12 (1): 1088. https://doi.org/10.1038/s41467-021-21246-9.

Juárez-Morales, José L., Reyna I. Martinez-De Luna, Michael E. Zuber, Alan Roberts, and Katharine E. Lewis. 2017. "Zebrafish Transgenic Constructs Label Specific Neurons in *Xenopus Laevis* Spinal Cord and Identify Frog V0v Spinal Neurons." *Developmental Neurobiology* 77 (8): 1007–20. https://doi.org/10.1002/dneu.22490.

Kakebeen, Anneke D., and Andrea E. Wills. 2019. "More Than Just a Bandage: Closing the Gap Between Injury and Appendage Regeneration." *Frontiers in Physiology* 10: 81. https://doi.org/10.3389/fphys.2019.00081.

Kakebeen, Anneke Dixie, Alexander Daniel Chitsazan, Madison Corinne Williams, Lauren M Saunders, and Andrea Elizabeth Wills. 2020. “Chromatin Accessibility Dynamics and Single Cell RNA-Seq Reveal New Regulators of Regeneration in Neural Progenitors.” *eLife* 9 (April): e52648. https://doi.org/10.7554/eLife.52648.

Katoh, Hiroyuki, Kazuya Yokota, and Michael G. Fehlings. 2019. “Regeneration of Spinal Cord Connectivity Through Stem Cell Transplantation and Biomaterial Scaffolds.” *Frontiers in Cellular Neuroscience* 13 (June): 248. https://doi.org/10.3389/fncel.2019.00248.

Katz, Hilary R., Anthony A. Arcese, Ona Bloom, and Jennifer R. Morgan. 2022. “Activating Transcription Factor 3 (ATF3) Is a Highly Conserved Pro-Regenerative Transcription Factor in the Vertebrate Nervous System.” *Frontiers in Cell and Developmental Biology* 10 (March): 824036. https://doi.org/10.3389/fcell.2022.824036.

Khavandegar, Armin, Luke J. Bolstad, Amgad S. Hanna, and Daniel J. Hellenbrand. 2025. “Regeneration after Spinal Cord Injury: A Review on the Crucial Aspects of V2a Interneurons.” *Journal of Neurotrauma*, October 7, 08977151251386031. https://doi.org/10.1177/08977151251386031.

Khokha, Mustafa K., Christina Chung, Erika L. Bustamante, et al. 2002. “Techniques and Probes for the Study of *Xenopus Tropicalis* Development.” *Developmental Dynamics* 225 (4): 499–510. https://doi.org/10.1002/dvdy.10184.

Koide, Tetsuya, Tadayoshi Hayata, and Ken W. Y. Cho. 2006. “Negative Regulation of Hedgehog Signaling by the Cholesterogenic Enzyme 7-Dehydrocholesterol Reductase.” *Development* 133 (12): 2395–405. https://doi.org/10.1242/dev.02393.

Kroehne, Volker, Dorian Freudenreich, Stefan Hans, Jan Kaslin, and Michael Brand. 2011. “Regeneration of the Adult Zebrafish Brain from Neurogenic Radial Glia-Type Progenitors.” *Development* 138 (22): 4831–41. https://doi.org/10.1242/dev.072587.

Kuehn, Emily, David S. Clausen, Ryan W. Null, Bria M. Metzger, Amy D. Willis, and B. Duygu Özpolat. 2022. “Segment Number Threshold Determines Juvenile Onset of Germline Cluster Expansion in *Platynereis Dumerilii*.” *Journal of Experimental Zoology Part B: Molecular and Developmental Evolution* 338 (4): 225–40. https://doi.org/10.1002/jez.b.23100.

Lai, Karen, Brian K. Kaspar, Fred H. Gage, and David V. Schaffer. 2003. “Sonic Hedgehog Regulates Adult Neural Progenitor Proliferation in Vitro and in Vivo.” *Nature Neuroscience* 6 (1): 21–27. https://doi.org/10.1038/nn983.

Lane, Maura, Michael Slocum, and Mustafa K. Khokha. 2022. “Raising and Maintaining *Xenopus Tropicalis* from Tadpole to Adult.” *Cold Spring Harbor Protocols* 2022 (4): pdb.prot106369. https://doi.org/10.1101/pdb.prot106369.

Lee, Andrew S, Chad Tang, Mahendra S Rao, Irving L Weissman, and Joseph C Wu. 2013. “Tumorigenicity as a Clinical Hurdle for Pluripotent Stem Cell Therapies.” *Nature Medicine* 19 (8): 998–1004. https://doi.org/10.1038/nm.3267.

Lee, Kevin J., Paula Dietrich, and Thomas M. Jessell. 2000. “Genetic Ablation Reveals That the Roof Plate Is Essential for Dorsal Interneuron Specification.” *Nature* 403 (6771): 734–40. https://doi.org/10.1038/35001507.

Lee, Soo-Kyung, and Samuel L. Pfaff. 2001. “Transcriptional Networks Regulating Neuronal Identity in the Developing Spinal Cord.” *Nature Neuroscience* 4 (11): 1183–91. https://doi.org/10.1038/nn750.

Lee-Liu, Dasfne, Gabriela Edwards-Faret, Víctor S. Tapia, and Juan Larraín. 2013. “Spinal Cord Regeneration: Lessons for Mammals from Non-mammalian Vertebrates.” *Genesis* 51 (8): 529–44. https://doi.org/10.1002/dvg.22406.

Leung, Brigid, and Sebastian M. Shimeld. 2019. “Evolution of Vertebrate Spinal Cord Patterning.” *Developmental Dynamics* 248 (11): 1028–43. https://doi.org/10.1002/dvdy.77.

Lewis, Cristy, and Paul A. Krieg. 2014. “Reagents for Developmental Regulation of Hedgehog Signaling.” *Methods (San Diego, Calif.)* 66 (3): 390–97. https://doi.org/10.1016/j.ymeth.2013.08.022.

Li, W.-C., Shin-ichi Higashijima, D. M. Parry, Alan Roberts, and S. R. Soffe. 2004. “Primitive Roles for Inhibitory Interneurons in Developing Frog Spinal Cord.” *The Journal of Neuroscience* 24 (25): 5840–48. https://doi.org/10.1523/JNEUROSCI.1633-04.2004.

Liem, Karel F, Gabi Tremml, Henk Roelink, and Thomas M Jessell. 1995. “Dorsal Differentiation of Neural Plate Cells Induced by BMP-Mediated Signals from Epidermal Ectoderm.” *Cell* 82 (6): 969–79. https://doi.org/10.1016/0092-8674(95)90276-7.

Lin, Gufa, and Jonathan M.W. Slack. 2008. “Requirement for Wnt and FGF Signaling in Xenopus Tadpole Tail Regeneration.” *Developmental Biology* 316 (2): 323–35. https://doi.org/10.1016/j.ydbio.2008.01.032.

Liu, Yuanyuan, Hurong Yu, Sarah K. Deaton, and Ben G. Szaro. 2012. “Heterogeneous Nuclear Ribonucleoprotein K, an RNA-Binding Protein, Is Required for Optic Axon Regeneration in *Xenopus Laevis*.” *The Journal of Neuroscience* 32 (10): 3563–74. https://doi.org/10.1523/JNEUROSCI.5197-11.2012.

Livet, Jean, Tamily A. Weissman, Hyuno Kang, et al. 2007. “Transgenic Strategies for Combinatorial Expression of Fluorescent Proteins in the Nervous System.” *Nature* 450 (7166): 56–62. https://doi.org/10.1038/nature06293.

Love, Nick R, Yaoyao Chen, Boyan Bonev, et al. 2011. “Genome-Wide Analysis of Gene Expression during Xenopus Tropicalis Tadpole Tail Regeneration.” *BMC Developmental Biology* 11 (1): 70. https://doi.org/10.1186/1471-213X-11-70.

Makanae, Aki, Kazumasa Mitogawa, and Akira Satoh. 2016. “Cooperative Inputs of Bmp and Fgf Signaling Induce Tail Regeneration in Urodele Amphibians.” *Developmental Biology* 410 (1): 45–55. https://doi.org/10.1016/j.ydbio.2015.12.012.

Marti, Elisa, David A. Bumcrot, Ritsuko Takada, and Andrew P. McMahon. 1995. “Requirement of 19K Form of Sonic Hedgehog for Induction of Distinct Ventral Cell Types in CNS Explants.” *Nature* 375 (6529): 322–25. https://doi.org/10.1038/375322a0.

Martin, Benjamin L., Sara M. Peyrot, and Richard M. Harland. 2007. “Hedgehog Signaling Regulates the Amount of Hypaxial Muscle Development during Xenopus Myogenesis.” *Developmental Biology* 304 (2): 722–34. https://doi.org/10.1016/j.ydbio.2007.01.022.

Matson, Kaya J. E., Daniel E. Russ, Claudia Kathe, et al. 2022. “Single Cell Atlas of Spinal Cord Injury in Mice Reveals a Pro-Regenerative Signature in Spinocerebellar Neurons.” *Nature Communications* 13 (1): 5628. https://doi.org/10.1038/s41467-022-33184-1.

Mchedlishvili, Levan, Hans H. Epperlein, Anja Telzerow, and Elly M. Tanaka. 2007. “A Clonal Analysis of Neural Progenitors during Axolotl Spinal Cord Regeneration Reveals Evidence for Both Spatially Restricted and Multipotent Progenitors.” *Development* 134 (11): 2083–93. https://doi.org/10.1242/dev.02852.

Mescher, Anthony L., Anton W. Neff, and Michael W. King. 2013. “Changes in the Inflammatory Response to Injury and Its Resolution during the Loss of Regenerative Capacity in Developing Xenopus Limbs.” *PLoS ONE* 8 (11): e80477. https://doi.org/10.1371/journal.pone.0080477.

Miller, Robert H., Kyl Dinsio, Rae Wang, Robert Geertman, Charles E. Maier, and Alison K. Hall. 2004. “Patterning of Spinal Cord Oligodendrocyte Development by Dorsally Derived BMP4.” *Journal of Neuroscience Research* 76 (1): 9–19. https://doi.org/10.1002/jnr.20047.

Montgomery, Jacob E., Timothy D. Wiggin, Luis M. Rivera-Perez, Christina Lillesaar, and Mark A. Masino. 2016. “Intraspinal Serotonergic Neurons Consist of Two, Temporally Distinct Populations in Developing Zebrafish.” *Developmental Neurobiology* 76 (6): 673–87. https://doi.org/10.1002/dneu.22352.

Morcos, Paul A., Yongfu Li, and Shan Jiang. 2008. “Vivo-Morpholinos: A Non-Peptide Transporter Delivers Morpholinos into a Wide Array of Mouse Tissues.” *BioTechniques* 45 (6): 613–23. https://doi.org/10.2144/000113005.

Muñoz, Rosana, Gabriela Edwards-Faret, Mauricio Moreno, Nikole Zuñiga, Hollis Cline, and Juan Larraín. 2015. “Regeneration of Xenopus Laevis Spinal Cord Requires Sox2/3 Expressing Cells.” *Developmental Biology* 408 (2): 229–43. https://doi.org/10.1016/j.ydbio.2015.03.009.

Nieuwkoop, Pieter Dirk, Jacob Faber, John Gerhart, and Marc Kirschner. 1994. *Normal Table of Xenopus Laevis (Daudin): A Systematical and Chronological Survey of the Development from the Fertilized Egg till the End of Metamorphosis*. Facsim. ed. With Hubrecht laboratorium. Garland.

NINDS. 2019. “Spinal Cord Injury Information Page.” March 27. https://www.ninds.nih.gov/disorders/all-disorders/spinal-cord-injury-information-page.

Nogueira-Rodrigues, Joana, Sérgio C. Leite, Rita Pinto-Costa, et al. 2022. “Rewired Glycosylation Activity Promotes Scarless Regeneration and Functional Recovery in Spiny Mice after Complete Spinal Cord Transection.” *Developmental Cell* 57 (4): 440-450.e7. https://doi.org/10.1016/j.devcel.2021.12.008.

Özugur, Suzan, Myra N. Chávez, Rosario Sanchez-Gonzalez, Lars Kunz, Jörg Nickelsen, and Hans Straka. 2022. “Transcardial Injection and Vascular Distribution of Microalgae in Xenopus Laevis as Means to Supply the Brain with Photosynthetic Oxygen.” *STAR Protocols* 3 (2): 101250. https://doi.org/10.1016/j.xpro.2022.101250.

Patel, Jeet H., Daniel J. Ong, Claire R. Williams, LuLu K. Callies, and Andrea E. Wills. 2022. “Elevated Pentose Phosphate Pathway Flux Supports Appendage Regeneration.” *Cell Reports* 41 (4): 111552. https://doi.org/10.1016/j.celrep.2022.111552.

Patel, Jeet H., Preston A. Schattinger, Evan E. Takayoshi, and Andrea E. Wills. 2022. “Hif1α and Wnt Are Required for Posterior Gene Expression during Xenopus Tropicalis Tail Regeneration.” *Developmental Biology* 483 (March): 157–68. https://doi.org/10.1016/j.ydbio.2022.01.007.

Peyrot, Sara M., John B. Wallingford, and Richard M. Harland. 2011. “A Revised Model of Xenopus Dorsal Midline Development: Differential and Separable Requirements for Notch and Shh Signaling.” *Developmental Biology* 352 (2): 254–66. https://doi.org/10.1016/j.ydbio.2011.01.021.

Puls, Brendan, Yan Ding, Fengyu Zhang, et al. 2020. “Regeneration of Functional Neurons After Spinal Cord Injury via in Situ NeuroD1-Mediated Astrocyte-to-Neuron Conversion.” *Frontiers in Cell and Developmental Biology* 8 (December): 591883. https://doi.org/10.3389/fcell.2020.591883.

Ralph, Patrick C., Sung-Woo Choi, Min Jung Baek, and Sang Jin Lee. 2024. “Regenerative Medicine Approaches for the Treatment of Spinal Cord Injuries: Progress and Challenges.” *Acta Biomaterialia* 189 (November): 57–72. https://doi.org/10.1016/j.actbio.2024.10.021.

Ramsbottom, Simon A., Richard J. Maguire, Simon W. Fellgett, and Mary Elizabeth Pownall. 2014. “Sulf1 Influences the Shh Morphogen Gradient during the Dorsal Ventral Patterning of the Neural Tube in *Xenopus Tropicalis*.” *Developmental Biology* 391 (2): 207–18. https://doi.org/10.1016/j.ydbio.2014.04.010.

Reimer, M. M., V. Kuscha, C. Wyatt, et al. 2009. “Sonic Hedgehog Is a Polarized Signal for Motor Neuron Regeneration in Adult Zebrafish.” *Journal of Neuroscience* 29 (48): 15073–82. https://doi.org/10.1523/JNEUROSCI.4748-09.2009.

Roberts, A., and J. D. W. Clarke. 1982. *The Neuroanatomy of an Amphibian Embryo Spinal Cord*. B (296): 195–212.

Roberts, Alan. 2000. “Early Functional Organization of Spinal Neurons in Developing Lower Vertebrates.” *Brain Research Bulletin* 53 (5): 585–93. https://doi.org/10.1016/S0361-

9230(00)00392-0.

Roberts, Alan, Wen-Chang Li, and Stephen R. Soffe. 2012. “A Functional Scaffold of CNS Neurons for the Vertebrates: The Developing Xenopus Laevis Spinal Cord.” *Developmental Neurobiology* 72 (4): 575–84. https://doi.org/10.1002/dneu.20889.

Rodemer, William, Jianli Hu, MichaelE Selzer, and MichaelI Shifman. 2020. “Heterogeneity in the Regenerative Abilities of Central Nervous System Axons within Species: Why Do Some Neurons Regenerate Better than Others?” *Neural Regeneration Research* 15 (6): 996. https://doi.org/10.4103/1673-5374.270298.

Rodrigo Albors, Aida, Gail A. Singer, Enric Llorens-Bobadilla, et al. 2023. “An Ependymal Cell Census Identifies Heterogeneous and Ongoing Cell Maturation in the Adult Mouse Spinal Cord That Changes Dynamically on Injury.” *Developmental Cell* 58 (3): 239-255.e10. https://doi.org/10.1016/j.devcel.2023.01.003.

Romero, Maria Montserrat Garcia, Gareth McCathie, Philip Jankun, and Henry Hamilton Roehl. 2018. “Damage-Induced Reactive Oxygen Species Enable Zebrafish Tail Regeneration by Repositioning of Hedgehog Expressing Cells.” *Nature Communications* 9 (October): 4010. https://doi.org/10.1038/s41467-018-06460-2.

Rowitch, David H., Benoit St.-Jacques, Scott M. K. Lee, Jonathon D. Flax, Evan Y. Snyder, and Andrew P. McMahon. 1999. “Sonic Hedgehog Regulates Proliferation and Inhibits Differentiation of CNS Precursor Cells.” *The Journal of Neuroscience* 19 (20): 8954–65. https://doi.org/10.1523/JNEUROSCI.19-20-08954.1999.

Saint-Amant, Louis, and Pierre Drapeau. 2001. “Synchronization of an Embryonic Network of Identified Spinal Interneurons Solely by Electrical Coupling.” *Neuron* 31 (6): 1035–46. https://doi.org/10.1016/S0896-6273(01)00416-0.

Saraswathy, Vishnu Muraleedharan, Lili Zhou, and Mayssa H. Mokalled. 2024. “Single-Cell Analysis of Innate Spinal Cord Regeneration Identifies Intersecting Modes of Neuronal Repair.” *Nature Communications* 15 (1): 6808. https://doi.org/10.1038/s41467-024-50628-y.

Satija, Rahul, Jeffrey A Farrell, David Gennert, Alexander F Schier, and Aviv Regev. 2015. “Spatial Reconstruction of Single-Cell Gene Expression Data.” *Nature Biotechnology* 33 (5): 495–502. https://doi.org/10.1038/nbt.3192.

Satoh, Akira, Tetsuya Endo, Masahiro Abe, et al. 2006. “Characterization of Xenopus Digits and Regenerated Limbs of the Froglet.” *Developmental Dynamics* 235 (12): 3316–26. https://doi.org/10.1002/dvdy.20985.

Satou, Chie, Yukiko Kimura, and Shin-ichi Higashijima. 2012. “Generation of Multiple Classes of V0 Neurons in Zebrafish Spinal Cord: Progenitor Heterogeneity and Temporal Control of Neuronal Diversity.” *The Journal of Neuroscience* 32 (5): 1771–83. https://doi.org/10.1523/JNEUROSCI.5500-11.2012.

Satou, Chie, Yukiko Kimura, Tsunehiko Kohashi, et al. 2009. “Functional Role of a Specialized Class of Spinal Commissural Inhibitory Neurons during Fast Escapes in Zebrafish.” *The Journal of Neuroscience* 29 (21): 6780–93. https://doi.org/10.1523/JNEUROSCI.0801-09.2009.

Schindelin, Johannes, Ignacio Arganda-Carreras, Erwin Frise, et al. 2012. “Fiji: An Open-Source Platform for Biological-Image Analysis.” *Nature Methods* 9 (7): 676–82. https://doi.org/10.1038/nmeth.2019.

Schlosser, Gerhard, and Katja Ahrens. 2004. “Molecular Anatomy of Placode Development in *Xenopus Laevis*.” *Developmental Biology* 271 (2): 439–66. https://doi.org/10.1016/j.ydbio.2004.04.013.

Schnapp, Esther, Martin Kragl, Lee Rubin, and Elly M. Tanaka. 2005. “Hedgehog Signaling Controls Dorsoventral Patterning, Blastema Cell Proliferation and Cartilage Induction during Axolotl Tail Regeneration.” *Development* 132 (14): 3243–53. https://doi.org/10.1242/dev.01906.

SCIMS, NSCISC. 2024. *Traumatic Spinal Cord Injury Facts and Figures at a Glance*. National Spinal Cord Injury Statistical Center, Spinal Cord Injury Model System. https://bpb-us-w2.wpmucdn.com/sites.uab.edu/dist/f/392/files/2024/06/Facts_and_Figures_2024_Final.pdf.

Segerdell, Erik, Virgilio G Ponferrada, Christina James-Zorn, et al. 2013. “Enhanced XAO: The Ontology of Xenopus Anatomy and Development Underpins More Accurate Annotation of Gene Expression and Queries on Xenbase.” *Journal of Biomedical Semantics* 4 (1): 31. https://doi.org/10.1186/2041-1480-4-31.

Shimomura, Atsushi, Dharmeshkumar Patel, Sarah M. Wilson, Karl R. Koehler, Rajesh Khanna, and Eri Hashino. 2015. “Tlx3 Promotes Glutamatergic Neuronal Subtype Specification through Direct Interactions with the Chromatin Modifier CBP.” *PLOS ONE* 10 (8): e0135060. https://doi.org/10.1371/journal.pone.0135060.

Singh, Bhairab N., Cyprian V. Weaver, Mary G. Garry, and Daniel J. Garry. 2018. “Hedgehog and Wnt Signaling Pathways Regulate Tail Regeneration.” *Stem Cells and Development* 27 (20): 1426–37. https://doi.org/10.1089/scd.2018.0049.

Slack, J. M. W., C. W. Beck, C. Gargioli, and B. Christen. 2004. “Cellular and Molecular Mechanisms of Regeneration in *Xenopus*.” *Philosophical Transactions of the Royal Society of London. Series B: Biological Sciences* 359 (1445): 745–51. https://doi.org/10.1098/rstb.2004.1463.

Smith, A., F. Avaron, D. Guay, B. K. Padhi, and M. A. Akimenko. 2006. “Inhibition of BMP Signaling during Zebrafish Fin Regeneration Disrupts Fin Growth and Scleroblasts Differentiation and Function.” *Developmental Biology* 299 (2): 438–54. https://doi.org/10.1016/j.ydbio.2006.08.016.

Stringer, Carsen, Tim Wang, Michalis Michaelos, and Marius Pachitariu. 2021. “Cellpose: A

Generalist Algorithm for Cellular Segmentation." *Nature Methods* 18 (1): 100–106. https://doi.org/10.1038/s41592-020-01018-x.

Stuart, Tim, Andrew Butler, Paul Hoffman, et al. 2019. "Comprehensive Integration of Single-Cell Data." *Cell* 177 (7): 1888-1902.e21. https://doi.org/10.1016/j.cell.2019.05.031.

Su, Zhida, Wenze Niu, Meng-Lu Liu, Yuhua Zou, and Chun-Li Zhang. 2014. "In Vivo Conversion of Astrocytes to Neurons in the Injured Adult Spinal Cord." *Nature Communications* 5 (1): 3338. https://doi.org/10.1038/ncomms4338.

Sugiura, Takuji, Yuka Taniguchi, Akira Tazaki, Naoto Ueno, Kenji Watanabe, and Makoto Mochii. 2004. "Differential Gene Expression between the Embryonic Tail Bud and Regenerating Larval Tail in *Xenopus Laevis*." *Development, Growth & Differentiation* 46 (1): 97–105. https://doi.org/10.1111/j.1440-169X.2004.00727.x.

Sun, Aaron X., Ricardo Londono, Megan L. Hudnall, Rocky S. Tuan, and Thomas P. Lozito. 2018. "Differences in Neural Stem Cell Identity and Differentiation Capacity Drive Divergent Regenerative Outcomes in Lizards and Salamanders." *Proceedings of the National Academy of Sciences* 115 (35). https://doi.org/10.1073/pnas.1803780115.

Tan, Ruolan, Xiaoxuan Hu, Xinyi Wang, et al. 2023. "Leptin Promotes the Proliferation and Neuronal Differentiation of Neural Stem Cells through the Cooperative Action of MAPK/ERK1/2, JAK2/STAT3 and PI3K/AKT Signaling Pathways." *International Journal of Molecular Sciences* 24 (20): 15151. https://doi.org/10.3390/ijms242015151.

Taniguchi, Yuka, Kenji Watanabe, and Makoto Mochii. 2014. "Notochord-Derived Hedgehog Is Essential for Tail Regeneration in Xenopus Tadpole." *BMC Developmental Biology* 14 (1): 27. https://doi.org/10.1186/1471-213X-14-27.

Tazaki, Akira, Elly M. Tanaka, and Ji-Feng Fei. 2017. "Salamander Spinal Cord Regeneration: The Ultimate Positive Control in Vertebrate Spinal Cord Regeneration." *Developmental Biology* 432 (1): 63–71. https://doi.org/10.1016/j.ydbio.2017.09.034.

The Gene Ontology Consortium, Suzi A Aleksander, James Balhoff, et al. 2023. "The Gene Ontology Knowledgebase in 2023." *GENETICS* 224 (1): iyad031. https://doi.org/10.1093/genetics/iyad031.

Thuret, Raphaël, Hélène Auger, and Nancy Papalopulu. 2015. "Analysis of Neural Progenitors from Embryogenesis to Juvenile Adult in *Xenopus Laevis* Reveals Biphasic Neurogenesis and Continuous Lengthening of the Cell Cycle." *Biology Open* 4 (12): 1772–81. https://doi.org/10.1242/bio.013391.

Timmer, John R., Charlotte Wang, and Lee Niswander. 2002. "BMP Signaling Patterns the Dorsal and Intermediate Neural Tube via Regulation of Homeobox and Helix-Loop-Helix Transcription Factors." *Development* 129 (10): 2459–72. https://doi.org/10.1242/dev.129.10.2459.

Ulloa, Fausto, and Elisa Martí. 2010. "Wnt Won the War: Antagonistic Role of Wnt over Shh

Controls Dorso-ventral Patterning of the Vertebrate Neural Tube." *Developmental Dynamics* 239 (1): 69–76. https://doi.org/10.1002/dvdy.22058.

Valiente, Manuel, and Oscar Marín. 2010. "Neuronal Migration Mechanisms in Development and Disease." *Current Opinion in Neurobiology* 20 (1): 68–78. https://doi.org/10.1016/j.conb.2009.12.003.

Wang, Jiayi, Wei Zou, Jingyun Ma, and Jing Liu. 2019. "Biomaterials and Gene Manipulation in Stem Cell-Based Therapies for Spinal Cord Injury." *Stem Cells and Development* 28 (4): 239–57. https://doi.org/10.1089/scd.2018.0169.

Wang, Lei-Lei, Zhida Su, Wenjiao Tai, Yuhua Zou, Xiao-Ming Xu, and Chun-Li Zhang. 2016. "The P53 Pathway Controls SOX2-Mediated Reprogramming in the Adult Mouse Spinal Cord." *Cell Reports* 17 (3): 891–903. https://doi.org/10.1016/j.celrep.2016.09.038.

Watson, Charles, and Gulgun Kayalioglu. 2009. "The Organization of the Spinal Cord." In *The Spinal Cord*. Elsevier. https://doi.org/10.1016/B978-0-12-374247-6.50005-5.

Wickham, Hadley. 2016. *Ggplot2: Elegant Graphics for Data Analysis*. Use R! Springer-Verlag New York. https://doi.org/10.1007/978-3-319-24277-4.

Willsey, Helen Rankin. 2021. "Whole-Mount RNA In Situ Hybridization and Immunofluorescence of *Xenopus* Embryos and Tadpoles." *Cold Spring Harbor Protocols* 2021 (10): pdb.prot105635. https://doi.org/10.1101/pdb.prot105635.

Wilson, Alexia C., and Lora B. Sweeney. 2023. "Spinal Cords: Symphonies of Interneurons across Species." *Frontiers in Neural Circuits* 17 (April): 1146449. https://doi.org/10.3389/fncir.2023.1146449.

Wullimann, Mario F., Elke Rink, Philippe Vernier, and Gerhard Schlosser. 2005. "Secondary Neurogenesis in the Brain of the African Clawed Frog, Xenopus Laevis, as Revealed by PCNA, Delta-1, Neurogenin-Related-1, and NeuroD Expression." *Journal of Comparative Neurology* 489 (3): 387–402. https://doi.org/10.1002/cne.20634.

Yajima, Hiroshi, Makoto Suzuki, Haruki Ochi, et al. 2014. "Six1 Is a Key Regulator of the Developmental and Evolutionary Architecture of Sensory Neurons in Craniates." *BMC Biology* 12 (1): 40. https://doi.org/10.1186/1741-7007-12-40.

Yam, Patricia T, and Frédéric Charron. 2013. "Signaling Mechanisms of Non-Conventional Axon Guidance Cues: The Shh, BMP and Wnt Morphogens." *Current Opinion in Neurobiology* 23 (6): 965–73. https://doi.org/10.1016/j.conb.2013.09.002.

Yang, Ciqing, Shuanqing Li, Xiaoying Li, et al. 2019. "Effect of Sonic Hedgehog on Motor Neuron Positioning in the Spinal Cord during Chicken Embryonic Development." *Journal of Cellular and Molecular Medicine* 23 (5): 3549–62. https://doi.org/10.1111/jcmm.14254.

Yang, Lixin, Feifei Wang, and Uwe Strähle. 2020. "The Genetic Programs Specifying Kolmer–

Agduhr Interneurons." *Frontiers in Neuroscience* 14 (October): 577879. https://doi.org/10.3389/fnins.2020.577879.

Yu, Haiyang, Shangbin Yang, Haotao Li, Rongjie Wu, Biqin Lai, and Qiujian Zheng. 2023. "Activating Endogenous Neurogenesis for Spinal Cord Injury Repair: Recent Advances and Future Prospects." *Neurospine* 20 (1): 164–80. https://doi.org/10.14245/ns.2245184.296.

Zechner, Dietmar, Thomas Müller, Hagen Wende, et al. 2007. "Bmp and Wnt/β-Catenin Signals Control Expression of the Transcription Factor Olig3 and the Specification of Spinal Cord Neurons." *Developmental Biology* 303 (1): 181–90. https://doi.org/10.1016/j.ydbio.2006.10.045.

Zhang, Fang, Patrizia Ferretti, and Jonathan D.W. Clarke. 2003. "Recruitment of Postmitotic Neurons into the Regenerating Spinal Cord of Urodeles." *Developmental Dynamics* 226 (2): 341–48. https://doi.org/10.1002/dvdy.10230.

Zhou, Lili, Anthony R. McAdow, Hunter Yamada, et al. 2023. "Progenitor-Derived Glia Are Required for Spinal Cord Regeneration in Zebrafish." *Development* 150 (10): dev201162. https://doi.org/10.1242/dev.201162.